Aus dem Institut für Laboratoriumsmedizin und Pathobiochemie, Molekulare Diagnostik des Fachbereichs Medizin der Philipps-Universität Marburg

Direktor:

Prof. Dr. med. Harald Renz

des Fachbereichs Medizin der Philipps-Universität Marburg

in Kooperation mit dem Institut für Bioverfahrenstechnik und Pharmazeutische Technologie der Technischen Hochschule Mittelhessen

Geschäftsführende Direktoren:

Prof. Dr.-Ing. Peter Czermak und Prof. Dr. rer. nat. Frank Runkel

KUMULATIVE DISSERTATION

Entwicklung eines protektiven dermalen Drug Delivery Systems für therapeutische DNAzyme gegen Hauterkrankungen wie die aktinische Keratose

Inauguraldissertation zur Erlangung des Doktorgrades der Naturwissenschaft

dem Fachbereich Medizin der Philipps-Universität Marburg

vorgelegt von

Kay Jens Marquardt

aus Offenbach

Marburg, 2016

Angenommen vom Fachbereich Medizin der Philips-Universität Marburg am: 12.12.2016.

Gedruckt mit Genehmigung des Fachbereichs.

Dekan: Herr Prof. Dr. H. Schäfer

Referenten: Herr Prof. Dr. H. Renz/Herr Prof. Dr. F. Runkel

1. Korreferent: Herr Prof. Dr. W. Pfützner

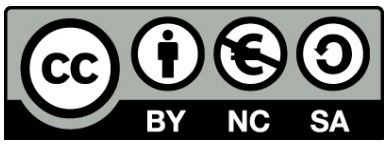

“We got the cure, we got the DNA”

Beatsteaks. “DNA”

Inhaltsverzeichnis

Abstract

DNAzymes are a group of synthetic nucleic acid based APIs that have the ability to inhibit protein translation by targeting the transcript of a specific gene. DNAzymes have already been tested in clinical trials with five different diseases. Two of the DNAzymes have been tested for dermal application against atopic dermatitis and skin cancer (squamous-cell carcinoma, basal cell carcinoma). The development of an appropriate dermal drug delivery system (DDS) is challenging, because DNAzymes are prone to enzymatic degradation and have problematic properties in terms of skin penetration. The task of this thesis was to develop a dermal DDS that addresses both issues. The dermal DDS should maintain the integrity of DNAzymes while enhancing the penetration and uptake of DNAzymes into human skin and the targeted keratinozytes. First, to ensure the integrity of this particularly group of APIs, the degradation of DNAzymes on human skin had to be identified and analysed. The analysis revealed that unprotected DNAzymes were rapidly degraded by a DNase II like activity. Therefore, protective systems were developed to protect against DNase II. Especially, complexation of DNAzymes with polycations, forming polyplexes, was able to sufficiently maintain the integrity of the API. Depending on the properties of the polycations a specific ratio (ξ) between the oppositely charged DNAzymes and polycations was necessary to fully protect. A ξ-ratio of about 1-2 along with a positive zeta potential increased in general the chances of an appropriate protection. The most effective protection was achieved with polycations of biodegradable chitosan. To enhance the penetration of DNAzymes through the skin barrier the submicron emulsion (SME) was identified as ideal candidate and the SME was developed as carrier system for DNAzymes. The SME increased the penetration of API into skin. The DNAzymes accumulated especially in the stratum corneum due to the SME's excipients. Consequently, the stratum corneum was able to act as an API reservoir. The SME and the chitosan polyplexes were finally combined to a so called protective dermal DDS. The protective dermal DDS enhanced the penetration into the skin and protected the DNAzymes. On cellular level the uptake of DNAzymes into the targeted keratinocytes were enhanced due to the polyplexes.

Einleitung

Erkrankungen der Haut sind ein wachsendes sozioökonomisches Problem der Gesellschaft. In einer deutschlandweiten Kohortenstudie wurden Erwerbstätige im Alter von 17-70 Jahren hinsichtlich therapiebedürftiger Hautläsionen untersucht. Bei 26,8 % dieser Bevölkerungsgruppe konnte eine Hautläsion mit Therapiebedarf festgestellt werden (Augustin et al., 2011). Dieses Resultat zeigt deutlich den hohen Bedarf in der Therapie von Hauterkrankungen auf, insofern, dass das Untersuchungsergebnis einen Rückschluss auf die Gesamtbevölkerung zulässt. Werden die Ergebnisse der Studie auf die erwerbsfähige Bevölkerung übertragen, so sind derzeit ungefähr 14 Mio. der deutschen und 88 Mio. der europäischen Bevölkerung betroffen (European Union, 2016). Die Therapie von Hauterkrankungen erfolgt idealerweise über die dermale Wirkstoffapplikation. Im Hinblick auf den therapeutischen Erfolg hat die lokale Bioverfügbarkeit des Wirkstoffes einen maßgeblichen Anteil. Um eine hohe Bioverfügbarkeit an dem Zielort in der Haut zu erreichen, muss eine angemessene perkutane Absorption erfolgen. Die Absorption des Wirkstoffes wird dabei entscheidend durch die Haut, den Wirkstoff selbst und das Trägersystem bestimmt.

Haut

Die Haut ist das größte Organ des Menschen und grenzt den Organismus von der Umwelt ab. Es ist ein komplexes Organ, das durch seinen vielschichtigen Aufbau zahlreiche Funktionen erfüllt. Als äußere Begrenzung kommt die Haut einer ihrer Hauptfunktionen nach, indem sie Schutz vor exogenen Noxen gewährt. Durch aktinische, mechanische, biochemische und immunologische Barrieren entgegnet die Haut dieser chronischen Belastung. Diese Barrieren werden durch einen passiven sowie aktiven Schutz gesichert. Die Unterscheidung der aktiven und passiven Barrieren wird durch die Art der Abwehr beschrieben. Die passive Hautbarriere verhindert eine Penetration exogener Noxen durch den speziellen Aufbau der Gewebestruktur. Die Gewebestruktur wird dabei maßgeblich durch die Epidermis und das Stratum corneum gebildet. Die stetige Proliferation der Keratinozyten in der Epidermis und deren terminale epidermale Differenzierung führen zu einer kontinuierlichen Rekonvaleszenz des Stratum corneum an der Hautoberfläche. Das Stratum corneum besteht aus mehreren Schichten von Korneozyten, die in eine Lipid-

Proteinmatrix eingebettet sind (Elias, 1983). Als Resultat bewirkt dieser Zustand, dass das lipophile Stratum corneum die Hauptdiffusionsbarriere für exogene und endogene Substanzen bildet (Scheuplein und Blank, 1971; Wertz et al., 1989). Gegenüber der passiven Barriere wird die aktive Barriere hingegen durch Prozesse beschrieben, die zu einer Veränderung der exogenen Noxen führt. Kommensale Bakterien an der Hautoberfläche sowie die Haut selbst sind der Ursprung für degradierende Proteine, die insbesondere chemischen und mikrobiellen Noxen entgegenwirken (Eckhart et al., 2012; Gallo und Nakatsuji, 2011). Zusätzlich wird auf der Hautoberfläche aktiv ein selektierendes Milieu geschaffen, das zur Folge hat, dass mikrobielle Noxen nicht resident werden oder penetrieren können (Sanford und Gallo, 2013). Ist dieser zuvor beschriebene komplexe Prozess der Homöostase der Haut gestört, ist diese gegenüber Erkrankungen anfälliger. In Kombination mit der chronischen Belastung durch äußere Noxen kann die äußere Barriere geschwächt werden und es zum Ausbruch von Erkrankungen kommen.

Hauterkrankung – Aktinische Keratose

Im Fall der aktinischen Keratose, welche als Vorform des Plattenephitelkarzinoms betrachtet werden kann, erfährt die Homöostase eine Disruption durch pathogene Veränderung der Keratinozyten (Nomura et al., 1997; Roewert-Huber et al., 2007). Die Folge ist eine Veränderung der Hautmorphologie. Da die Veränderungen durch UV-Strahlung induziert werden können, zeigt insbesondere Australien eine hohe Prävalenz, die bei der Population der über 40-Jährigen bei 60 % liegt (Marks et al., 1986). Aufgrund der Tatsache, dass weder die Chancen einer vollständigen Regression noch das Risiko einer Progression zu einem invasiven Plattenephitelkarzinom abzuschätzen sind, hält die „International League of Dermatological Societies“ ein therapeutisches Vorgehen für notwendig (Werner et al., 2015). In ihrer derzeitigen Therapieempfehlung werden invasive Methoden wie ablative Verfahren bis hin zur chirurgischen Exzision im Fall von Einzelläsionen als Methoden der Wahl betrachtet. Jedoch ist die invasive Therapie an exponierten Stellen problematisch und für ein großflächiges Vorgehen ungeeignet. Das Beispiel der aktinischen Keratose verdeutlicht den Handlungsbedarf in Hinblick auf die Erforschung geeigneter Wirkstoffe für neue Therapieansätze im Bereich der Dermatopharmazie.

Nukleinsäurebasierende Wirkstoffe

Einen vielversprechenden neuen Therapieansatz bilden die therapeutischen Oligonukleotide. Der überwiegende Teil der potenziellen Wirkstoffe greift auf post-transkriptioneller Ebene in der Zielzelle ein. Hierbei wird die Translation von spezifischen mRNAs inhibiert, deren Expression eine Schüsselrolle in der Pathogenese zugeschrieben wird. Repräsentanten dieser Technologie sind nicht codierende Oligonukleotide wie die Antisense Oligonucleotides, small interfering RNAs, Ribozyme sowie DNAzyme (Bhindi et al., 2007). Im Hinblick auf die Entwicklung neuer Therapieansätze in der Dermatopharmazie besitzen die DNAzyme, als synthetisches Analogon zu den natürlich vorkommenden Ribozymen, erfolgsversprechende Vorteile. Die speziellen 10-23 DNAzyme bestehen aus einem DNA-basierenden Einzelstrang, welcher in eine katalytische Domäne und zwei flankierende Bindungsarme unterteilt werden kann (Santoro und Joyce, 1997). Über die Flexibilität der Bindungsarme kann eine Ziel-RNA selektiv adressiert werden, während die katalytische Domäne die Ziel-RNA spaltet (Cairns et al., 1999). Der Prozess der Spaltung unterliegt einer enzymatischen Kinetik mit mehrfacher Substratumsetzung (Santoro und Joyce, 1998). Die enzymatische Kinetik in Kombination mit einer erhöhten Stabilität in biologischen Matrices im Vergleich zu RNA-basierenden Wirkstoffen erhöht die zu erwartende therapeutische Potenz. Die hohe Selektivität bezüglich der primären als auch sekundären Zielstruktur sowie die Unabhängigkeit gegenüber endogenen zellulären Faktoren wie RNase H, Dicer und RISC (RNA-induced silencing complex) verringern zudem das Risiko unerwünschter Wirkungen wie beispielsweise „off-target effects“ (Fellmann und Lowe, 2014; Kole et al., 2012; Santoro und Joyce, 1998). Hinsichtlich einer Therapie gegen Hauterkrankungen werden derzeit drei DNAzyme entwickelt. Diese adressieren entzündungsassoziierte Erkrankungen wie atopische Dermatitis (klinische Prüfung: NCT02079688), Psoriasis (Präklinik) oder Hautkarzinome (Plattenepithelkarzinom, Basalzellkarzinom) sowie deren Vorstufe in Form der aktinischen Keratose (Zhang et al., 2006). Die Applikation der therapeutischen DNAzyme soll für jede der genannten Erkrankungen lokal erfolgen. Dadurch wird zwar das Problem einer gewebespezifischen Distribution umgangen, jedoch ist ein Wirkstofftransport in die Haut erforderlich (Larson et al., 2007).

Wirkstofftransport

Die Penetration in die Haut wird im Allgemeinen durch den Prozess der passiven Diffusion beschrieben (Scheuplein und Blank, 1971). Um die Diffusion eines Wirkstoffes durch die passive Barriere der Haut zu fördern, werden dermale Drug Delivery Systeme (DDS) entwickelt. Während für gängige Wirkstoffgruppen bereits zahlreiche Ansätze des zu wählenden dermalen DDS etabliert sind, besteht im Bereich der Biomoleküle und im Speziellen für DNAzyme ein noch ausbaufähiges Forschungspotenzial. Zumeist wird auf einen aktiven Wirkstofftransport der Biomoleküle zurückgegriffen, da eine erhöhte Penetrationseffizienz zu erwarten ist. Physikalische Methoden wie Iontophorese, Elektroporation oder mechanische, invasive Methoden wie Mikronadeln, Abrasion, Ablation oder Perforation sind hierbei Methoden der Wahl. Diese Methoden gehen mit einem hohen apparativen Aufwand an stationärer Stelle oder einem invasiv-destruktiven Eingriff an der Haut des Patienten einher. Bedingt durch die Methoden sind Applikationsort und -fläche beschränkt und meist ist eine nachträgliche Versorgung der Applikationsstelle notwendig. Zusätzlich erfordern die aktiven Methoden bei einer Langzeittherapie meist einhergehend mit einer hochfrequentierten Dosierung eine gute Patientencompliance. Demgegenüber stoßen passive Methoden des Wirkstofftransports auf größere Akzeptanz bei den Patienten. Ohne invasiven Eingriff oder stationäre Behandlung steigt das Maß an Therapietreue. Mittels einer geeigneten passiven Methode kann eine etwaige irreversible Schädigung der Haut umgangen werden. Eine großflächige Applikation auch an exponierten Hautstellen ist möglich. Die Umsetzung einer passiven Methode kann durch den Gebrauch galenischer Trägersysteme erreicht werden. Diese Trägersysteme zeichnen sich durch nicht aktive Hilfsstoffe aus, die in der Lage sind, unter anderem die Penetration des Wirkstoffes zu fördern.

Wirkstoffschutz

Während des Wirkstofftransports zum Zielort ist der Aspekt der Integrität des Wirkstoffes zwingend zu berücksichtigen. Ist der Wirkstoff gegenüber einer Degradierung durch die aktive Barriere der Haut anfällig, kann der Wirkstoff durch Modulierung geschützt werden (Dass et al., 2002). Jedoch kann eine Modulierung in *in-vivo*-Untersuchungen zu unvorhergesehenen und unerwünschten Wirkungen oder verringerter therapeutischer Potenz führen

(Fluiter et al., 2005; Rockwell et al., 1997). Typische DNA-Modulierungen wurden bereits an DNAzymen getestet, aus denen sich einzig das invertierte Thymidin am 3‘-Ende durchgesetzt hat und Anwendung bei den drei genannten DNAzymen gegen Hauterkrankungen findet.

Zielsetzung

Das Ziel der vorliegenden Arbeit bestand darin, ein protektives DDS zur dermalen Applikation von therapeutischen DNAzymen zu entwickeln. Das dermale protektive DDS sollte den Wirkstofftransport in die Haut fördern, gleichzeitig den Schutz des Wirkstoffes gewährleisten und schlussendlich die zelluläre Aufnahme des Wirkstoffes begünstigen. Die Wirkstoffgruppe der 10-23 DNAzyme stellte herausfordernde Ansprüche an das zu entwickelnde dermale DDS, insofern die Eigenschaften der DNAzyme sowohl deren Penetration als auch deren Stabilität beeinträchtigen. Um diesen komplexen Anforderungen zu begegnen, bestand die Strategie der vorliegenden Arbeit darin, die relevanten Teilaspekte separiert voneinander zu analysieren und die daraus resultierenden Erkenntnisse in einem letzten Schritt zielführend zu verknüpfen. Das somit entwickelte protektive dermale DDS sollte im pharmazeutischen Umfeld realisierbar sein, d. h. die eingesetzten Substanzen sollten der Pharmaqualität entsprechen und die Herstellung des DDS einer einfachen und umsetzbaren Methode unterliegen. Die Eignung der finalen Entwicklung wurde anhand des potenziellen Wirkstoffes zur Therapie der aktinischen Keratose validiert.

Ergebnisse

Im Folgenden sind die Ergebnisse der für das Promotionsthema relevanten Veröffentlichungen dargestellt. Die Gliederung der Veröffentlichungen unterliegt der strategischen und somit einer inhaltlichen und nicht chronologischen Anordnung. Die Referenzen zu den Ergebnissen befinden sich in der Referenzliste der jeweilig genannten Veröffentlichung. Die Einteilung der Ergebnisse spiegelt die drei Phasen der Entwicklung eines geeigneten protektiven dermalen DDS für DNAzyme wider: Der erste Teil beschreibt grundlegende Untersuchungen zur Auswahl eines geeigneten Trägersystems für die Wirkstoffgruppe der DNAzyme. Im zweiten Teil wird die Degradierung eines DNAzyms auf der humanen Haut genauer analysiert und der Schutz durch polyplexbildende Polykationen begutachtet. Aufgrund der vorangegangenen Ergebnisse kann im dritten Teil aus der Addition der Submicronemulsion (SME), als geeignetes Trägersystem und des Chitosan-Polyplexes, als geeignetes Schutzsystem, ein protektives dermales DDS für das DNAzym gegen aktinische Keratose entwickelt und hinsichtlich der Wirkstoffpenetration und -integrität validiert werden.

Ansätze zur dermalen Applikation von DNAzymen

In der Veröffentlichung *„Development of drug delivery systems for the dermal application of therapeutic DNAzymes“* (Schmidts, Marquardt et al., 2012) wurden unterschiedliche Trägersysteme hinsichtlich ihrer möglichen Eignung zur Applikation eines DNAzymes untersucht. Die Auswahl der zu entwickelnden Trägersysteme beruhte auf zwei Aspekten. Zum einen sollte das Trägersystem die Penetration des Wirkstoffes in die Haut fördern und zum anderen sollte das Trägersystem den Wirkstoff vor Degradierung schützen. Die Microemulsion (ME) und die SME wurden aufgrund ihrer allgemein guten penetrationsfördernden Eigenschaften ausgewählt. Demgegenüber wurden die Wasser-in-Öl-Emulsion (W/O-Emulsion) sowie die Wasser-in-Öl-in-Wasser-Emulsion (W/O/W-Emulsion) hinsichtlich ihrer Eigenschaft ausgewählt, den Wirkstoff in der wässrigen Phase einzukapseln und somit vor einer Degradierung zu schützen. Die Effekte der zwei unterschiedlich zugrunde gelegten Formulierungsstrategien können im Folgenden an der SME und der W/O/W-Emulsion nachvollzogen werden, insofern beide Trägersysteme die besten Ergebnisse erzielten. In den ersten vergleichenden Studien wurden das Freisetzungsverhalten und das Penetrationsverhalten des DNAzymes aus den unterschiedlichen Trägersystemen bzw. in die Haut simuliert und analysiert. Die Wirkstofffreisetzung aus der SME zeigte eine sofortige steady state-Phase mit anschließender Plateauphase nach 2 Stunden. In der Plateauphase lag der Wirkstoffgehalt im Akzeptormedium bei 1/3 des wässrigen Referenzstandards. Die W/O/W-Emulsion hingegen zeigte nach 6 Stunden eine sehr geringe Freisetzung nahe dem Wert 0 %.

In der Penetrationsstudie mit einem *ex-vivo*-Modell mit intakter Haut der *Sus scrofa domestica* (Hausschwein) wurden die Trägersysteme bezüglich ihrer penetrationsfördernden Eigenschaften untersucht. In einem infinite-dose-Experiment (300 µl/cm^2), d. h. mit einem Überschuss an Galenik, zeigte die SME im Vergleich zur W/O/W-Emulsion und dem wässrigen Standard eine überlegende Wirkstoffakkumulation in den Hautpräparaten. Dabei war insbesondere eine Akkumulation des Wirkstoffes im Stratum corneum zu beobachten. Veränderungen des hydrodynamischen Durchmessers der Öltropfen, der durch den HLB-Wert (hydrophile-lipophile balance value) der SME gesteuert wurde, hatten keinen Einfluss auf die Penetrationseffizienz des

Wirkstoffes. Dieser erste experimentelle Aufbau entsprach den „International Council for Harmonisation“, (ICH)-Leitlinien, vernachlässigte allerdings den Aspekt der Scherung und Verdunstung der Galenik beim Auftragen und Einwirken auf der Haut. Um diesen beiden Aspekten Rechnung zu tragen, wurde die Penetrationsstudie mit einer geringeren Galenikmenge (finite dose, 11,4 µl/cm^2) und Scherung durchgeführt. In diesem Fall invertieren die Ergebnisse und zeigten eine 3,3-fach höhere Akkumulation des DNAzymes in den Hautpräparaten durch die W/O/W-Emulsion, zusätzlich zu einer erhöhten zellulären Aufnahme. Zusammenfassend beschreiben die Ergebnisse, dass die SME eine gute Freisetzung sowie penetrationsfördernde Eigenschaften für das DNAzym besitzt, jedoch die schützenden Eigenschaften der W/O/W-Emulsion bei dem Auftragen von geringen Mengen überlegen waren. Hinsichtlich der Wirkstoffdegradierung wurden weitere Untersuchungen an der Hautstruktur durchgeführt. Die *ex-vivo*-Haut der *Sus scrofa domestica* wurde absichtlich geschädigt, indem die Schichten des Stratum corneum sukzessive entfernt wurden. Die abgenommenen Hautschichten wurden bezüglich ihrer degradierenden Aktivität gegenüber dem DNAzym untersucht. Die degradierende Aktivität war an der Hautoberfläche am höchsten und verringerte sich mit jeder weiteren abgenommen Schicht, wodurch sich ein gradueller Verlauf zeigte. Mit dem Ablösen des Stratum corneum verminderte sich zudem die Akkumulation des Wirkstoffes durch die SME in den Hautpräparaten um den Faktor von circa 1,5.

Degradierung und Schutz von DNAzymen auf der humanen Haut

Die Veröffentlichung „*Degradation and protection of DNAzymes on human skin*“ (Marquardt, Eicher, et al., 2016) vertieft den Aspekt der Degradierung und des Schutzes von DNAzymen gegenüber der aktiven Barriere der Haut. Basierend auf der These, dass die Degradierung durch endogene und exogene Enzyme verursacht wird, wurde in einem ersten Schritt die Identität des degradierenden Enzymes bestimmt. In einem *ex-vivo*-Versuchsaufbau wurde das Abbaumuster des DNAzyms auf humaner Haut qualifiziert. Die Hautschuppen verschiedener Personen (kaukasischer Typus) wurden unter geeigneten Bedingungen mit dem DNAzym inkubiert. Beim Abbau von DNA-basierenden Wirkstoffen entstehen DNA-Fragmente, welche mithilfe der Anionenaustausch HPLC nachgewiesen werden können. Mit dieser Analysemethode ist es möglich, einzelne DNA-

Fragmente bezüglich ihrer Länge aufzutrennen und in einem Chromatogramm zu visualisieren. Das Chromatogramm zeigte DNA-Fragmente im Bereich von 30-33 Nukleotiden sowie zwei Abbauprodukte im Bereich von 19 Nukleotiden. Das detektierte Abbaumuster wurde mit dem Abbauschema verschiedener Arten von Desoxyribonukleasen (DNasen) verglichen. Die DNasen zeigten jeweils ein spezifisches Abbaumuster mit charakteristischen DNA-Fragmenten, wobei die spezifischen Abbaumuster durch Veränderungen der Reaktionsparameter, wie pH-Wert (im Bereich 5,0 und 6,6) und Dauer der Reaktion, nicht beeinflusst wurden. Im Vergleich mit der Haut zeigte die DNase II ein ähnliches Abbaumuster. Demzufolge besitzt die menschliche Haut eine mit der DNase II vergleichbare Abbauaktivität.

Nach erfolgreicher Identitätsbestimmung wurde die Umsatzgeschwindigkeit degradierender Enzyme und der damit einhergehenden abbauenden Aktivität bestimmt. Auf Basis des *ex-vivo*-Versuchsaufbaus wurde die Aktivität auf zwei unterschiedliche Arten detektiert. Im ersten Fall erfolgte die Detektion mithilfe eines kovalent gebundenen Fluoreszenzmarkers und des korrespondierenden Black Hole Quenchers. Durch Degradierung des DNAzyms wurden Fluoreszenzmarker und Quencher sterisch getrennt, die Fluoreszenzlöschung aufgehoben und somit das Fluoreszenzsignal messbar. Die Zunahme der Fluoreszenz war indirekt das Maß der Degradierungsaktivität gegenüber dem DNAzym und konnte in Echtzeit detektiert werden. Die zweite Art der Detektion hatte den Vorteil einer direkten Quantifizierung. Mithilfe der Anionenaustausch HPLC konnte die Reduktion des intakten Wirkstoffes analysiert werden, wobei die Datenaufnahme auf eine Endpunktdetektion beschränkt war. Trotz der methodischen Unterschiede konnten beide Analysemethoden eine spezifische Aktivität von 5,9 ± 0,1 Units/mg bei einem pH-Wert von 5,0 übereinstimmend quantifizieren. Das Ergebnis wurde relativ zu aufgereinigten DNase II Standards ermittelt. Diese Standards unterlagen den Aktivitätsangaben des Herstellers, wobei die Ermittlung der Aktivität nicht mit den vorliegenden Reaktionsbedingungen übereinstimmte. Eine unabhängige Quantifizierung der Aktivität ohne Standards war durch die Anionenaustausch HPLC möglich und ergab einen geringeren Wert von $(5,6 \pm 0,3)*10^{-5}$ Units/mg.

Um den Wirkstoff auf der Haut vor Degradierung zu schützen, wurden Schutzsysteme basierend auf Polyplexen entwickelt. Zur Herstellung der Polyplexe wurden verschiedene Polykationen genutzt. Die Auswahl der Polykationen setzte sich aus unterschiedlichen Arten von Chitosan-Polymeren und einem standardgebräuchlichen verzweigtem Polyethylenimin (PEI) zusammen. Die Charakterisierung der Polykationen wurde durch den Hersteller übernommen und um den Grad der Protonierung der Aminogruppen in Abhängigkeit des pH-Werts ergänzt. Im Vergleich zu den Chitosan-Polymeren zeichnete sich das PEI durch eine 4,2-fach höhere Ladungsdichte aus. Lediglich 56 % der freien Aminogruppen des PEIs waren bei pH 5,0 protoniert, während im Fall der Chitosan-Polymere annähernd alle Aminogruppen protoniert waren. Folglich entsprach das N/P-Verhältnis der Chitosan-Polymere dem des Ladungsverhältnis ($N/P = \xi_C$), während im Fall des PEIs das N/P-Verhältnis in etwa dem doppeltem Ladungsverhältnis entsprach ($N/P \approx 2*\xi_P$). Das N/P-Verhältnis beschreibt das Verhältnis zwischen der Anzahl an Aminogruppen des Polykations und der Anzahl an Phosphatgruppen des DNAzyms. Das Ladungsverhältnis (ξ) hingegen beschreibt das Verhältnis zwischen den gegensätzlich geladenen Gruppen des Polykations und des DNAzyms. Die aus dem DNAzym und den unterschiedlichen Polykationen entstandenen Polyplexe wurden bezüglich ihrer physikochemischen Eigenschaften charakterisiert. Das Ladungsverhältnis bestimmte dabei generell die Eigenschaften des Polyplexes. Mit zunehmendem Ladungsverhältnis erhöhten sich der Grad der Komplexierung, das Zeta-Potenzial sowie die Stabilität der verschiedenen Polyplexe. In einem Ladungsverhältnis zwischen 1 und 2 wechselte das Zeta-Potenzial der Polyplexe seine Ladung. In diesem Wendepunkt besaßen die Polyplexe ihre größte Partikelgröße und Partikelgrößenverteilung. Ab einem Ladungsverhältnis von 2 erreichte der Komplexierungsgrad des Wirkstoffes sein Maximum, das mit einer maximal positiven Ladung der Polyplexe einhergeht. Hinsichtlich ihrer Eignung als Schutzsystem wurden die Polyplexe in einem *in-vitro*-Versuchsaufbau getestet. Das *in-vitro*-Screening basiert dabei auf den Ergebnissen der *ex-vivo*-Hautuntersuchungen und simuliert die DNAzym-Degradierung auf der humanen Hautoberfläche. Abhängig von dem Ladungsverhältnis zeigten die Polyplexe aller Polykationen einen ausreichenden Schutz gegenüber

enzymatischer Degradierung. Über dem jeweiligen kritischen Ladungsverhältnis (ξ_{kri}) konnte das DNAzym vollständig geschützt werden. Die niedrigsten kritischen Ladungsverhältnisse benötigten Chitosan S, gefolgt von den anderen Chitosan-Polyplexen. Mit Ausnahme von Chitosan S korrelierte das kritische Ladungsverhältnis mit dem maximalen Grad an Komplexierung. Das PEI wiederum zeigte das höchste kritische Ladungsverhältnis oberhalb des Wertes der maximalen Komplexierung. Zusätzlich zum *in-vitro*-Screening wurden die Polyplexe des Chitosan S des Weiteren mit menschlicher *ex-vivo*-Vollhaut inkubiert. Erneut zeigte sich ein ähnliches Ergebnis wie bei dem *in-vitro*-Screening. Einzig das ξ_{kri} veränderte sich von 1,01 auf 1,26.

Entwicklung eines protektiven dermalen Drug Delivery Systems für DNAzyme

In der Veröffentlichung „*Development of a protective dermal drug delivery system for therapeutic DNAzymes*“ (Marquardt, Eicher et al., 2014) wird die Entwicklung eines protektiven dermalen DDS für DNAzyme unter besonderer Berücksichtigung des Wirkstoffschutzes und des Wirkstofftransports beschrieben. Im Rahmen der Entwicklung stützt sich die Veröffentlichung auf eine mikroskopisch-spektrale Auswertungsmethode, die in der Veröffentlichung „*Evaluation and quantification of spectral information in tissue by confocal microscopy*“ (Mäder, Marquardt, et al., 2012) entwickelt wurde.

Die Entwicklung eines geeigneten DDS setzt die Nutzung eines kompatiblen Konservierungsmittels voraus. In einem geeigneten Versuchsaufbau mit ausgewählten DAC (Deutscher Arzneimittel-Codex) konformen Konservierungsmitteln zeigte einzig die Benzoesäure eine Inkompatibilität mit dem DNAzym. Die verbleibenden Konservierungsmittel wurden genutzt, um eine konservierte SME zu entwickeln. In einem Konservierungsbelastungstest, basierend auf den Angaben des Europäischen Arzneibuchs, konnte ausschließlich die mit Propylenglykol konservierte SME einen geeigneten Schutz gegenüber mikrobieller Kontamination erzielen. Unabhängig einer Wirkstoffbeladung konnte die Stabilität aller konservierten SME bezüglich physikochemischer Eigenschaften, wie pH-Wert, Tropfengröße und Tropfengrößenverteilung, über einen Zeitraum von 3 Monaten gewährleistet

werden. In dem untersuchten Zeitraum lag die Wirkstoffwiederfindung aller konservierten SMEs in einem Bereich von 100 ± 12 %.

Hinsichtlich der Entwicklung eines additiven Schutzsystems wurden zwei konträre Strategien verfolgt. Im Fall der entwickelten Liposome konnte eine Einschlusseffizienz des Wirkstoffes von 6 % erreicht werden, was in dem DNAzym Degradierungstest zu einem signifikant höheren Schutz gegenüber dem wässrigen Standard führte. Allerdings unterlag der Schutz einer zeitlichen Beschränkung und näherte sich nach 2 Stunden dem Wert der liposomalen Kontrollformulierung ohne Wirkstoffeinschluss an. Demgegenüber zeigten die entwickelten Chitosan-Polyplexe einen zeitunabhängigen Schutz. Über den untersuchten Zeitraum konnten 81 % des Wirkstoffes kontinuierlich geschützt werden. Der Wirkstoff war bei einem Ladungsverhältnis von 0,7 nahezu vollständig komplexiert. Die protektiven Eigenschaften wurden nach der Kombination mit der in Proyplenglykol konservierten SME zwar weiterhin beibehalten, jedoch konnte erneut eine zeitabhängige Degradierung des DNAzymes beobachtet werden. Parallel konnte in diesem Versuchsaufbau gezeigt werden, dass der Wirkstoff in der SME ohne Polyplexe vollständig abgebaut wurde. Die entstandene Kombination wurde als protektives DDS bezeichnet und nachfolgenden *in-vitro*-Untersuchungen unterzogen. Der Fokus der Studien lag auf der Degradierung, Penetration und Verteilung des Wirkstoffes und wurde an einem *ex-vivo*-Hautmodell der *Sus scrofa domestica* durchgeführt. Nach 24 Stunden Versuchsdauer konnte ein vollständiger Schutz des DNAzymes auf der Haut nachgewiesen werden. Die Penetration des Wirkstoffes in die Haut war, im Vergleich zum wässrigen Standard, um den Faktor 3,3 erhöht. Ohne die SME zeigten die Chitosan-Polyplexe keine penetrationsfördernden Eigenschaften und waren in der Penetrationsstudie dem wässrigen Standard unterlegen. Die Verteilung des DNAzymes in der Haut wurde mittels konfokaler Laser-Scanning-Mikroskopie visualisiert. Das fluoreszenzmarkierte DNAzym wurde spezifisch angeregt und das Emissionsspektrum der Haut gerastert aufgenommen. Um den Farbstoff zu identifizieren, wurde das Emissionsspektrum mit einem Referenzspektrum korreliert und über einen statistischen Schwellwert dem Farbstoff oder der Autofluoreszenz der Haut zugewiesen. Das Ergebnis der Analyse zeigte eine Wirkstoffkumulation durch das protektive DDS im Stratum corneum und den

äußeren Schichten der Epidermis. Die zelluläre Aufnahme des fluoreszenzmarkierten Wirkstoffes in die Hautzellen wurde in der Zellkultur an HaCaT-Keratinozyten untersucht. Mit Hilfe der Chitosan-Polyplexe fluoreszierten ein Viertel der untersuchten Zellen, während sich das Fluoreszenzsignal innerhalb der Zelle akkumulierte. Hierbei konnte eine Wiederfindung des intakten Wirkstoffes von 12 % in den Keratinozyten nachgewiesen werden.

Diskussion

Die Therapie von Erkrankungen setzt eine therapeutisch wirksame Bioverfügbarkeit des Wirkstoffes im Körper voraus. Um eine hohe Bioverfügbarkeit am Wirkort zu erlangen, ist in vielen Fällen ein DDS unabdingbar. Die Auswahl der DDS ist dabei abhängig von Faktoren wie Applikationsort, Ziel und dem Wirkstoff selbst. In der vorliegenden Arbeit wird speziell für therapeutische DNAzyme ein protektives dermales DDS entwickelt. Die Entwicklung wird anhand eines Modell-DNAzymes durchgeführt, welches zur Therapie von aktinischer Keratose eingesetzt werden soll.

Auf Grundlage dieser Zielsetzung sind die menschliche Haut und das Zytosol der Keratinozyten als Applikationsort bzw. Wirkort festgelegt. Die Haut als schützende Barriere zwischen Organismus und Umwelt stellt hohe Anforderung an die Entwicklung des DDS. Die generelle Barrierefunktion setzt sich dabei aus zahlreichen aufbauenden Teilaspekten zusammen. Der vielschichtige Aufbau der Haut, terminale Differenzierung, Tight Junctions, Immunabwehr, residente Bakterien sowie sekretive Enzyme sorgen in der Haut für eine schützende Homöostase (Naik et al., 2012; Proksch et al., 2008). Zusätzlich zur Barrierefunktion der Haut stellt auch der Wirkstofftypus besondere Ansprüche an das DDS. Der dieser Arbeit zugrunde liegende Wirkstofftyp ist ein Biomolekül bestehend aus Desoxyribonukleinsäure. Charakteristisch für diese neue Art der Wirkstoffe sind ein hohes Molekulargewicht, eine negative Ladung und deren hydrophile Eigenschaft. Des Weiteren unterliegt der Wirkstoff im physiologischen Umfeld einer enzymatischen Degradierung. Diese diffizilen Eigenschaften erschweren die Entwicklung eines geeigneten dermalen DDS. In dem aktuellen Review „*Nucleic acid delivery into skin for the treatment of skin diseases*“ benennen die Autoren drei wichtige Herausforderungen, die es generell bei dem Transport von Nukleinsäure in die Haut zu überwinden gilt: 1. Erhalt der Integrität des Wirkstoffes, 2. Penetration des Wirkstoffes in die Haut sowie 3. Zelluläre Aufnahme des Wirkstoffes (Zakrewsky et al., 2015). Diese drei Aspekte werden als hinreichend notwendig betrachtet, um an ihnen im Folgenden die Entwicklung eines geeigneten dermalen DDS für therapeutische DNAzyme zu diskutieren.

Integrität des Wirkstoffes

Die Desoxyribonukleotidkette des zugrunde liegenden Wirkstoffes ist anfällig gegenüber hydrolytischer Degradierung (Lindahl, 1993). Eine Degradierung führt zu einer Verringerung oder zum Erlöschen der therapeutischen Potenz. Bei der topischen Applikation des Wirkstoffes auf der Haut unterlag der Wirkstoff einer Degradierung, welche durch die aktive Hautbarriere hervorgerufen wurde. Die degradierende Aktivität nahm von innen nach außen zu und hatte die höchste Aktivität an der Hautoberfläche. An der Hautoberfläche kann die Hydrolyse durch die umgebende Matrix katalysiert werden. Dabei kann es zu einer säureinduzierten Katalyse durch den pH-Wert der Oberfläche sowie zu einer enzymatischen Katalyse durch exogene und endogene Enzyme kommen. Ziel war es, die degradierende Aktivität zu identifizieren, deren Umsatzgeschwindigkeit zu quantifizieren und in der Konsequenz ein System zu entwickeln, welches den Wirkstoff vor Degradierung schützt.

Durch eine säurekatalysierte Degradierung kann eine Spaltung der N-glykosidischen Bindung am Wirkstoff erfolgen, was zu einer Depurinierung oder in selteneren Fällen zu einer Depyrimidierung führt (Lindahl, 1993; Pogocki und Schöneich, 2000). Das entstehende Produkt ist anfällig gegenüber einer β-Eliminierung, sodass es zu einem Strangbruch des Phosphatrückgrats kommt (Lindahl, 1993). Diesbezügliche *in-vitro*-Untersuchungen im physiologischen pH-Bereich der Haut konnten keine erhöhte Degradierung des DNAzymes im Vergleich zwischen sauren und neutralen pH-Wert aufzeigen. Demnach ist die Wahrscheinlichkeit einer speziellen säurekatalysierten Hydrolyse des Wirkstoffes auf der Haut als gering einzuschätzen.

Andererseits wurde ein hohes Maß an enzymatisch katalysierter Hydrolyse an der humanen Hautoberfläche detektiert. Die Degeneration des Wirkstoffes erfolgt hierbei über die Phosphorhydrolasen, welche den DNA-Strang sowohl am Ende als auch innerhalb der Nukleotidkette spalten können. Die Nukleasen bauen endo- und exogene DNA ab und tragen dazu bei, die Homöostase und die Barrierefunktion der Haut aufrechtzuerhalten (Eckhart et al., 2012; Howell et al., 2003). Zur Identifizierung der enzymatischen Aktivität wurde das Abbaumuster der humanen Hautoberfläche mit dem Abbaumuster unterschiedlicher Typen von DNasen verglichen. Obgleich das DNAzym als

Substrat nur eine geringe Nukleotidlänge aufweist, bildeten die abgebauten DNA-Fragmente ein spezifisches Muster, das der DNase II zugeordnet werden konnte. Die Detektionsmethode erwies sich als robust, insofern weder pH-Wertänderung noch unterschiedliche Reaktionszeiten zu Veränderungen der spezifischen Abbaumuster der unterschiedlichen DNasen führten. Das entstandene Abbaumuster der hauteigenen DNasen wurde unter anderem durch ein CpG-A-Motiv geprägt, das eine endosomale Toll-like-Rezeptor 9-Aktivierung nach sich ziehen kann (Chan et al., 2015). Die Aktivierung des Toll-like-Rezeptor 9 trägt zur Interferon Ausschüttung bei und ist ein wichtiger Faktor in der köpereigenen Immunantwort gegenüber exogener DNA aus Viren und Bakterien. Die DNase II selbst wird im Lysosom der Hautzellen detektiert und wird vermutlich über die Keratinosome in das Stratum corneum sekretiert (Fischer et al., 2011; Ohkouchi et al., 2013). In Anlehnung an Fischer et al. ist die DNase-II-Aktivität der Haut auf die DNase 2a und L-DNase II zurückzuführen (Fischer et al., 2011).

Eine 3‘-5‘ Exonukleaseaktivität oder eine DNase I-Aktivität, wie sie im Blut vorkommt, konnte für die Modell DNAzyme nicht identifiziert werden (Cherepanova et al., 2007). Obwohl TREX2 als Vertreter der Exonuklease in der Haut nachgewiesen werden kann, konnte keine diesbezügliche Aktivität festgestellt werden (Parra et al., 2009). Der Grund basiert auf der bereits bestehenden Wirkstoffmodulation, welche durch die Einführung eines zusätzlichen, invertierten Thymidins am 3‘-Ende das DNAzym vor einer 3‘-5‘-Exonuklease-Aktivität schützt (Takei et al., 2002). Ebenfalls wurde keine DNase-I-Aktivität festgestellt, obgleich in den *ex-vivo*-Versuchen der pH-Wert dem Optimum der DNase I angeglichen wurde. Das Fehlen einer DNase-I-Aktivität widerspricht dem Usus, DNase I als Standard zu nutzen, um *in-vitro*-Stabilitätsstudien durchzuführen, welche die enzymatische Degradierung der Haut simulieren sollen (Schmidts et al., 2011).

Nach der Qualifizierung der degradierenden Aktivität wurde die Umsatzgeschwindigkeit erfolgreich quantifiziert. Bei der Quantifizierung galt es zu berücksichtigen, dass die entstehenden Abbauprodukte des Wirkstoffes dem Enzym erneut als kompetitives Substrat zur Verfügung standen. Da jedoch eine degradierende Veränderung des Wirkstoffmoleküls im pharmazeutischen Sinne

zum Funktionsverlust führt, wurde einzig die Aktivität des Enzymes gegenüber dem intakten Wirkstoff quantifiziert. Da keine vergleichbaren Messwerte in der Literatur beschrieben wurden, wurden zwei unterschiedliche Messmethoden genutzt, um die Umsatzgeschwindigkeit zu bestimmen. Die Messmethoden gründen zum einen auf dem Prinzip der fluoreszenzbasierenden Förster-Resonanz-Elektronen-Transmission und zum anderen auf der UV-Messung des größenseparierten intakten Wirkstoffes. Trotz der unterschiedlichen Messmethoden zeigten die Messungen vergleichbare Umsatzgeschwindigkeiten im Ergebnis. Die Werte bezogen sich relativ zu einem aufgereinigten DNase-II-Standard. Die Hersteller dieser Standards ermitteln grundsätzlich die Aktivität des Enzyms anhand doppelsträngiger DNA. Der Wirkstoff hingegen ist ein Einzelstrang und wird daher langsamer umgesetzt (Harosh et al., 1991). Als Konsequenz ergab die Quantifizierung ohne Bezug zum DNase-II-Standard einen stark erniedrigten Wert im Vergleich zur relativen Umsatzgeschwindigkeit.

Zusammenfassend beschreiben die ermittelten Erkenntnisse die humane Hautoberfläche als ein Kompartiment, welches den Wirkstoff durch die DNase II aktiv nach kurzer Verweilzeit degradiert und gleichzeitig das Immunsystem durch TLR9 stimulieren kann. Ein erfolgreiches DDS muss diese aktive Barriere überwinden, indem es die Integrität des Wirkstoffes sicherstellt.

Diesbezüglich wurden in einem ersten *in–vitro*-Versuch zwei unterschiedliche Schutzstrategien verfolgt. Diese beruhten zum einem auf der Einkapselung des Wirkstoffes in unilamellare Liposome und zum anderen in der Komplexierung des Wirkstoffes zu Polyplexen. Während bei der Herstellung der protektiven Systeme eine vollständige Komplexierung zu Polyplexen erreicht wurde, konnte bei den Liposomen hingegen nur eine geringe Einschlusseffizienz erreicht werden. Die Einschlusseffizienz lag im Bereich der nach Xu et al. berechneten theoretischen Einschlusseffizienz, allerdings unterhalb von 10 % (Xu et al., 2012). Auf Grundlage der geringen Einschlusseffizienz erzielte die liposomale Formulierung einen geringen und zudem zeitlich begrenzten Schutz des Wirkstoffes. Im Vergleich gewährleisteten die auf Polykationen basierenden Polyplexe einen nahezu vollständigen Schutz über den gesamten Untersuchungszeitraum hinweg. Der Schutz wurde dabei durch die

Wirkstoffkomplexierung erreicht, die sowohl über elektrostatische Wechselwirkung als auch über hydrophobe Wechselwirkung zwischen dem DNAzym und dem Polykation erfolgen kann (Dautzenberg und Jaeger, 2002; Liu et al., 2005). Im Polyplex schirmt das Polykation den Wirkstoff sterisch ab und verhindert somit eine enzymatische Degradierung.

Basierend auf diesen Erkenntnissen wurde die Untersuchung zur Eignung verschiedener Polykationen zur Polyplexbildung intensiviert. Als bioabbaubares, biokompatibles Polykation wurden unterschiedliche Chitosan-Polymere ausgewählt, welche sich im Molekulargewicht, im Deacetylierungsgrad sowie in der Hydrophilie unterschieden (Kean und Thanou, 2010). Als Vergleich wurde das in der Gentechnik als Goldstandard bezeichnete PEI genutzt (Patnaik und Gupta, 2013). Die Charakterisierung hinsichtlich Partikelgröße, Zeta-Potenzial, Komplexierungsgrad und Stabilität der hergestellten Polyplexe ergab, dass, unabhängig von dem Typus des Polykations, die Eigenschaften durch das Ladungsverhältnis ξ geprägt wurden. Hierbei zeigte der Einfluss des ξ-Verhältnisses auf alle Eigenschaften keine Unregelmäßigkeiten. Die Polyplexe wurden hinsichtlich ihrer schützenden Eigenschaften gegenüber der aktiven Barriere der Hautoberfläche in einem weiteren standardisierten *in-vitro*-Versuchsaufbau getestet. Ein hoher Wert des ξ-Verhältnisses und ein Zeta-Potenzial im Bereich des positiven Plateaus sind gute Indikatoren für einen ausreichenden Schutz des Wirkstoffes. Demgegenüber zeigte insbesondere der ermittelte Komplexierungsgrad ein indifferentes Bild. Das zugrunde liegende Messprinzip basiert auf der kompetitiven Verdrängung des positiv geladenen Fluoreszenzfarbstoffes von dem negativ geladenen Wirkstoff durch die komplexierenden Polykationen. Durch das Messprinzip wird die Komplexierung mittels elektrostatischer Wechselwirkung bei gleichzeitiger Diskriminierung der hydrophoben Wechselwirkung analysiert. In den Untersuchungen zeigte PEI eine vollständige Komplexierung bei dem vergleichsweise niedrigsten ξ-Wert. In dem Wirkstoff-Degradierungsversuch benötigte PEI jedoch ein höheres ξ-Verhältnis, um einen ausreichenden Schutz zu gewährleisten. Folglich stellte in diesem Fall ein maximaler Komplexierungsgrad keinen Indikator für einen ausreichenden Schutz dar. Diese Divergenz kann im Vergleich der Eigenschaften zwischen PEI und Chitosan S erläutert werden. Das Chitosan S ist ein größeres Polymer mit höherem monomeren Molekulargewicht und

geringerer Ladungsdichte. Das hohe Molekulargewicht der Monomere sorgt nach der Bindung an den Wirkstoff für eine bessere Abschirmung der einzelnen Wirkstoffmonomere, während die Größe des Polymers sowie die geringe Ladungsdichte die Flexibilität des Polymers verbessern (Liu et al., 2007). Die Flexibilität fördert das „Umschlingen“ des Chitosan-Polymers um das Wirkstoffmolekül und verhindert die Annäherung degradierender Enzyme (Rudzinski und Aminabhavi, 2010). Die Tatsache, dass bei einem gemessenen Komplexierungsgrad von nur 50 % der Wirkstoff vollständig geschützt wurde, weist auf eine zusätzliche hydrophobe Wechselwirkung zwischen Chitosan und Wirkstoff hin, die hingegen unter dem Einsatz von PEI nicht ermittelt werden konnte.

Ausnahmslos konnte ein ausreichender Schutz des Wirkstoffes gegenüber der aktiven Hautbarriere mittels jedes der untersuchten Polykationen erzielt werden. Unterschiede zeigten ausschließlich die Effizienzen des Schutzes, welcher durch den benötigten ξ_{krit}-Wert bestimmt wurde. Die Chitosan-Polymere und insbesondere das Chitosan S zeigten die höchste Effizienz, während PEI die geringste Effizienz aufwies. Infolgedessen waren die Chitosan-Polymere dem PEI überlegen. Werden die Polykationen hinsichtlich einer therapeutischen Applikation beurteilt, kann eine ähnliche Einordung erfolgen. Zwar wird in der Literatur den PEI-Polymeren eine hohe Transfektionseffizienz sowie ein Endosomaustritt zugeschrieben, das möglicherweise zu einer Erhöhung der Wirkstoffkonzentration im Zytoplasma führen kann, allerdings besitzt es als nicht abbaubares Polymer ebenfalls eine erhöhte Tendenz zur Toxizität (Boussif et al., 1995; Kawakami et al., 2006). Demgegenüber zeichneten sich im Allgemeinen die Chitosan-Polymere durch ihre Bioabbaubarkeit und -kompatibilität aus und sind somit dem PEI vorzuziehen, da sie eine geringe Tendenz der Toxizität aufweisen (Kean und Thanou, 2010).

Zusätzlich zu den *in-vitro*-Versuchen wurden die Chitosan S-Polyplexe in ein Trägersystem bestehend aus einer SME eingearbeitet und auf der *ex-vivo*-Haut der *Sus scrofa domestica* inkubiert. Hierbei sollten die schützenden Effekte des Chitosan-Polyplexes in der SME auf *ex-vivo*-Haut untersucht und zusätzlich eine mögliche Inkompatibilität zwischen Polyplex und Trägersystem aufgedeckt werden. Zwar zeigten die Polylexe in der SME im *in-vitro*-Versuch eine

zeitabhängige Degradierung des Wirkstoffes, jedoch konnte diese Beobachtung im *ex-vivo*-Modell nicht aufrechterhalten werden. Über den gesamten Untersuchungszeitraum gewährleisteten die Polyplexe einen vollständigen Schutz des Wirkstoffes auf der Haut im Vergleich zum vollständig degradierten wässrigen Standard. Des Weiteren konnte ein schützender Effekt durch die SME selbst ausgeschlossen werden. Ohne die Polyplexe wurde der Wirkstoff in der SME rasch degradiert, da dieser in der äußeren wässrigen Phase der Emulsion vorlag und dadurch direkt mit der degradierenden Hautoberfläche in Kontakt stand. Erst durch die Wirkstoffkomplexierung zu Polyplexen erreicht der Wirkstoff einen effektiven Schutz, obwohl sich die Polyplexe immer noch in der äußeren Phase befinden. Folglich können die Chitosan-Polyplexe in jegliche wässrige Phase – auch weiterer Trägersysteme – eingearbeitet werden, solange keine Inkompatibilität vorliegt, welche die Komplexierung beeinträchtigt.

Nach erfolgreichem Schutz des Wirkstoffes auf der Haut kann dieser in die Haut penetrieren. In der Hautmatrix befinden sich endogene Polyelektrolyte, die durch komplementäre Verdrängung negativen Einfluss auf die Stabilität der Chitosan-Polyplexe nehmen können (Danielsen et al., 2005). Die Folge zeigte sich bei der Inkubation der Polyplexe mit menschlicher Vollhaut bei dem sich der ξ_{krit} von 1,1 auf 1,26 erhöhte. Befindet sich der Polyplex unbeschadet in die Haut, kann dieser in die Hautzellen aufgenommen werden. Bei der zellulären Aufnahme wird der Polyplex über das Endosom/Lysosom aufgenommen (Dass et al., 2002). Howell et al. beschreiben, dass die DNase II in diesen Zellkompartimenten die prädominante Desoxyribonuklease und der limitierende Engpass in der Zellaufnahme ist (Howell et al., 2003). Danach ist das DNAzym durch die Polyplexe auch auf zellulärer Ebene geschützt.

Penetration des Wirkstoffes

Die topische Applikation des Wirkstoffes und die damit benötigte Wirkstoffpenetration an den Zielort in der Haut stellt eine große Herausforderung an das dermale DDS. Der Erfolg der Penetration wird durch die Eigenschaften des Trägersystems, des Wirkstoffes und den Zustand der Haut bestimmt. In dieser Arbeit war nur das Trägersystem frei zu wählen, während der Zustand der Haut durch die Hauterkrankung und der Wirkstoff durch das Nutzen von DNAzymen festgelegt war. Insbesondere die

charakteristischen Eigenschaften der Wirkstoffgruppe, wie der geringe Octanol/Wasser-Verteilungskoeffizient, die negative Ladung und das hohe Molekulargewicht, sind für die Wirkstoffpenetration problematisch. Die Folge ist eine geringe Penetration des Wirkstoffes, sodass in den *ex-vivo*-Versuchen mit einem wässrigen Standard eine Wiederfindung in der Haut von lediglich 0,02 % nachgewiesen werden konnte. Die geringe Bioverfügbarkeit des Wirkstoffes wurde dabei sowohl durch die bereits beschriebene aktive Barriere als auch die passive Barriere der Haut negativ beeinflusst. Die passive Barriere stellt dabei die Hauptpermeabilitätsbarriere dar und wird hauptsächlich durch das Stratum corneum gebildet. Durch Abtragen des Stratum corneum und die damit einhergehende Schädigung der passiven Barriere wurde die Penetration des Wirkstoffes erhöht.

Die Ergebnisse belegen die Notwendigkeit, ein penetrationsförderndes Trägersystem zu entwickeln, welches die Wirkstoffpenetration auch in die intakte Haut fördert. In einem ersten Auswahlverfahren mittels *ex-vivo*-Hautmodellen wurden zwei potenzielle Trägersysteme identifiziert, die W/O/W-Emulsion und die SME. Die SME zeigte gegenüber dem Wirkstoff eine hohe penetrationsfördernde Wirkung, konnte jedoch keinen Schutz vor einer Degradierung gewährleisten. Demgegenüber hatte das komplexe System der W/O/W-Emulsion den Vorteil, den Wirkstoff in die innere wässrige Phase durch eine innere Ölphase einzuschließen. Allerdings wurde durch die Entwicklung der additiven Schutzsysteme in Form von Polyplexen sowohl der Schutz durch die komplexe W/O/W-Emulsion als auch das Hauptdefizit der SME obsolet. Folglich stellt die SME eine ideale Grundlage zur Entwicklung eines dermalen DDS dar und erfüllt zugleich die Zielsetzung der vorliegenden Arbeit sowohl eine einfache als auch umsetzbare Methode zu etablieren. Die SME ist allgemein ein zweiphasiges System mit einer dispersen Ölphase. Die Größe der Öltropfen befindet sich im Nanometerbereich und kann über den Hydrophilie-Lipophilie-Gleichgewicht-Wert (hydrophilic-lipophilic-balance, HLB-Wert) der Emulgatoren reguliert werden (Schmidts et al., 2012). Im idealen Verhältnis der emulgierenden Hilfsstoffe, am erforderlichen HLB-Wert (required HLB-Wert), weisen die Öltropfen die kleinste Größe auf. Die dadurch hergestellten unterschiedlichen Tropfengrößen der SME hatten weder einen Einfluss auf die Penetration des Wirkstoffes noch auf die Liberation des Wirkstoffes aus dem

Trägersystem. Die vergleichsweise schnelle Wirkstofffreisetzung aus der SME war durch die geringe Viskosität des Trägersystems und die Lokalisation des Wirkstoffes in der äußeren Phase begründet. Einzig der allgemein hohe Verteilungskoeffizient der SME wirkte sich negativ auf die Freisetzung aus.

Um die SME als Trägersystem zu nutzen, musste ein etwaiges mikrobielles Wachstum in dem Trägersystem unterbunden werden. Demzufolge wurden unterschiedliche Konservierungsmittel getestet und hinsichtlich ihrer konservierenden Eigenschaften sowie Kompatibilität gegenüber dem Trägersystem und dem Wirkstoff bewertet. Einzig Propylenglykol hielt allen drei Anforderungen stand. Alle übrigen Konservierungsmittel konnten im Konservierungsbelastungstest nicht bestehen. Die Benzoesäure zeigte zudem eine Inkompatibilität gegenüber dem Wirkstoff.

Die mittels Propylenglykol konservierte SME wurde mit den Chitosan-Polyplexen kombiniert, um ein protektives dermales DDS zu entwickeln. Der effektive Wirkstoffschutz durch die Kombination in den Degradierungsversuchen wurde bereits als eine der notwendigen Bedingung für ein DDS erörtert. Im Folgenden gilt es, die penetrationsfördernden Eigenschaften der SME im DDS als eine weitere Notwendigkeit zu diskutieren.

Da die gute Freisetzung der SME zu einer guten pharmazeutischen Verfügbarkeit an der Hautoberfläche führte, wurde eine steady-state-Phase schneller erreicht, in der kontinuierlich der Wirkstoff an die Haut freigesetzt wurde. Folglich erhöhte sich der Konzentrationsgradient zwischen Hautoberfläche und Stratum corneum und förderte dadurch die Penetration. Ebenfalls erhöhten die genutzten Polyplexe den Konzentrationsgradienten, indem diese den Wirkstoff auf der Hautoberfläche vor Degradierung schützten. Neben dem Konzentrationsgradienten hatten im Speziellen die Hilfsstoffe der SME einen positiven Einfluss auf die Penetration, indem sie den Diffusionskoeffizienten beeinflussten. Die ausgewählten Hilfsstoffe der SME verfügen über hautmodulierende Eigenschaften, welche die Wirkstoffpenetration fördern. Konkret sind die Hilfsstoffe in der Lage, die Eigenschaften des Stratum corneum durch Veränderungen der Lipidbereiche, Modifizierung der Proteinbestandteile sowie durch Beeinflussung der Wirkstoffverteilung zu verändern (Neubert et al., 2001). Die

penetrationsfördernden Hilfsstoffe der SME lassen sich in verschiedene Kategorien mit unterschiedlichen Effekten einteilen. So zählt der eingearbeitete Stearylalkohol zu den Fettalkoholen. Über langkettige Fettalkohole wurde berichtet, dass diese zur Lipidextraktion und zur Lipiddisruption im Stratum corneum führen (Dias et al., 2008; Kandimalla et al., 2010). Darüber hinaus kann der Stearylakohol auch als Co-Emulgator betrachtet werden und fällt zusätzlich in die Kategorie der nichtionischen Tenside. Zu dieser Gruppe gehören zudem die Emulgatoren Glycerolmonostearat, Ceteareth-20 und Laureth-9. Diese Gruppe zeichnet sich allgemein durch ein gering irritatives Potenzial im Vergleich zu ionischen Tensiden aus und erreicht seine penetrationsfördernden Eigenschaften durch die Adsorption an den Grenzflächen sowie die Disruption der Lipidschicht (Abraham, 1997; Park et al., 2000). Weitere Bestandteile der SME wie das Glycerol und das Propylenglykol zählen zu den mehrwertigen Alkoholen. Grundsätzlich werden diese als Cosolventien in Trägersystemen eingesetzt. Insbesondere für das Propylenglykol wird zusätzlich in der Literatur auf eine penetrationsfördernde Eigenschaft verwiesen. Danach soll der Wirkstoff durch den Lösungsmittelstrom des penetrierenden Propylenglykols mitgerissen werden. Dieser Effekt wird als konvektive Penetration (solvent drag) beschrieben (Herkenne et al., 2008). Die eingearbeiteten Triglyceride, das Oleyloleat sowie das Cetearyl-Isononanoat können in die Kategorie der Fettsäuren und Fettsäurederivate eingeordnet werden. Die Ölsäure des Oleyloleats erhöht beispielsweise die Fluidität der Lipide und erreicht dadurch eine verstärkte Penetration (Aungst, 1989; Golden et al., 1987). Zusätzlich kann es hydrophile Pools im Stratum corneum bilden, in denen es zu einer Bildung von einem Wirkstoffreservoir kommen kann (Ongpipattanakul et al., 1991).

Zusammenfassend zeigt die Auflistung, dass die SME aus einer Vielzahl von Hilfsstoffen mit penetrationsfördernden Effekten (chemical penetration enhancers) besteht, welche 47,5 % (v/w) der Formulierung ausmachen. Dadurch ist es zu erklären, dass eine vergleichsweise hohe Penetration gegenüber anderen Formulierungen erreicht werden konnte.

Verteilung und zellulärer Aufnahme des Wirkstoffes

Das Ziel des Wirkstofftransports bei der topischen Therapie von Hauterkrankungen befindet sich vorwiegend in den oberen Hautschichten. Um die Verteilung des Wirkstoffes in der Haut nach der Penetration zu überprüfen, wurde der Wirkstoff mit einem Fluoreszenzfarbstoff markiert und anhand des emittierenden Signals lokalisiert. Jedoch besitzt die Haut als biologische Matrix eine Autofluoreszenz, welche je nach Signal-to-Noise-Verhältnis die Messungen erheblich verfälschen kann (Schenke-Layland et al., 2006). Um dieses Problem zu adressieren, wurde eine Methode entwickelt, welche anhand des Emissionsspektrums zwischen dem Farbstoff und der Autofluoreszenz unterscheiden kann. Ein großer Vorteil dieser Methode ist die intensitätsunabhängige Identifizierung. Dadurch konnten sogar geringe Fluoreszenzsignale in der Haut ihrem Ursprung zugeteilt werden. Eine Limitierung erfährt die Methode dadurch, dass das Fluoreszenzsignal unabhängig von der Integrität des Wirkstoffes und folglich nicht direkt mit der Wirkstoffkonzentration gleichzusetzen ist. Hinsichtlich der Verteilung des Fluoreszenzsignals in der Haut konnte die Methode eindeutige Ergebnisse aufzeigen. Die SME erreichte eine hohe Akkumulation des spezifischen Fluoreszenzfarbstoffsignals in den oberen Hautschichten der intakten Haut, insbesondere im Stratum corneum. Das Stratum corneum bildete somit ein Wirkstoffreservoir, aus dem der Wirkstoff stetig in die Epidermis freigesetzt werden konnte. Die Einlagerung des Wirkstoffes in dem Stratum corneum ist dabei durch die bereits diskutierten Hilfsstoffe, wie das Oleyloleat, begründet. Die vergleichenden Trägersysteme, wie z. B. die W/O/W-Emulsion, konnten einen ähnlichen Effekt nicht aufzeigen. Wurde die passive Penetrationsbarriere durch das Abtragen des Stratum corneum geschwächt, verlor die SME im Gegensatz zu den anderen Trägersystemen an Penetrationseffizienz. Folglich adressiert die SME spezielle Hauterkrankungen, wie die aktinische Keratose, mit intakter Hautbarriere.

Nach erfolgreicher Penetration des Wirkstoffes durch das genutzte protektive dermale DDS verbleibt die zelluläre Aufnahme als letzte Hürde. Die Zielzellen des speziellen Wirkstoffes waren die Keratinozyten. Die Aufnahme und Verteilung des Wirkstoffes wurde erneut mit dem fluoreszenzmarkierten Wirkstoff überprüft. Es konnte nachgewiesen werden, dass ein Viertel der

HaCaT-Zellen ein Fluoreszenzsignal des Fluoreszenzmarkers aufwiesen. Das Fluoreszenzsignal konnte innerhalb der Zellen lokalisiert werden und bestätigt somit, dass der Wirkstoff in die Zelle aufgenommen wurde. Die signifikant höhere Aufnahmeeffizienz des Wirkstoffes im Vergleich zu dem wässrigen Standard wurde durch die Komplexierung mit dem Chitosan-Polymer zu Polyplexen erzielt. Als Polykation verfügt Chitosan über die Möglichkeit, die negative Ladung des DNAzyms ganz oder partiell zu überdecken. Dadurch wird die Wahrscheinlichkeit erhöht, die negativ geladene Zellmembran zu überwinden (Huang et al., 2004). Zudem wurde bewiesen, dass 12 % des aufgetragenen Wirkstoffes in der Zelle intakt vorlagen.

In Bezug auf die eingangs erläuterten Aspekte der Integrität, Penetration und zellulären Aufnahme des Wirkstoffes wird abschließend Folgendes festgehalten: In dem entwickelten protektiven DDS konnte durch das Nutzen von Chitosan-Polyplexen die Integrität und die zelluläre Aufnahme des DNAzymes sichergestellt werden. In Kombination mit der SME wurde eine erhöhte Penetration in die Haut erzielt. Zusammenfassend adressiert das protektive DDS erfolgreich alle drei von Zakrewsky et al. aufgestellten Hauptaspekte des Transports von Nukleinsäure in die Haut.

Zusammenfassung der Erkenntnisse

Die therapeutischen DNAzyme stellen als neue Wirkstoffgruppe einen vielversprechend Ansatz bei der Therapie von Hauterkrankungen dar. Derzeit sind fünf DNAzyme in der klinischen Wirkstoffprüfung von denen zukünftig wiederum zwei gegen Hauterkrankungen eingesetzt werden sollen. Für eine erfolgreiche Therapie muss der Wirkstoff an den Zielort in der Haut penetrieren und dort intakt vorliegen. Allerdings erschweren allgemein die Eigenschaften der Wirkstoffgruppe den Wirkstofftransport und den Erhalt der Wirkstoffintegrität. Zudem besitzt die Haut eine Barrierefunktion, die es zu überwinden gilt, um eine hohe Bioverfügbarkeit in den pathogen veränderten Hautzellen zu erreichen. Die Hautbarriere lässt sich in eine passive und aktive Barriere unterteilen. Während die aktive Barriere der Integrität des Wirkstoffes schadet, verhindert die passive Barriere die Wirkstoffdiffusion. In Bezug auf die aktive Barriere konnte nachgewiesen werden, dass das ungeschützte DNAzym auf der humanen Hautoberfläche durch DNase II degradiert wird. Durch eine Komplexierung mit Polykationen zu Polyplexen konnte der Wirkstoff auf der Haut geschützt werden. In Abhängigkeit der Eigenschaften des Polykations waren unterschiedliche ξ-Verhältnisse nötig, um den Schutz zu gewährleisten. Ein ξ-Verhältnis im Bereich von 1-2 und darüber hinaus im positiven Zeta-Potenzial erhöht die Chance auf einen ausreichenden Schutz. Als Polykationen eigneten sich insbesondere bioabbaubare Chitosan-Polymere, welche im Vergleich zu Polyethylenimin laut Literatur eine geringere Toxizität aufweisen. In Bezug auf die passive Hautbarriere konnte diese mittels Submicronemulsion (SME) überwunden werden. Selbst die größeren Polyplex-Partikel konnten durch die SME in die Haut penetrieren. Dabei erhöhten die Hilfsstoffe der SME die Penetration und erreichen eine Akkumulation des Wirkstoffes in dem Stratum corneum der intakten Haut. Somit stand das Stratum corneum als Wirkstoffreservoir zur Verfügung. Die Polyplexe wiederum erreichen auf zellulärer Ebene eine erhöhte Aufnahme des Wirkstoffes in HaCaT-Zellen. Die Kombination aus Chitosan-Polyplexen und SME führte zu dem Ergebnis eines protektiven dermalen DDS, das sowohl die Penetration als auch die Zellaufnahme fördert und darüber hinaus den Wirkstoff schützt.

Literaturverzeichnis

Abraham, W., 1997. Surfactant effects on skin barrier, in: Rieger, M.M., Rhein, L.D. (Eds.), Surfactants in cosmetics, 2nd ed., rev. and expanded ed. Marcel Dekker, New York, pp. 473–487.

Augustin, M., Herberger, K., Hintzen, S., Heigel, H., Franzke, N., Schäfer, I., 2011. Prevalence of skin lesions and need for treatment in a cohort of 90 880 workers. British Journal of Dermatology 165 (4), 865–873.

Aungst, B.J., 1989. Structure/effect studies of fatty acid isomers as skin penetration enhancers and skin irritants. Pharmaceutical research 6 (3), 244–247.

Bhindi, R., Fahmy, R.G., Lowe, H.C., Chesterman, C.N., Dass, C.R., Cairns, M.J., Saravolac, E.G., Sun, L.-Q., Khachigian, L.M., 2007. Brothers in arms: DNA enzymes, short interfering RNA, and the emerging wave of small-molecule nucleic acid-based gene-silencing strategies. The American journal of pathology 171 (4), 1079–1088.

Boussif, O., Lezoualc'h, F., Zanta, M.A., Mergny, M.D., Scherman, D., Demeneix, B., Behr, J.P., 1995. A versatile vector for gene and oligonucleotide transfer into cells in culture and in vivo: polyethylenimine. Proc. Natl. Acad. Sci. U.S.A. 92 (16), 7297–7301.

Cairns, M.J., Hopkins, T.M., Witherington, C., Wang, L., Sun, L.Q., 1999. Target site selection for an RNA-cleaving catalytic DNA. Nat. Biotechnol. 17 (5), 480–486.

Chan, M.P., Onji, M., Fukui, R., Kawane, K., Shibata, T., Saitoh, S.-i., Ohto, U., Shimizu, T., Barber, G.N., Miyake, K., 2015. DNase II-dependent DNA digestion is required for DNA sensing by TLR9. Nat Commun 6, 5853.

Cherepanova, A., Tamkovich, S., Pyshnyi, D., Kharkova, M., Vlassov, V., Laktionov, P., 2007. Immunochemical assay for deoxyribonuclease activity in body fluids. J Immunol Methods 325 (1-2), 96–103.

Danielsen, S., Strand, S., Lange Davies, C. de, Stokke, B.T., 2005. Glycosaminoglycan destabilization of DNA-chitosan polyplexes for gene delivery depends on chitosan chain length and GAG properties. Biochimica et biophysica acta 1721 (1-3), 44–54.

Dass, C.R., Saravolac, E.G., Li, Y., Sun, L.-Q., 2002. Cellular Uptake, Distribution, and Stability of 10-23 Deoxyribozymes. Antisense and Nucleic Acid Drug Development 12 (5), 289–299.

Dautzenberg, H., Jaeger, W., 2002. Effect of charge density on the formation and salt stability of polyelectrolyte complexes. Macromol Chem Phys 203 (14), 2095–2102.

Dias, M., Naik, A., Guy, R.H., Hadgraft, J., Lane, M.E., 2008. In vivo infrared spectroscopy studies of alkanol effects on human skin. European journal of pharmaceutics and biopharmaceutics : official journal of Arbeitsgemeinschaft für Pharmazeutische Verfahrenstechnik e.V 69 (3), 1171–1175.

Eckhart, L., Fischer, H., Tschachler, E., 2012. Mechanisms and emerging functions of DNA degradation in the epidermis. Front Biosci (Landmark Ed) 17, 2461–2475.

Elias, P.M., 1983. Epidermal lipids, barrier function, and desquamation. The Journal of investigative dermatology 80 Suppl, 44s–49.
European Union, 2016. Eurostat: Population on 1 January by broad age group and sex. http://appsso.eurostat.ec.europa.eu/nui/submitViewTableAction.do. Accessed 10 Mai 2016.
Fellmann, C., Lowe, S.W., 2014. Stable RNA interference rules for silencing. Nature cell biology 16 (1), 10–18.
Fischer, H., Scherz, J., Szabo, S., Mildner, M., Benarafa, C., Torriglia, A., Tschachler, E., Eckhart, L., 2011. DNase 2 is the main DNA-degrading enzyme of the stratum corneum. PLoS ONE 6 (3), e17581.
Fluiter, K., Frieden, M., Vreijling, J., Koch, T., Baas, F., 2005. Evaluation of LNA-modified DNAzymes targeting a single nucleotide polymorphism in the large subunit of RNA polymerase II. Oligonucleotides 15 (4), 246–254.
Gallo, R.L., Nakatsuji, T., 2011. Microbial symbiosis with the innate immune defense system of the skin. J. Invest. Dermatol. 131 (10), 1974–1980.
Golden, G.M., McKie, J.E., Potts, R.O., 1987. Role of stratum corneum lipid fluidity in transdermal drug flux. Journal of pharmaceutical sciences 76 (1), 25–28.
Harosh, I., Binninger, D.M., Harris, P.V., Mezzina, M., Boyd, J.B., 1991. Mechanism of action of deoxyribonuclease II from human lymphoblasts. Eur. J. Biochem. 202 (2), 479–484.
Herkenne, C., Naik, A., Kalia, Y.N., Hadgraft, J., Guy, R.H., 2008. Effect of propylene glycol on ibuprofen absorption into human skin in vivo. Journal of pharmaceutical sciences 97 (1), 185–197.
Howell, D.P.-G., Krieser, R.J., Eastman, A., Barry, M.A., 2003. Deoxyribonuclease II is a lysosomal barrier to transfection. Mol. Ther. 8 (6), 957–963.
Huang, M., Khor, E., Lim, L.-Y., 2004. Uptake and cytotoxicity of chitosan molecules and nanoparticles: effects of molecular weight and degree of deacetylation. Pharmaceutical research 21 (2), 344–353.
Kandimalla, K.K., Babu, R.J., Singh, M., 2010. Biphasic flux profiles of melatonin: the Yin-Yang of transdermal permeation enhancement mediated by fatty alcohol enhancers. Journal of pharmaceutical sciences 99 (1), 209–218.
Kawakami, S., Ito, Y., Charoensit, P., Yamashita, F., Hashida, M., 2006. Evaluation of proinflammatory cytokine production induced by linear and branched polyethylenimine/plasmid DNA complexes in mice. J. Pharmacol. Exp. Ther. 317 (3), 1382–1390.
Kean, T., Thanou, M., 2010. Biodegradation, biodistribution and toxicity of chitosan. Adv. Drug Deliv. Rev. 62 (1), 3–11.
Kole, R., Krainer, A.R., Altman, S., 2012. RNA therapeutics: beyond RNA interference and antisense oligonucleotides. Nature reviews. Drug discovery 11 (2), 125–140.

Larson, S.D., Jackson, L.N., Chen, L.A., Rychahou, P.G., Evers, B.M., 2007. Effectiveness of siRNA uptake in target tissues by various delivery methods. Surgery 142 (2), 262–269.

Lindahl, T., 1993. Instability and decay of the primary structure of DNA. Nature 362 (6422), 709–715.

Liu, W., Sun, S., Cao, Z., Zhang, X., Yao, K., Lu, W.W., Luk, K D K, 2005. An investigation on the physicochemical properties of chitosan/DNA polyelectrolyte complexes. Biomaterials 26 (15), 2705–2711.

Liu, X., Howard, K.A., Dong, M., Andersen, M.Ø., Rahbek, U.L., Johnsen, M.G., Hansen, O.C., Besenbacher, F., Kjems, J., 2007. The influence of polymeric properties on chitosan/siRNA nanoparticle formulation and gene silencing. Biomaterials 28 (6), 1280–1288.

Marks, R., Foley, P., Goodman, G., Hage, B.H., Selwood, T.S., 1986. Spontaneous remission of solar keratoses: the case for conservative management. The British journal of dermatology 115 (6), 649–655.

Naik, S., Bouladoux, N., Wilhelm, C., Molloy, M.J., Salcedo, R., Kastenmuller, W., Deming, C., Quinones, M., Koo, L., Conlan, S., Spencer, S., Hall, J.A., Dzutsev, A., Kong, H., Campbell, D.J., Trinchieri, G., Segre, J.A., Belkaid, Y., 2012. Compartmentalized Control of Skin Immunity by Resident Commensals. Science 337 (6098), 1115–1119.

Neubert, R., Marsch, W., Wohlrab, W.A., 2001. Dermatopharmazie: Vehikel - Wirkstoffe - Pharmakologie ; mit 29 Tabellen. Wiss. Verl.-Ges, Stuttgart, XI, 178 S.

Nomura, T., Nakajima, H., Hongyo, T., Taniguchi, E., Fukuda, K., Li, L.Y., Kurooka, M., Sutoh, K., Hande, P.M., Kawaguchi, T., Ueda, M., Takatera, H., 1997. Induction of cancer, actinic keratosis, and specific p53 mutations by UVB light in human skin maintained in severe combined immunodeficient mice. Cancer research 57 (11), 2081–2084.

Ohkouchi, S., Shibata, M., Sasaki, M., Koike, M., Safig, P., Peters, C., Nagata, S., Uchiyama, Y., 2013. Biogenesis and proteolytic processing of lysosomal DNase II. PloS one 8 (3), e59148.

Ongpipattanakul, B., Burnette, R.R., Potts, R.O., Francoeur, M.L., 1991. Evidence that oleic acid exists in a separate phase within stratum corneum lipids. Pharm. Res. 8 (3), 350–354.

Park, E.S., Chang, S.Y., Hahn, M., Chi, S.C., 2000. Enhancing effect of polyoxyethylene alkyl ethers on the skin permeation of ibuprofen. Int J Pharm 209 (1-2), 109–119.

Parra, D., Manils, J., Castellana, B., Viña-Vilaseca, A., Morán-Salvador, E., Vázquez-Villoldo, N., Tarancón, G., Borràs, M., Sancho, S., Benito, C., Ortega, S., Soler, C., 2009. Increased Susceptibility to Skin Carcinogenesis in TREX2 Knockout Mice. Cancer Res. 69 (16), 6676–6684.

Patnaik, S., Gupta, K.C., 2013. Novel polyethylenimine-derived nanoparticles for in vivo gene delivery. Expert Opin Drug Deliv 10 (2), 215–228.

Pogocki, D., Schöneich, C., 2000. Chemical stability of nucleic acid-derived drugs. Journal of pharmaceutical sciences 89 (4), 443–456.

Proksch, E., Brandner, J.M., Jensen, J.-M., 2008. The skin: an indispensable barrier. Experimental dermatology 17 (12), 1063–1072.
Rockwell, P., O'Connor, W.J., King, K., Goldstein, N.I., Zhang, L.M., Stein, C.A., 1997. Cell-surface perturbations of the epidermal growth factor and vascular endothelial growth factor receptors by phosphorothioate oligodeoxynucleotides. Proceedings of the National Academy of Sciences of the United States of America 94 (12), 6523–6528.
Roewert-Huber, J., Stockfleth, E., Kerl, H., 2007. Pathology and pathobiology of actinic (solar) keratosis - an update. The British journal of dermatology 157 Suppl 2, 18–20.
Rudzinski, W.E., Aminabhavi, T.M., 2010. Chitosan as a carrier for targeted delivery of small interfering RNA. Int J Pharm 399 (1-2), 1–11.
Sanford, J.A., Gallo, R.L., 2013. Functions of the skin microbiota in health and disease. Semin. Immunol. 25 (5), 370–377.
Santoro, S.W., Joyce, G.F., 1997. A general purpose RNA-cleaving DNA enzyme. Proc. Natl. Acad. Sci. U.S.A. 94 (9), 4262–4266.
Santoro, S.W., Joyce, G.F., 1998. Mechanism and utility of an RNA-cleaving DNA enzyme. Biochemistry 37 (38), 13330–13342.
Schenke-Layland, K., Riemann, I., Damour, O., Stock, U.A., König, K., 2006. Two-photon microscopes and in vivo multiphoton tomographs--powerful diagnostic tools for tissue engineering and drug delivery. Advanced drug delivery reviews 58 (7), 878–896.
Scheuplein, R.J., Blank, I.H., 1971. Permeability of the skin. Physiological reviews 51 (4), 702–747.
Schmidts, T., Dobler, D., von den Hoff, Sylvia, Schlupp, P., Garn, H., Runkel, F., 2011. Protective effect of drug delivery systems against the enzymatic degradation of dermally applied DNAzyme. Int J Pharm 410 (1-2), 75–82.
Schmidts, T., Schlupp, P., Gross, A., Dobler, D., Runkel, F., 2012. Required HLB Determination of Some Pharmaceutical Oils in Submicron Emulsions. Journal of Dispersion Science and Technology 33 (6), 816–820.
Takei, Y., Kadomatsu, K., Itoh, H., Sato, W., Nakazawa, K., Kubota, S., Muramatsu, T., 2002. 5'-,3'-inverted thymidine-modified antisense oligodeoxynucleotide targeting midkine. Its design and application for cancer therapy. The Journal of biological chemistry 277 (26), 23800–23806.
Werner, R.N., Stockfleth, E., Connolly, S.M., Correia, O., Erdmann, R., Foley, P., Gupta, A.K., Jacobs, A., Kerl, H., Lim, H.W., Martin, G., Paquet, M., Pariser, D.M., Rosumeck, S., Röwert-Huber, H.-J., Sahota, A., Sangueza, O.P., Shumack, S., Sporbeck, B., Swanson, N.A., Torezan, L., Nast, A., 2015. Evidence- and consensus-based (S3) Guidelines for the Treatment of Actinic Keratosis - International League of Dermatological Societies in cooperation with the European Dermatology Forum - Short version. Journal of the European Academy of Dermatology and Venereology : JEADV 29 (11), 2069–2079.

Wertz, P.W., Swartzendruber, D.C., Kitko, D.J., Madison, K.C., Downing, D.T., 1989. The role of the corneocyte lipid envelopes in cohesion of the stratum corneum. The Journal of investigative dermatology 93 (1), 169–172.
Xu, X., Khan, M.A., Burgess, D.J., 2012. Predicting hydrophilic drug encapsulation inside unilamellar liposomes. Int J Pharm 423 (2), 410–418.
Zakrewsky, M., Kumar, S., Mitragotri, S., 2015. Nucleic acid delivery into skin for the treatment of skin disease: Proofs-of-concept, potential impact, and remaining challenges. Journal of controlled release : official journal of the Controlled Release Society 219, 445–456.
Zhang, G., Luo, X., Sumithran, E., Pua, V.S.C., Barnetson, R.S.C., Halliday, G.M., Khachigian, L.M., 2006. Squamous cell carcinoma growth in mice and in culture is regulated by c-Jun and its control of matrix metalloproteinase-2 and -9 expression. Oncogene 25 (55), 7260–7266.

Erklärung über Anteil an Publikationen

I. Schmidts, Thomas; Marquardt, Kay; Schlupp, Peggy; Dobler, Dorota; Heinz, Florian; Mäder, Ulf et al. (2012): Development of drug delivery systems for the dermal application of therapeutic DNAzymes. In: *International Journal Pharmaceutics* 431 (1-2), S. 61–69.

Beitrag 20%: Teilweise Durchführung der Experimente. Teilweise Analyse und Diskussion der Daten. Teilweise Verfassen des Manuskripts. Die internationale, peer-reviewed Fachzeitschrift hatte im Jahr 2012 einen 5 Jahres Impactfaktor von 4,011 und ist im SCImago Journal Ranking in der Kategorie „Pharmaceutical Science“ auf Platz 14 von 198 Fachzeitschriften gelistet.

II. Marquardt, Kay; Eicher, Anna-Carola; Dobler, Dorota; Höfer, Frank; Mäder, Ulf; Schmidts, Thomas; Renz, Harald; Runkel, Frank (2016): Degradation and protection of DNAzymes on human skin. In: *European Journal of Pharmaceutics and Biopharmaceutics* 107, S. 80–87.

Beitrag 70%: Design und Durchführung der Experimente. Analyse und Diskussion der Daten. Selbstständiges Verfassen des Manuskripts. Die internationale, peer-reviewed Fachzeitschrift hatte im Jahr 2014 einen 5 Jahres Impactfaktor von 4,394 und ist im SCImago Journal Ranking in der Kategorie „Pharmaceutical Science“ auf Platz 9 von 200 Fachzeitschriften gelistet.

III. Maeder, Ulf; Marquardt, Kay; Beer, Sebastian; Bergmann, Thorsten; Schmidts, Thomas; Heverhagen, Johannes T. et al. (2012): Evaluation and quantification of spectral information in tissue by confocal microscopy. In: *Journal of Biomedical Optics* 17 (10), S. 106011.

Beitrag 20%: Teilweise Design und Durchführung der Experimente. Teilweise Analyse und Diskussion der Daten. Teilweise Verfassen des Manuskripts. Die internationale, peer-reviewed Fachzeitschrift hatte im Jahr 2012 einen 5 Jahres Impactfaktor von 2,926 und ist im SCImago Journal Ranking in der Kategorie „Biomaterials“ auf Platz 16 von 62 Fachzeitschriften gelistet.

IV. Marquardt, Kay; Eicher, Anna-Carola; Dobler, Dorota; Mäder, Ulf; Schmidts, Thomas; Renz, Harald; Runkel, Frank (2014): Development of a protective dermal drug delivery system for therapeutic DNAzymes. In: *International Journal Pharmaceutics* 479 (1), S. 150–158.

Beitrag 70%: Design und Durchführung der Experimente. Analyse und Diskussion der Daten. Selbstständiges Verfassen des Manuskripts. Die internationale, peer-reviewed Fachzeitschrift hatte im Jahr 2014 einen 5 Jahres Impactfaktor von 4,011 und ist im SCImago Journal Ranking in der Kategorie „Pharmaceutical Science“ auf Platz 13 von 200 Fachzeitschriften gelistet.

Ausgewählte Publikationen

I. Development of drug delivery systems for the dermal application of therapeutic DNAzymes. In: *International Journal Pharmaceutics* 431 (1-2), S. 61–69.

International Journal of Pharmaceutics 431 (2012) 61–69

Contents lists available at SciVerse ScienceDirect

International Journal of Pharmaceutics

journal homepage: www.elsevier.com/locate/ijpharm

Development of drug delivery systems for the dermal application of therapeutic DNAzymes

Thomas Schmidts[a], Kay Marquardt[a], Peggy Schlupp[a], Dorota Dobler[a], Florian Heinz[a], Ulf Mäder[b], Holger Garn[c], Harald Renz[d], Jana Zeitvogel[e], Thomas Werfel[e], Frank Runkel[a,*]

[a] Institute of Bioprocess Engineering and Pharmaceutical Technology, Technische Hochschule Mittelhessen – University of Applied Science, Giessen, Germany
[b] Institute of Medical Physics and Radiation Protection, Technische Hochschule Mittelhessen – University of Applied Science, Giessen, Germany
[c] Sterna Biologicals GmbH & Co. KG, Biomedical Research Center, Marburg, Germany
[d] Institute of Laboratory Medicine, Philipps University, Marburg, Germany
[e] Department of Dermatology, Allergy and Venereology, Division for Immunodermatology and Allergy Research, Hannover Medical School, Germany

ARTICLE INFO

Article history:
Received 21 December 2011
Received in revised form 5 April 2012
Accepted 8 April 2012
Available online 15 April 2012

Keywords:
DNAzyme
Oligonucleotides
W/O/W multiple emulsion
Submicron emulsion
Skin penetration

ABSTRACT

DNAzymes are potent novel drugs for the treatment of inflammatory diseases such as atopic dermatitis. DNAzymes represent a novel class of pharmaceuticals that fulfil a causal therapy by interruption of the inflammation cascade at its origin. There are two challenges regarding the dermal application of DNAzymes: the large molecular weight and the sensitivity to DNases as part of the natural skin flora. To overcome these limitations suitable carrier systems have to be considered. Nano-sized drug carrier systems (submicron emulsions, microemulsions) are known to improve the skin uptake of drugs due to their ability to interact with the skin's lipids. To protect the drug against degradation, the hydrophilic drug may be incorporated into the inner aqueous phase of carrier systems, such as water-in-oil-in-water multiple emulsions. In the present study various emulsions of pharmaceutical grade were produced. Their physicochemical properties were determined and the influence of preservation systems on stability was tested. Drug release and skin uptake studies using various skin conditions and experimental set-ups were conducted. Furthermore, cellular uptake was determined by flow cytometric analysis. The investigations revealed that the developed multiple emulsion is a suitable and promising drug carrier system for the topical application of DNAzyme.

1. Introduction

Chronic inflammatory diseases of the skin such as atopic dermatitis are increasingly prevalent worldwide mainly in industrialised countries. They represent complex skin disorders that develop on the basis of a genetic predisposition under the influence of certain environmental factors. The current understanding is that immunological mechanisms are mainly involved in the pathology of these diseases with activation of different T cell subpopulations selectively contributing to the development of either disease or a disease state (Leung, 2000; Leung and Soter, 2001). In atopic dermatitis, the immune hypothesis invokes an imbalance in the T lymphocytes, with Th2 cells predominating in the acute phase; this results, among other things, in the cytokine production of various interleukins such as IL-4, IL-5, IL-12 and IL-13 (Garlisi et al., 1995; Grünig et al., 1998; Maggi, 1998). Therefore, most current therapies are still based on general anti-inflammatory drugs that may reduce symptoms without directly interfering with the disease-causing mechanisms. Novel concepts for approaches include the use of antisense-based molecules such as antisense DNA, DNAzymes, small interfering RNA (siRNA) and ribozymes that interfere with the mRNA of proteins that are involved in the pathogenesis of the respective disease (Kim et al., 2009). DNAzymes represent a novel class of antisense molecules that have not yet been established for the treatment of any human disease. 10–23 DNAzymes are a group of RNA-cleaving DNA molecules that contain a catalytic domain (Cieslak et al., 2003; Silverman, 2005; Tritz et al., 2005) and cleave the RNA sequence at a phosphodiester bond between an unpaired purine and a paired pyrimidine residue (Santoro and Joyce, 1998). 10–23 DNAzymes targeting GATA-3 mRNA have recently been developed, and their anti-asthmatic effect in mouse models has been successfully demonstrated (Sel et al., 2008). As GATA-3 plays a central role in Th2 cell differentiation (Barnes, 2008) and in promoting Th2 responses (Zhu et al., 2006), similar results are expected for the treatment of inflammatory skin diseases with the mRNA-cleaving GATA-3 10–23 DNAzyme. Therefore, this oligonucleotide model was chosen as a promising API candidate for the treatment of

* Corresponding author. Tel.: +49 0 641 309 2550; fax: +49 0 641 309 2553.
E-mail address: Frank.Runkel@kmub.thm.de (F. Runkel).

0378-5173/$ – see front matter © 2012 Elsevier B.V. All rights reserved.
http://dx.doi.org/10.1016/j.ijpharm.2012.04.034

atopic dermatitis. For the effective treatment of atopic dermatitis, it is necessary to transport the oligonucleotide into the epidermis and to the inflammatory infiltrate. However, the topical application of such molecules is still challenging owing to their limited bioavailability, which is due to several reasons (Akhtar et al., 2000). For example, penetration into the skin compartments is often restricted due to the rather large size of these molecules, which often exceeds 10 kDa. In addition, as a result of size and chemical composition, oligonucleotide molecules are generally not easily taken up by cells; thus the transfection efficiency of target cells in the skin is often low (Bally et al., 1999). Moreover, oligonucleotide-degrading enzymes such as RNases and DNases may destroy the integrity of such molecules before they come into contact with their target structures. DNA-cleaving enzymes might be located on both the skin and in skin tissue. The deoxynucleases on the skin are mainly produced by several microorganisms, which belong to the natural skin flora such as Staphylococcus (Langlois et al., 1989; Wierup, 1978). Drug carrier systems for topical application of such sensitive and large DNA molecules pursue improvement of skin uptake and protection against degradation. Therefore, different systems were evaluated. With regard to the encapsulation properties of DNAzymes, systems with an inner water phase (water-in-oil (W/O) emulsion and water-in-oil-in-water (W/O/W) emulsion) were chosen as appropriate candidates. With respect to their excellent transport properties, a microemulsion and a submicron emulsion with hydrophilic DNAzymes located in the outer water phase were chosen. Due to their distinct structure and properties, multiple emulsions are of particular interest for several drug delivery approaches, including the dermal application of encapsulated drugs in pharmaceutical products (Fukushima et al., 1987; Khopade and Jain, 1999; Lindenstruth and Müller, 2004; Schmidts et al., 2010). Microemulsion (ME) and submicron emulsion (SME) represent carrier systems below one micrometre in size and allow improved drug penetration and permeation into the skin compared to conventional formulations (Bouchemal et al., 2004; Delgado-Charro et al., 1997; Djekic and Primorac, 2008; Kanikkannan and Singh, 2002; Schmalfuß et al., 1997).

In the present study, a W/O/W emulsion, a W/O emulsion, an SME and an ME were produced, their physicochemical properties were determined over time and the formulations were tested for sufficient preservation. Furthermore, drug release and skin uptake studies using various skin conditions and experimental set-ups were conducted and were analysed by HPLC, hybridisation-ELISA and fluorescence microscopy. Finally, a W/O/W emulsion and a SME were compared regarding celluar uptake of the drug by flow cytometric analysis.

2. Materials and methods

2.1. Materials

All ingredients were obtained in pharmaceutical grade. Light and heavy paraffin oil, isopropyl palmitate, sodium chloride (NaCl), magnesium sulphate heptahydrate ($MgSO_4$), propylene glycol, glycerol 85%, potassium sorbate, citric acid, butylene glycol, propyl-4-hydroxybenzoate and hydrophobic basis gel (DAC) were supplied by Fagron (Germany). Cetostearyl isononanoate and Coco-Caprylate/Caprate were provided by Cognis (Germany). Ethyl Oleate, Sorbitan Oleate (Span®80), Oleth-5, Oleth-10 and Steareth-20 were provided by Croda (Germany). Soy lecithin, methyl-4-hydroxybenzoate and triglycerol diisostearate were purchased from Caelo (Germany). Caprylocaproyl macrogol-8-glycerides (Labrasol®) and Polyglyceryl-6-dioleate (Plurol Oleique®) were obtained from Gattefossé (France). Acrylamide/Sodium acryloyldimethyl Taurate Copolymer/Isohexadecane/Polysorbate®80 (Sepineo®P600) was obtained from Seppic (Germany). Methanol (gradient grade), water (gradient grade), sulphuric acid, ethylenediamine tetra-acetic acid (EDTA) and sodium hydroxide (NaOH) were obtained from VWR (Germany). Benzoic acid was obtained from Euro OTC Pharma (Germany), and the Phenoxyethanol was from Th. Geyer (Germany). An unlabelled and a 6-carboxyfluorescein (FAM) labelled 10–23 DNAzyme was provided by Sterna Biologicals (Germany) representing the sodium salt of DNAzyme, a single-stranded DNA molecule composed of 34 deoxynucleotide bases with a molecular weight of 10.6 kDa (unlabelled). UltraPure™ Tris Hydrochloride (Tris–HCl) was supplied by Invitrogen (Germany). NaCl and magnesium chloride ($MgCl_2$), both nuclease-free, were obtained from Applied Biosystems (Germany). Polysorbate 20 (Tween®20) and Sodium dodecyl sulphate ultra-pure (SDS) were purchased from Carl Roth (Germany). Trizma® hydrochloride and Trizma® base were supplied by Sigma–Aldrich (Germany). Oligonucleotide probes labelled with either digoxigenin or biotin were synthesised by Operon (Germany). Anti-digoxigenin-peroxidase and BM Blue POD substrate were supplied by Roche Diagnostics (Germany). Phosphate buffered saline (PBS) without Mg^{2+} and Ca^{2+} was supplied by Biochrom AG (Germany), and proteinase K was purchased from Qiagen (Germany). Dispase II was obtained from Roche Molecular Biochemicals (Germany). Trypsin/EDTA and Trypsin Inhibitor were both supplied by Pan (Germany). Collagenase was purchased from Worthington Biochemical Corporation (USA) and Hyaluronidase from Sigma–Aldrich.

2.2. Preparation of delivery systems

DNAzyme was added to the water phase of the formulations. Regarding the multiple emulsion, DNAzyme was added to the inner water phase at a total quantity of 0.4 wt%. For skin penetration studies, 10% of the DNAzyme was replaced by *the fluorescent labelled* FAM-DNAzyme.

W/O emulsions were prepared at room temperature. The water phase (5 wt% glycerol, 0.3 wt% $MgSO_4$, 0.14 wt% potassium sorbate, 0.07 wt% citric acid and 63.9 wt% distilled water) was added slowly to the oil phase (3.0 wt% triglycerol diisostearate, 1.2 wt% isopropyl palmitate, 1.2 wt% Cetostearyl Isononanoate, 0.2 wt% soy lecithin and 24.6 wt% hydrophobic basis gel) and stirred with a mortar and pestle until a homogeneous emulsion was obtained.

W/O/W emulsions were prepared using a 2-step procedure previously reported by Matsumoto et al. (Matsumoto et al., 1976). First, the primary W/O emulsion was produced. Second, the obtained primary emulsion (40.0 wt%) was dispersed in the aqueous phase containing the hydrophilic emulsifier. In detail, the simple W/O emulsions were produced by adding the aqueous phase (0.065 M $MgSO_4$ solution containing the DNAzyme) to the oil phase (15.8 wt% heavy paraffin oil, 4.0 wt% Sorbitan oleate and 0.2 wt% soy lecithin) followed by a homogenisation step using a rotor-stator homogeniser (Diax 600, Heidolph, Germany) for 2 min at 9500 rpm. Next the chilled primary emulsion was slowly added to the outer water phase (1.0 wt% Steareth-20 and 58.7 wt% preserved water) under stirring at 1200 rpm using a EUROSTAR digital stirrer (IKA, Germany) at room temperature. Finally, 0.3 wt% Sepineo®P600 was added as thickening agent under gentle stirring.

An ME was obtained by gently mixing the appropriate quantities of the components plus the DNAzyme at room temperature. The oil phase consisted of 7.20 wt% Labrasol®, 4.80 wt% Plurol Oleique®, 2.50 wt% cetostearyl isononanoate and 2.50 wt% isopropyl palmitate. The water phase consisted of 2.49 wt% glycerol, 16.60 wt% propylene glycol, 0.30 wt% $MgSO_4$ and 63.21 wt% distilled water.

SMEs were prepared as followed. The water phase (a blend of Oleth-3 and Oleth-10 in total 6.0 wt%, 3.0 wt% glycerol, 0.3 wt%

$MgSO_4$ and 75.3 wt% preserved water) and oil phase (5.0 wt% Coco-Caprylate/Caprate, 5.0 wt% cetearyl isononanoate, 5.0 wt% Ethyl oleate) were heated separately to 70 °C. The two phases were then combined and homogenised for 1 min using a rotor/stator homogeniser at 24,000 rpm. Three different SMEs were produced with HLB values of 10, 11 and 12. Oleth-3 and Oleth-10 were used to adjust the HLB value.

2.3. Characterisation of the drug delivery systems

Droplet size analysis was performed with respect to the requirements of the samples. The mean droplet sizes (*z*-Average) of W/O emulsion and ME were determined by dynamic light scattering (High Performance Particle Sizer, Malvern Instruments, UK). W/O emulsions were diluted 1:1000 with light paraffin oil (viscosity: 33 mPa s) prior to measurement, while the MEs were measured undiluted. The droplet sizes of the multiple W/O/W emulsions and the SMEs were determined by laser diffraction (Mastersizer S, Malvern Instruments, UK). The results are presented as the mean diameter $D(v,0.5)$ based on the volume distribution. Determination of the viscosity was performed at 25 °C using the RheoStress 300 Rheometer (ThermoHaake, Germany) with a cone and plate geometry of 20 mm in diameter and a 2° angle. The apparent viscosity was measured over a shear rate of 0.1–100 s^{-1} and presented as the mean value ($n = 3$). All of the above mentioned parameters were recorded over a period of 3 months.

2.4. Preservative efficacy test

Preservative efficacy tests were performed according to the European Pharmacopoeia (2008) using the microbial strains: *Staphylococcus aureus*, *Escherichia coli*, *Pseudomonas aeruginosa*, *Candida albicans* and *Aspergillus niger*. The microbial impurities were determined after storage at 25 °C for one week. Preservative efficiency test was considered a success when the count of bacteria is reduced within one week by more than 99.9% and fungus by more than 99.0%.

2.5. Drug release studies

The DNAzyme release from the drug delivery systems was studied using the Franz diffusion cell set-up (surface area 1.76 cm^2 and 12 mL acceptor volume) (Gauer Glas, Germany). A pre-soaked mixed cellulose ester membrane (pore size 0.2 μm, Ø 25 mm, Whatman, Germany) was placed between the donor and receptor compartment. The acceptor medium (distilled water) was continuously stirred (500 rpm) and the temperature was maintained at 32.5 °C. After equilibration (30 min), 500 μL of the investigated formulation was applied on the top side of the membrane and the released DNAzyme was monitored by collecting samples (300 μL) of the acceptor fluid at different time points. Sampling time was adjusted for every formulation. The samples were analysed by hybridization-Enzyme Linked Immunosorbent Assay (ELISA). All experiments were repeated three times and are presented as the mean value ± SD.

2.6. Skin penetration studies

DNAzyme skin uptake studies were performed in vitro using the Franz diffusion cell set-up (OECD, 2004a,b). Porcine skin was chosen due to its similarity to human skin in terms of its morphology and permeability characteristics (Diembeck et al., 1999) and due to its availability. Therefore, untreated porcine ears (domestic pig) were obtained directly from a local slaughterhouse, and immediately transferred to the lab under cool conditions. Porcine ears were washed by rinsing with mildly warm water and wiped with paper towels, and the bristles were carefully shortened by trimming. Full thickness porcine skin was either used immediately (fresh skin) or stored at −20 °C (frozen skin; up to 6 months) and thawed prior to use in experiments. Untreated skin (intact skin) and skin with an impaired barrier were used to conduct skin uptake studies. To simulate the impaired barrier of atopic dermatitis skin, the porcine skin underwent a tape stripping procedure following Simonsen and Fullerton (2007), which was controlled by transepidermal water loss (TEWL) measurements. On the day of the experiment, the prepared skin samples were mounted into the Franz diffusion cell with PBS as the acceptor fluid and equilibrated for 30 min at 32.5 °C. Then, the investigated formulations were evenly applied as either an infinite dose (500 μL) or a finite dose (20 μL) onto the skin surface for 24 h. To mimic potential human exposure, the finite dose was applied and gently massaged for 1 min. At the end of the experiment, any remaining formulation was removed by a wash-off procedure. Skin samples were analysed by hybridisation-ELISA and fluorescence microscopy. Skin sections for the fluorescence microscope analysis were stamped out, shock frozen and stored at −20 °C. The remaining parts were reduced to small pieces and covered with lysis buffer (50 mM Tris–HCl, 25 mM EDTA, 100 mM NaCl, 0.5% SDS) plus proteinase K overnight. The samples were then centrifuged, and the supernatant was used to conduct hybridisation-ELISA. All experiments were repeated three times and are presented as the mean value ± SD.

2.7. Cellular uptake of DNAzymes

Fluorescence activated cell sorter (FACS, Calibur, BD Bioscience, Germany) was used to determine the cellular uptake of the FAM-DNAzyme. Skin penetration studies (finite dose experimental set up, chapter 2.6) were conducted and the total amount of DNAzyme was replaced by FAM-DNAzyme. At the end of the experiment, cells were isolated out of the epidermis and measured by FACS. Therefore, punch biopsies (4 mm) were taken, and incubated over night at 4 °C in 1 mL Dispase II (2.4 U/mL). Subsequently, the epidermis was taken-off the dermis and incubated for 5 min at 37 °C in 1 mL Trypsin (0.05%)/EDTA (0.02%). The enzymatic digestion was stopped by adding the same amount of Trypsin Inhibitor to the epidermis. To obtain a single cell suspension, cells were separated by using a cell strainer (40 μm). After two additional wash steps with PBS cells were measured by FACS and analysed using Cell QuestPro software (BD Bioscience). Results are presented as geometric mean value (GeoMean), representing the mean value of the total fluorescence of the cell population, and percentage of FAM-DNAzyme positive cells (%pos). Therefore, the threshold values were adjusted in order to obtain low values of skin cells treated with the placebo formulations.

2.8. Fluorescence microscopy analysis

For fluorescence microscopy analysis, 10-μm-thick cryosections were prepared with the Leica CM 1850UV (Leica, Germany). Slices were analysed using the fluorescence microscope DMI 6000B (Leica, Germany) with the L5 filter cube. The fluorescent pictures analysis is based on summing the pixel intensity values (total intensity) and counting the number of the summed pixels. Then the total intensity is normalised to the number of the included pixels representing the intensity per pixel for the given image; at least 15 images were analysed for each sample, and values are presented as the mean ± SD.

2.9. DNase activity assay

To determine the DNase activity on the skin surface, the first three tape strips obtained by skin tape stripping were analysed. The

single tape strips were incubated for 20 min with 1.5 ml of 10 mM sodium acetate buffer (pH 5.0) and 0.5 mL of an aqueous DNAzyme solution (0.1625 mg/mL). The samples were filtered (0.2 μm pore size), and the remaining DNAzyme amount was analysed by HPLC (Schmidts et al., 2011).

2.10. Quantification of the DNAzyme

DNAzyme recovery and stability testing in the developed drug delivery systems as well as testing of DNase activity on the skin surface was performed by a slightly modified anion-exchange HPLC method (DNAPac PA-100 4 mm × 250 mm anion-exchange column and guard column (Dionex, USA)) previously described by Schmidts et al. (2011). Briefly, equilibration buffer (A) consists of 20 mM Tris–HCl, 20% methanol and 263 mM NaCl, and elution buffer (B) consists of 20 mM Tris–HCl, 20% methanol and 650 mM NaCl. Both buffers were adjusted to pH 7. The following gradient was run with a flow of 1.0 mL/min: 0–11 min (100% A), 11–50 min (from 100% A to 100% B), 50–56 min (100% B), 56–60 min (from 100% B to 100% A) and 60–70 min (100% A). If necessary, sample preparation was done by sonication at 50 °C for 30 min prior to HPLC analysis.

Samples obtained by skin penetration studies and drug release studies were analysed by a hybridisation-ELISA. The hybridisation–ELISA developed for the specific detection of DNAzyme (Dicke, 2009) was adjusted for the present requirements and performed as follows. Samples were diluted within a concentration range between 1 ng/mL and 78 ng/mL (dilution buffer: 20 mM Tris–HCl, 2.6% SDS, 0.5 mM $MgCl_2$; pH 7.4). Then 100 μL of the hybridisation buffer (20 mM Tris–HCl, 52.5 mM NaCl, 0.5 mM $MgCl_2$; pH 7.4), 80 μL dilution buffer and 0.22 μL of a mixture of oligonucleotide probes labelled with digoxigenin or biotin (each with 0.5 mg/mL) were added to 30 μL of the sample. This solution was incubated for 5 min at 75 °C and then immediately chilled to room temperature. Next, 100 μL of this solution was incubated in a 96-well streptavidin-coated microtiter plate (StreptaWell, High Bind, Roche) for 2 h at 37 °C and washed ten times with a buffer (20 mM Tris Base, 150 mM NaCl, 0.1% Tween®20; pH 10.0). Each well was filled with 100 μL of an antibody mixture (100 μL hybridisation buffer plus 0.5 μL anti-digoxigenin-peroxidase (anti-digoxigenin-POD, 250 mU/mL)), incubated by gently shaking for 1.5 h at 37 °C and washed again as previously described. Subsequently, 100 μL of BM Blue POD substrate was transferred into each well and incubated for 5 min in darkness. The reaction was stopped with 50 μL 2 M H_2SO_4, and the absorbance was measured with a Multiskan FC photometer (Thermo Fisher Scientific, Germany) at 450 nm and 650 nm as the sample and reference wavelengths, respectively. The calculation was done by a logarithmic standard curve.

3. Results

3.1. Selection of preservatives for the delivery systems

To identify the applicable preservative agent for the investigated drug delivery systems, various commonly used preservative systems were examined by visual observation regarding microbiological and physical stability (Table 1).

Propylene glycol as one component of the ME was sufficient to preserve this formulation. With regard to the W/O/W emulsion, preservatives showed a bearing influence on the physical stability leading to coalescence and phase separation. Only the application of 0.05% of benzoic acid showed sufficient microbiological and physical stability. Based on the preservative efficacy test and the stability data, the formulations were preserved as follows: the W/O emulsion contained 0.14% potassium sorbate, the ME contained 20% propylene glycol in the water phase, the SME contained 0.20% potassium sorbate and the W/O/W emulsion contained 0.05% benzoic acid.

Table 1
Influence of different preservative systems on the microbiological and physical stability of various drug delivery systems; (−) failed, (+) passed, (○) no data. Concentrations are given as total amount of the formulation.

Preservative	Preservative efficacy test	Stability (3 months)
W/O emulsion		
0.14% potassium sorbate	+	+
ME		
16.60% propylene glycol	+	+
SME		
0.10% Parabens[a]	−	+
20.00% propylene glycol	+	−
10.00% propylene glycol/0.10% Parabens[a]	−	+
5.00% butylene glycol/0.10% Parabens[a]	−	+
0.20% potassium sorbate	+	+
W/O/W emulsion		
0.10% Parabens[a]	−	+
0.20% Parabens[a]	−	−
0.40% Parabens[a]	−	−
20.00% propylene glycol	○	−
10.00% propylene glycol/0.10% Parabens[a]	−	−
5.00% butylene glycol/0.10% Parabens[a]	−	−
5.00% butylene glycol/0.10% Parabens[a]/0.50% Phenoxyethanol	○	−
8.00% butylene glycol/0.10% Parabens[a]	−	−
8.00% butylene glycol	−	−
0.14% potassium sorbate	○	−
0.20% benzoic acid	+	−
0.05% benzoic acid	+	+

[a] Parabens (75% methyl-4-hydroxybenzoate and 25% propyl-4-hydroxybenzoate).

3.2. Stability of delivery systems

To compare different drug delivery systems, the physicochemical properties were determined. First, stable placebo formulations were developed. The placebo formulations ($n = 3$) were considered as stable if the physicochemical parameters did not change within 3 months (stored at 25 °C and 60% RH). Next, these formulations were produced with DNAzyme, and the physicochemical parameters of the formulations were observed over 3 months (Table 2).

Regarding the droplet size and viscosity in the long-term stability analysis, the addition of DNAzyme did not appreciably influence these parameters in the case of the W/O emulsion, the ME and the SMEs. Only in the case of multiple emulsions was an increase of droplet sizes and a slight decrease in viscosity observed over three months. DNAzyme stability in the different formulations ranged in the order of W/O/W ≫ W/O ≫ ME ≥ SMEs. ME and SMEs showed a considerable decrease of DNAzyme content of about 35% after three months. Only with the W/O/W emulsion was a sufficient DNAzyme stability observed over three months. Additionally, regarding the different SMEs, the droplet size depended on the HLB of the surfactant blend.

3.3. Drug release studies

Drug release of the different formulations and an aqueous solution of DNAzyme were studied. First, the three SMEs, varying in droplet size, were compared (Fig. 1A). DNAzyme released from the three SMEs is very similar, and an influence of the droplet size could not be detected. In general, SMEs showed an immediate release; about 22.3 ± 1.3% was released within the first hour increasing up to 30.1 ± 3.2% after five hours.

Table 2
Physicochemical parameters of DNAzyme containing formulations.

	pH	Viscosity [mPa s]	$D(v,0.5)$ [μm]	z-Average [nm]	Recovery [%]
W/O emulsion					
Day 1	–	4954	–	816	97.3 ± 1.1
Month 1	–	4703	–	800	88.9 ± 1.5
Month 3	–	4764	–	900	88.8 ± 0.3
ME					
Day 1	6.9	9.1	–	95	99.3 ± 1.4
Month 1	6.6	9.6	–	105	99.8 ± 2.9
Month 3	6.4	11.8	–	114	65.6 ± 0.8
SME HLB = 10					
Day 1	4.6	2.4	0.23	–	104.1 ± 0.9
Month 1	4.6	2.6	0.23	–	100.6 ± 1.3
Month 3	4.5	2.7	0.22	–	62.6 ± 0.3
SME HLB = 11					
Day 1	4.6	2.6	0.40	–	102.3 ± 2.0
Month 1	4.6	2.6	0.40	–	101.4 ± 0.5
Month 3	4.6	2.6	0.37	–	62.9 ± 0.6
SME HLB = 12					
Day 1	4.6	2.8	0.77	–	100.8 ± 1.7
Month 1	4.6	2.9	0.77	–	100.2 ± 1.2
Month 3	4.5	3.1	0.75	–	66.3 ± 0.8
W/O/W emulsion					
Day 1	5.8	935.0	14.65	–	98.3 ± 0.5
Month 1	5.7	903.8	17.99	–	100.5 ± 0.5
Month 3	5.2	803.8	29.27	–	103.5 ± 0.3

Fig. 1B shows the comparison among the different formulations and an aqueous DNAzyme solution. The amount of DNAzyme released was in the following order: aqueous solution > SME (HLB 12) ≥ ME > W/O/W emulsion > W/O emulsion. Drug release was strongly dependent on the drug carrier system. An undisturbed release was recognised with the aqueous solution (81.4 ± 4.3% after two hours). While DNAzyme from SME (HLB 12) was released immediately and yielded a plateau phase after two hours, ME showed a delayed release and a lag time of 90 min and was continuously increasing over time. DNAzyme released from W/O/W emulsion and W/O emulsion was either close to the quantification limit or not detectable at all. Less than 0.1% of the DNAzyme was released after 24 h.

3.4. DNase activity assay

To study the influence of DNase activity of the skin on the penetration studies, the degradation of DNAzyme was determined. Fig. 2 represents the data of the DNase activity experiment of fresh and frozen skin on top of the *stratum corneum* (tape 1) up to tape 3. The results exhibited a reduction of DNase activity from the top of the skin (tape 1) to the deeper skin layers. The frozen-thawed skin showed a similar decreasing profile but an overall lower amount of DNase activity.

3.5. Skin penetration studies

DNAzyme transport into the skin was compared with respect to the different drug carrier systems and different experimental designs. The comparison of the three SMEs, differing in droplet size, showed no significant difference (Fig. 3).

To compare the influence of the different drug carrier systems, the DNAzyme transport into skin was studied (Fig. 4A + B). The penetration of DNAzyme into impaired and intact skin ranged in the order SME (HLB 12) > ME ≫ aqueous solution (aq. s.) > W/O/W and W/O emulsion after 24 h. In general, the DNAzyme uptake from impaired skin was slightly increased compared to the intact skin except with the SME (HLB 12). Examination of the fluorescence assay showed similar results (Fig. 4B), thus are in agreement with the results by hybridisation-ELISA.

Fig. 5 depicts representative examples of fluorescence microscopy images of vertically cross-sectioned skin following topical application of DNAzyme in various formulations prepared for the fluorescence assay (Fig. 4B). The permeation of FAM-DNAzyme was restricted to the epidermal layer, especially the stratum corneum.

The most promising drug carrier systems regarding drug transport into the skin, SME (HLB 12), and DNAzyme stability, W/O/W emulsion, were subjected to further penetration studies using fresh

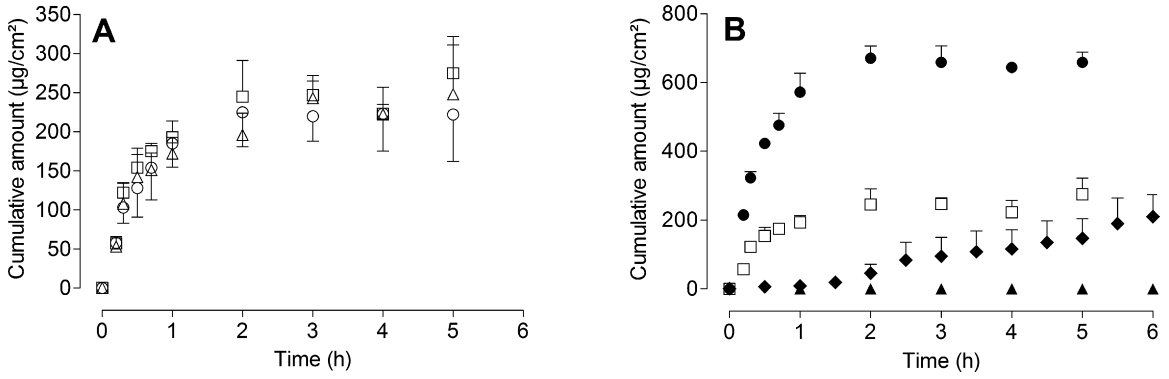

Fig. 1. Cumulative drug release (HPLC analysis) of DNAzyme from various drug carrier systems. (A) SME with different HLB values: (○) HLB 10, (△) HLB 11, (□) HLB 12. (B) Various drug carrier systems (●) aqueous solution, (□) SME (HLB 12), (♦) ME, (▲) W/O/W emulsion, W/O emulsion below limit of detection; (mean ± SD, $n = 3$).

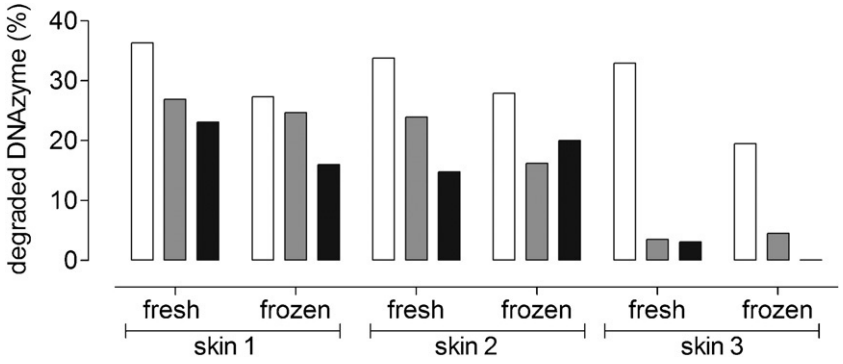

Fig. 2. Results of the DNase activity assay of fresh and frozen skin samples by tape stripping; analysed by HPLC.

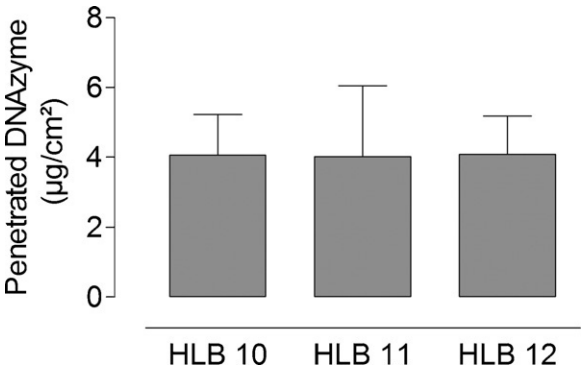

Fig. 3. DNAzyme skin uptake of SMEs varying in HLB values and droplet sizes. Infinite dose approach and frozen skin with intact skin barrier (mean ± SD, $n = 6$); 24 h, analysed by hybridization ELISA.

skin (Fig. 6) and the finite dose approach to mimic a more realistic experimental design (Fig. 7).

DNAzyme uptake from W/O/W emulsion into skin was not significantly affected by the skin conditions, but it exhibited a slightly higher DNAzyme uptake with the frozen skin (Fig. 6). Regarding the SME, a significant decreased amount of DNAzyme uptake was seen with fresh intact skin compared to the frozen intact skin, while no difference was seen with the impaired skin.

Finally, the influence of finite dose application under a low pressure massage on the skin uptake of DNAzyme was investigated to mimic the common conditions. Then, a formulation was applied on the skin. This experiment showed a nearly 4-fold higher DNAzyme uptake from the W/O/W emulsion (0.26 ± 0.15 µg/cm^2) compared to the SME (0.07 ± 0.03 µg/cm^2; HLB 12) (Fig. 7).

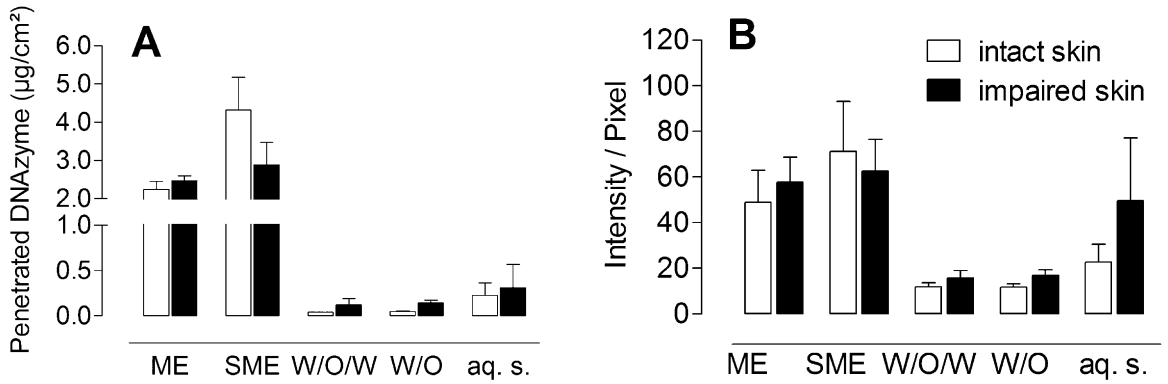

Fig. 4. DNAzyme skin uptake of various drug carrier systems; results of (A) hybridisation ELISA and (B) fluorescence assay. Infinite dose approach, frozen skin for 24 h (mean ± SD, $n \geq 3$).

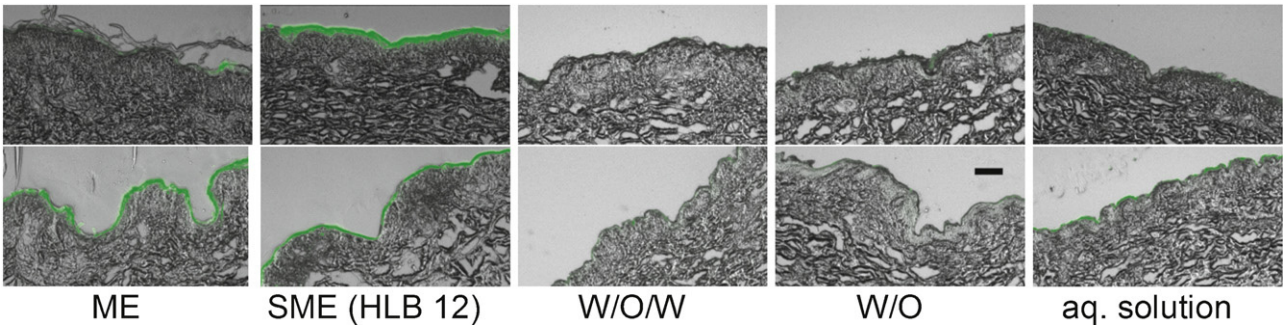

Fig. 5. Fluorescence microscopy images of vertically cross-sectioned skin following topical application of FAM-DNAzyme (green) in various formulations. Scale bar represents 100 µm. Pictures in the upper row represent the intact skin, and those in the lower row represent the impaired skin. (For interpretation of the references to colour in this figure legend, the reader is referred to the web version of the article.)

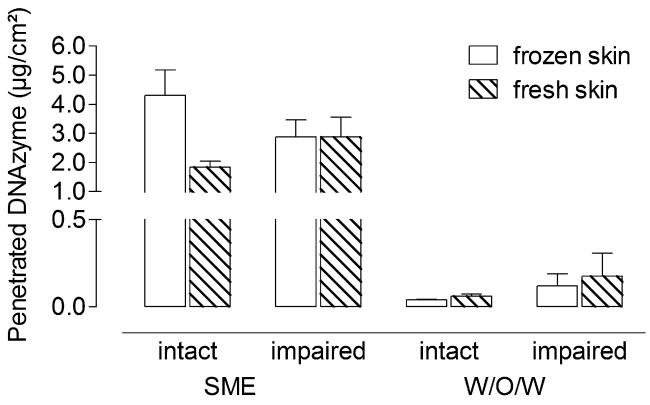

Fig. 6. DNAzyme skin uptake analysed by hybridisation-ELISA; Infinite dose and 24 h analysed by hybridisation-ELISA (mean ± SD, $n \geq 3$).

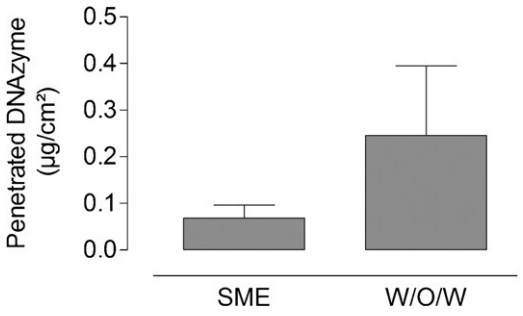

Fig. 7. DNAzyme skin uptake analysed by hybridisation-ELISA. Finite dose approach with low pressure application on fresh intact skin for 24 h analysed by hybridisation-ELISA (mean ± SD, $n = 6$).

3.6. Cellular uptake of DNAzymes

To determine the cellular uptake of the FAM-DNAzyme, FACS analysis of cells obtained from skin penetration studies with W/O/W and SME were done. As depicted in Fig. 8, it is shown that the penetrated FAM-DNAzyme was taken up by viable epidermal cells, mainly keratinocytes. Cellular uptake of the FAM-DNAzyme is improved by the W/O/W emulsion as compared to the SME resulting in an obvious higher increase of the respective uptake parameters as compared to the SME.

4. Discussion

The dermal therapy of skin diseases is often limited due to insufficient therapeutic drug levels at the target site. Therefore, the identification and application of suitable drug carrier systems are essential for a successful therapy. On the one hand, 10–23 DNAzyme is a relatively large molecule (10.6 kDa); therefore, appropriate inactive ingredients have to be chosen to enhance or even enable skin uptake. On the other hand, the DNAzyme is extremely sensitive towards DNases naturally occurring on the skin surface and in the skin tissue, therefore an encapsulation of the drug, in multiple emulsions, would be preferable.

The aim of this study was to identify formulations that best meet these requirements. Therefore, two drug carrier systems, SME and ME, with excellent penetration-enhancing properties due to their excellent drug solubility characteristics, alternation of skin lipids and small droplet size (Friedman et al., 1995; Kreilgaard, 2002) were developed. Furthermore, two formulations with the DNAzyme encapsulated in the inner aqueous phase were produced: a conventional W/O emulsion and, as innovative approach, a W/O/W multiple emulsion. Particular attention was paid to the preservation of the developed formulations due to the expected influence on the formulation stability. The preservatives tested and concentrations used were chosen according to the German Pharmaceutical Codex (DAC). No incompatibility occurred when the preservative potassium sorbate (0.14%) for the W/O emulsion and propylene glycol (16.60%) as formulation constituent of the ME was used and the preservative efficacy test was successful. The selection of an appropriate preservative for the W/O/W emulsion and the SME was more difficult. One possible explanation could be the influence of the inactive ingredients, e.g., soy lecithin, on the efficiency of the preservative (Darwish and Bloomfield, 1995; Kohn et al., 1963) and the distribution of the preservative between the aqueous and lipophilic phase of the emulsions (Kurup et al., 1991). Furthermore, W/O/W emulsions are extremely sensitive towards variation of components and additives (Schmidts et al., 2010). However, 0.05% benzoic acid and 0.20% potassium sorbate showed an appropriate preservation for W/O/W emulsion and W/O emulsion, respectively.

Regarding the stability of the formulations, the SME, ME and W/O emulsion did not meet the requirements for the recovery of the DNAzyme over 3 months. Degradation of the DNAzyme over time might be attributed to the non-encapsulated drug in the outer water phase in the case of ME and SME (Schmidts et al., 2011), DNase contamination during non-aseptic sampling for the stability testing or unspecific interactions with the formulation

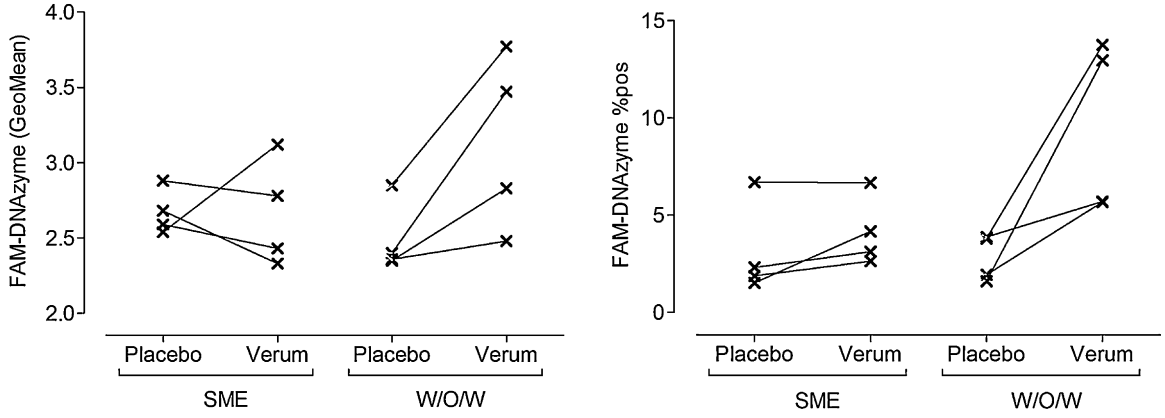

Fig. 8. Results of the FACS analysis of the cellular uptake of FAM-DNAzyme after skin penetration studies ($n = 4$). Left: geometric mean value (GeoMean). Right: percentage of FAM-DNAzyme positive cells (%pos).

components (Langlois et al., 1989). In contrast, only the W/O/W emulsion revealed sufficient DNAzyme recovery and protection during the period of observation that can be attributed to an appropriate encapsulation.

Next, the pharmacokinetic data of the developed DNAzyme containing formulations by drug release and skin penetration studies were collected. A comparison of the three different SMEs showed no significant influence of the droplet size on the drug release and skin uptake of DNAzyme. In contrast, Verma et al. (2003) showed a size-dependent influence of liposomes on drug penetration. One explanation might be the width of the droplet size distribution and therefore an overlapping droplet size of the developed SMEs. Furthermore, it must be considered that the hydrophilic DNAzyme was solubilised in the outer water phase.

Drug release is influenced both by the formulation and the drug properties. The formulation viscosity, the drug distribution among the phases (partition coefficient) and the thermodynamic activity of the drug define the diffusion coefficient and thus the drug release. An expected fast and unimpeded diffusion of the DNAzyme from aqueous solution was observed. DNAzyme was released from various formulations in the order SME (HLB 12) ≥ ME > W/O/W emulsion > W/O emulsion, which is in agreement with the results of Ferreira et al. (1994), who showed that the hydrophilic glucose was released fastest from an O/W emulsion, but was barely released from a W/O/W emulsion and a W/O emulsion. While the maxima of DNAzyme released from the SME and ME were comparable, the DNAzyme release was delayed with the ME. This can be associated with the higher viscosity of the ME as well as the possible inner structure of the ME, e.g., the formation of a bicontinuous structure (Kreilgaard, 2002) that hampers an immediate release. The extent of DNAzyme released from SME was less compared to the aqueous solution and might be attributed to the SME ingredients that block the pores of the membrane. Finally, the DNAzyme release from W/O/W and W/O emulsion was practically non-exist, which is a result of the DNAzyme encapsulation in the inner water phase of W/O/W and W/O emulsion and the high viscosity of the systems.

However, drug release studies are not sufficient enough to predict skin uptake due to the lack of skin–vehicle interactions. Thus, skin penetration was investigated to elucidate the most suitable drug carrier system regarding protective effect and skin uptake. DNAzyme may be used in the treatment of atopic dermatitis that is characterised by a defective skin barrier. Therefore, both skin conditions, intact and impaired skin, were investigated. Skin uptake followed the order SME > ME ≫ aqueous solution > W/O/W and W/O for both impaired and intact skin after infinite dose application for 24 h. The enhanced DNAzyme uptake by the SME and ME compared to the aqueous solution is attributed to the well-known enhancing properties of these carrier systems (Friedman et al., 1995; Schwarz et al., 1995). Furthermore, the low DNAzyme uptake by the W/O/W and W/O emulsions might be a result of a delayed drug release of the encapsulated DNAzyme. As expected, the DNAzyme uptake was slightly enhanced when the skin barrier was impaired. However, this is not true in case of SME. Drug penetration is higher using intact skin compared to impaired skin where the stratum corneum is absent. This phenomenon might be attributed to the oil blend used, especially ethyl oleate, the ethyl ester of oleic acid. Oleic acid is able to facilitate a transport of hydrophilic substances into the skin by increasing the fluidity of lipid portion (Kanikkannan and Singh, 2002) and the generation of water pools within the stratum corneum (Ongpipattanakul et al., 1991). Thus, the enhancing effect of the SME is less expressed in the absence of the stratum corneum layer. Fluorescence microscopic images revealed that the DNAzyme was mainly located in the upper skin. As the target GATA-3 is mainly expressed in the inflammation infiltrate containing T cells but also in eosinophils, basophils, mast cells and epithelial cells (Justice et al., 2002; Masuda et al., 2004; Zon et al., 1993), the observed DNAzyme uptake should be sufficient for an appropriate treatment of atopic dermatitis. Next, the influence of fresh skin on the DNAzyme uptake was investigated using the SME and the W/O/W emulsion. Skin penetration studies revealed the influence of DNase activity on the uptake of DNAzyme. While no significant difference was observed for the encapsulated and thus protected DNAzyme in the W/O/W emulsion, DNAzyme uptake from SME clearly exceeded that of fresh skin with an intact skin barrier. The DNase activity assay showed that DNase activity was highest with fresh skin and consequently degraded the DNAzyme in the outer aqueous phase of the SME. Furthermore, DNase activity showed a decreasing profile following the stratum corneum layers from the outside inwards (Fig. 2). Subsequently, the difference between fresh and frozen skin is less distinctive with the impaired skin.

Florence and Whitehill (1981, 1982) showed that several mechanism of W/O/W multiple emulsions breakdown exist, for example by rupture of the oily membrane due to the expulsion of the internal water droplets or the diffusion of the water through the oil phase owing to osmotic effects. Thus, the entrapped drug can be released (Raynal et al., 1993). As a breakdown of the oily membrane can also be induced by moderate shear stress (Muguet et al., 2001; Olivieri et al., 2003), the influence of the topical application (a shear rate of 1000 s^{-1} is commonly reached in topical application (Olivieri et al., 2003)) was investigated. DNAzyme uptake with finite dose set-up and application of the formulation under a gentle massage led to the superiority of the W/O/W emulsion over the SME. This indicates that the oily membrane of the developed W/O/W multiple emulsion broke down under the applied shear, and the DNAzyme was released and successfully penetrated into the skin. The targets of the DNAzyme are the cells of the viable epidermis. In order to proof an uptake of DNAzyme by the cells of the epidermis, FACS analysis of viable epidermal cells was performed. The FACS analysis revealed that the FAM-DNAzyme uptake by the skin is not limited to the interstitial of the epidermal compartment and the stratum corneum. Importantly, Compared to the SME the W/O/W emulsion mediated a higher drug uptake which confirmed the data obtained by the skin penetration studies.

5. Conclusion

In summary, different drug carrier systems for the topical application of DNAzyme were developed and investigated with regard to the physicochemical stability and skin uptake. The encapsulation of the hydrophilic DNAzyme into the inner aqueous phase of the W/O/W multiple emulsion and the W/O emulsion clearly improved the DNAzyme stability. DNAzyme uptake from SME to the skin indicates that composition components, e.g., ethyl oleate, interact with the *stratum corneum*, leading to enhanced DNAzyme penetration compared to skin with impaired barrier, which is characterised by a reduced *stratum corneum*. The release and consequently skin uptake of DNAzyme from the W/O/W multiple emulsion can be induced by shear commonly applied at topical application. With regard to the experimental set-up, the results emphasise the reduction of skin DNase activity due to deep freeze storage. To conclude, the developed W/O/W multiple emulsion is a suitable and promising drug carrier system for the transport of DNAzyme across the skin and into epidermal cells of the atopic dermatitis affected skin.

Acknowledgments

We would like to thank the Federal Ministry of Economics and Technology on the basis of a decision of the German Bundestag

for the financial support (ZIM - Zentrales Innovationsprogramm Mittelstand), grant number KF2268904FR0.

References

Akhtar, S., Hughes, M.D., Khan, A., Bibby, M., Hussain, M., Nawaz, Q., Double, J., Sayyed, P., 2000. The delivery of antisense therapeutics. Adv. Drug Deliv. Rev. 44, 3–21.

Bally, M.B., Harvie, P., Wong, F.M.P., Kong, S., Wasan, E.K., Reimer, D.L., 1999. Biological barriers to cellular delivery of lipid-based DNA carriers. Adv. Drug Deliv. Rev. 38, 291–315.

Barnes, P.J., 2008. Role of GATA-3 in allergic diseases. Curr. Mol. Med. 8, 330–334.

Bouchemal, K., Briançon, S., Perrier, E., Fessi, H., 2004. Nano-emulsion formulation using spontaneous emulsification: solvent, oil and surfactant optimisation. Int. J. Pharm. 280, 241–251.

Cieslak, M., Szymanski, J., Adamiak, R.W., Cierniewski, C.S., 2003. Structural rearrangements of the 10–23 DNAzyme to beta 3 integrin subunit mRNA induced by cations and their relations to the catalytic activity. J. Biol. Chem. 278, 47987–47996.

Darwish, R.M., Bloomfield, S.F., 1995. The effect of co-solvents on the antibacterial activity of paraben preservatives. Int. J. Pharm. 119, 183–192.

Delgado-Charro, M.B., Iglesias-Vilas, G., Blanco-Méndez, J., López-Quintela, M.A., Marty, J.-P., Guy, R.H., 1997. Delivery of a hydrophilic solute through the skin from novel microemulsion systems. Eur. J. Pharm. Biopharm. 43, 37–42.

Dicke, T.M., 2009. Charakterisierung GATA-3-spezifischer DNAzyme und Analyse der therapeutischen Wirksamkeit in experimentellen Modellen des Asthma bronchiale, Dissertation. Philipps - Universität Marburg, Marburg.

Diembeck, W., Beck, H., Benech-Kieffer, F., Courtellemont, P., Dupuis, J., Lovell, W., Paye, M., Spengler, J., Steiling, W., 1999. Test guidelines for in vitro assessment of dermal absorption and percutaneous penetration of cosmetic ingredients. European Cosmetic, Toiletry and Perfumery Association. Food Chem. Toxicol. 37, 191–205.

Djekic, L., Primorac, M., 2008. The influence of cosurfactants and oils on the formation of pharmaceutical microemulsions based on PEG-8 caprylic/capric glycerides. Int. J. Pharm. 352, 231–239.

Ferreira, L.A.M., Seiller, M., Grossiord, J.L., Marty, J.P., Wepierre, J., 1994. Vehicle influence on in vitro release of metronidazole: role of w/o/w multiple emulsion. Int. J. Pharm. 109, 251–259.

Florence, A.T., Whitehill, D., 1981. Some features of breakdown in water-in-oil-in-water multiple emulsions. J. Colloid Interface Sci. 79, 243–256.

Florence, A.T., Whitehill, D., 1982. The formulation and stability of multiple emulsions. Int. J. Pharm. 11, 277–308.

Friedman, D.I., Schwarz, J.S., Weisspapir, M., 1995. Submicron emulsion vehicle for enhanced transdermal delivery of steroidal and nonsteroidal antiinflammatory drugs. J. Pharm. Sci. 84, 324–329.

Fukushima, S., Nishida, M., Nakano, M., 1987. Preparation of and drug release from W/O/W type double emulsions containing anticancer agents using an oily lymphographic agent as an oil phase. Chem. Pharm. Bull. (Tokyo) 35, 3375–3381.

Garlisi, C.G., Falcone, A., Kung, T.T., Stelts, D., Pennline, K.J., Beavis, A.J., Smith, S.R., Egan, R.W., Umland, S.P., 1995. T cells are necessary for Th2 cytokine production and eosinophil accumulation in airways of antigen-challenged allergic mice. Clin. Immunol. Immunopathol. 75, 75–83.

Grünig, G., Warnock, M., Wakil, A.E., Venkayya, R., Brombacher, F., Rennick, D.M., Sheppard, D., Mohrs, M., Donaldson, D.D., Locksley, R.M., Corry, D.B., 1998. Requirement for IL-13 independently of IL-4 in experimental asthma. Science 282, 2261–2263.

Justice, J.P., Borchers, M.T., Lee, J.J., Rowan, W.H., Shibata, Y., Van Scott, M.R., 2002. Ragweed-induced expression of GATA-3, IL-4, and IL-5 by eosinophils in the lungs of allergic C57BL/6J mice. Am. J. Physiol. Lung Cell. Mol. Physiol. 282, L302–L309.

Kanikkannan, N., Singh, M., 2002. Skin permeation enhancement effect and skin irritation of saturated fatty alcohols. Int. J. Pharm. 248, 219–228.

Khopade, A.J., Jain, N.K., 1999. Multiple emulsions containing rifampicin. Pharmazie 54, 915–919.

Kim, S.T., Lee, K.M., Park, H.J., Jin, S.E., Ahn, W.S., Kim, C.K., 2009. Topical delivery of interleukin-13 antisense oligonucleotides with cationic elastic liposome for the treatment of atopic dermatitis. J. Gene Med. 11, 26–37.

Kohn, S.R., Gershenfeld, L., Barr, M., 1963. Effectiveness of antibacterial agents presently employed in ophthalmic preparations as preservatives against Pseudomonas aeruginosa. J. Pharm. Sci. 52, 967–974.

Kreilgaard, M., 2002. Influence of microemulsions on cutaneous drug delivery. Adv. Drug Deliv. Rev. 54 (Suppl.), S77–S98.

Kurup, T., Wan, L., Chan, L., 1991. Availability and activity of preservatives in emulsified systems. Pharm. Acta Helv. 66, 76.

Langlois, B.E., Harmon, R.J., Akers, K., Aaron, D.K., 1989. Comparison of methods for determining DNase and phosphatase activities of staphylococci. J. Clin. Microbiol. 27, 1127–1129.

Leung, D.Y., 2000. Atopic dermatitis: new insights and opportunities for therapeutic intervention. J. Allergy Clin. Immunol. 105, 860–876.

Leung, D.Y., Soter, N.A., 2001. Cellular and immunologic mechanisms in atopic dermatitis. J. Am. Acad. Dermatol. 44, S1–S12.

Lindenstruth, K., Müller, B.W., 2004. W/O/W multiple emulsions with diclofenac sodium. Eur. J. Pharm. Biopharm. 58, 621–627.

Maggi, E., 1998. The Th1/Th2 paradigm in allergy. Immunotechnology 3, 233–244.

Masuda, A., Yoshikai, Y., Kume, H., Matsuguchi, T., 2004. The interaction between GATA proteins and activator protein-1 promotes the transcription of IL-13 in mast cells. J. Immunol. 173, 5564–5573.

Matsumoto, S., Kita, Y., Yonezawa, D., 1976. An attempt at preparing waterin-oil-in-water multiple-phase emulsions. J. Colloid Interface Sci. 57, 353–361.

Muguet, V., Seiller, M., Barratt, G., Ozer, O., Marty, J.P., Grossiord, J.L., 2001. Formulation of shear rate sensitive multiple emulsions. J. Control. Release 70, 37–49.

OECD, 2004a. Guidance Document for the Conduct of Skin Absorption Studies. OECD Publishing.

OECD, 2004b. Test No. 428: Skin Absorption: In Vitro Method.

Olivieri, L., Seiller, M., Bromberg, L., Besnard, M., Duong, T.N., Grossiord, J.L., 2003. Optimization of a thermally reversible W/O/W multiple emulsion for shear-induced drug release. J. Control. Release 88, 401–412.

Ongpipattanakul, B., Burnette, R., Potts, R., Francoeur, M., 1991. Evidence that oleic acid exists in a separate phase within stratum corneum lipids. Pharm. Res. 8, 350–354.

Pharmacopoeia, E., 2008. Monographie 6.0/5.01.03.00 (Efficacy of Antimicrobial Preservation), 6th ed.

Raynal, S., Grossiord, J.L., Seiller, M., Clausse, D., 1993. A topical W/O/W multiple emulsion containing several active substances: formulation, characterization and study of release. J. Control. Release 26, 129–140.

Santoro, S.W., Joyce, G.F., 1998. Mechanism and utility of an RNA-cleaving DNA enzyme. Biochemistry 37, 13330–13342.

Schmalfuß, U., Neubert, R., Wohlrab, W., 1997. Modification of drug penetration into human skin using microemulsions. J. Control. Release 46, 279–285.

Schmidts, T., Dobler, D., Schlupp, P., Nissing, C., Garn, H., Runkel, F., 2010. Development of multiple W/O/W emulsions as dermal carrier system for oligonucleotides: effect of additives on emulsion stability. Int. J. Pharm. 398, 107–113.

Schmidts, T., Dobler, D., von den Hoff, S., Schlupp, P., Garn, H., Runkel, F., 2011. Protective effect of drug delivery systems against the enzymatic degradation of dermally applied DNAzyme. Int. J. Pharm. 410, 75–82.

Schwarz, J.S., Weisspapir, M.R., Friedman, D.I., 1995. Enhanced transdermal delivery of diazepam by submicron emulsion (SME) Creams. Pharm. Res. 12, 687–692.

Sel, S., Wegmann, M., Dicke, T., Sel, S., Henke, W., Yildirim, A.O., Renz, H., Garn, H., 2008. Effective prevention and therapy of experimental allergic asthma using a GATA-3-specific DNAzyme. J. Allergy Clin. Immunol. 121, 910–916, e915.

Silverman, S.K., 2005. In vitro selection, characterization, and application of deoxyribozymes that cleave RNA. Nucleic Acids Res. 33, 6151–6163.

Simonsen, L., Fullerton, A., 2007. Development of an in vitro skin permeation model simulating atopic dermatitis skin for the evaluation of dermatological products. Skin Pharmacol. Physiol. 20, 230–236.

Tritz, R., Habita, C., Robbins, J.M., Gomez, G.G., Kruse, C.A., 2005. Catalytic nucleic acid enzymes for the study and development of therapies in the central nervous system: review article. Gene Ther. Mol. Biol. 9A, 89–106.

Verma, D.D., Verma, S., Blume, G., Fahr, A., 2003. Particle size of liposomes influences dermal delivery of substances into skin. Int. J. Pharm. 258, 141–151.

Wierup, M., 1978. Production of coagulase, deoxyribonuclease and heat-stable deoxyribonuclease by canine isolates of staphylococci. Zentralbl. Bakteriol. Orig. A 242, 431–435.

Zhu, J., Yamane, H., Cote-Sierra, J., Guo, L., Paul, W.E., 2006. GATA-3 promotes Th2 responses through three different mechanisms: induction of Th2 cytokine production, selective growth of Th2 cells and inhibition of Th1 cell-specific factors. Cell Res. 16, 3–10.

Zon, L., Yamaguchi, Y., Yee, K., Albee, E., Kimura, A., Bennett, J., Orkin, S., Ackerman, S., 1993. Expression of mRNA for the GATA-binding proteins in human eosinophils and basophils: potential role in gene transcription. Blood 81, 3234–3241.

II. Degradation and protection of DNAzymes on human skin. In: *European Journal of Pharmaceutics and Biopharmaceutics* 107, S. 80–87.

European Journal of Pharmaceutics and Biopharmaceutics 107 (2016) 80–87

Contents lists available at ScienceDirect

European Journal of Pharmaceutics and Biopharmaceutics

journal homepage: www.elsevier.com/locate/ejpb

Research paper

Degradation and protection of DNAzymes on human skin

Kay Marquardt [a,*], Anna-Carola Eicher [a], Dorota Dobler [a], Frank Höfer [a], Thomas Schmidts [a], Jens Schäfer [b], Harald Renz [c], Frank Runkel [a,d]

[a] Institute of Bioprocess Engineering and Pharmaceutical Technology, University of Applied Sciences Mittelhessen, Wiesenstrasse 14, 35390 Giessen, Germany
[b] Pharmaceutical Technology and Biopharmacy, Ketzerbach 63, 35032 Marburg, Philipps-University Marburg, Germany
[c] Institute of Laboratory Medicine and Pathobiochemistry, Molecular Diagnostic, Baldinger Strasse, 35043 Marburg, Philipps-University Marburg, Germany
[d] Faculty of Biology and Chemistry, Justus-Liebig University Giessen, Heinrich-Buff-Ring 17, 35392 Giessen, Germany

ARTICLE INFO

Article history:
Received 12 April 2016
Revised 29 June 2016
Accepted in revised form 1 July 2016
Available online 1 July 2016

Chemical compounds studied in this article:
Chitosan (PubChem CID: 21896651)
Chitosan oligosaccharide lactate (PubChem CID: 16213812)
Deoxyribonuclease II (PubChem SID: 135286563)
Polyethyleneimine (PubChem CID: 9033)

Keywords:
DNAzyme
DNase
Chitosan
Human skin
Polyethylenimine
Polyplex

ABSTRACT

DNAzymes are catalytic nucleic acid based molecules that have become a new class of active pharmaceutical ingredients (API). Until now, five DNAzymes have entered clinical trials. Two of them were tested for topical application, whereby dermally applied DNAzymes had been prone to enzymatic degradation. To protect the DNAzymes the enzymatic activity of human skin has to be examined. Therefore, the enzymatic activity of human skin was qualitatively and quantitatively analyzed. Activity similar to that of DNase II could be identified and the specific activity was determined to be 0.59 Units/mg. These results were used to develop an *in vitro* degradation assay to screen different kinds of protective systems on human skin. The chosen protective systems consisted of biodegradable chitosans or polyethylenimine, which forms polyplexes when combined with DNAzymes. The polyplexes were characterized in terms of particle size, zeta potential, stability and degree of complexation. The screening revealed that the protective efficiency of the polyplexes depended on the polycation and the charge ratio (ξ). At a critical ξ ratio between 1.0 and 4.1 and at a maximal zeta potential, sufficient protection of the DNAzyme was achieved. The results of this study will be helpful for the development of a protective dermal drug delivery systems using polyplexes.

1. Introduction

The group of 10–23 DNAzymes is a new class of APIs. The DNAzymes provide a combination of high specificity and enzymatic activity [1,2]. A vast variety of 10–23 DNAzymes have been designed for the therapy of different kinds of diseases such as cancer, immune system defects and viral infections [3–6]. Currently, five DNAzymes have entered clinical trials and are suitable for local administration [7]. Two of them, namely hgd40 and the Dz13, could address skin diseases, such as atopic dermatitis or actinic keratosis. Both DNAzymes have already been tested for dermal application [8,9]. However, a dermal application of DNAzymes is challenging, because DNA-based molecules are prone to enzymatic degradation. The skin exhibits a broad range of DNA-degrading molecules besides DNase I [10]. In particular on the skin surface, there is an abundance of deoxyribonucleases (DNase) of endogenous and exogenous origin [11–14]. Correct identification of DNAzyme-degrading activity on the skin can be useful to develop an appropriate drug delivery system (DDS), which will protect against degradation. Approaches to protect DNA-based APIs are encapsulation or complexation with liposomes, nanoparticles or polyplexes. Previously, we presented a dermal DDS which combined polyplexes with a penetration enhancing submicron emulsion (SME). In this study due to the SME, the polyplexes were able to penetrate into the skin, whereas the DNAzyme was accumulating in the SC and first layers of the epidermis at targeted site [9]. Polyplexes are formed between two oppositely charged polyelectrolytes, mostly driven by electrostatic interaction [15]. The properties of the polyplexes are influenced by the selection of the polycation and the ratio between DNA's phosphates and the polycation's protonated amino groups (ξ ratio). The protective

* Corresponding author.
E-mail address: Kay.Marquardt@lse.thm.de (K. Marquardt).

http://dx.doi.org/10.1016/j.ejpb.2016.07.001
0939-6411/

efficiency of the polyplex was validated with the DNase I standard test. A more realistic validation of dermally applied polyplexes is still pending.

The aim of this work was to screen polyplexes adapted especially for dermally applied DNAzymes. Therefore, the main DNAzyme-degrading enzyme on human skin as well as degrading activity was determined. The results were used to develop an *in vitro* screening to validate different kinds of polyplexes for protective efficiency.

2. Materials and methods

2.1. Materials

DNAzyme Dz13 sodium salt was synthesized by Integrated DNA Technologies (Leuven, Belgium). The single stranded DNA consisted of 34 deoxyribonucleotides, including an inverted thymidine at the 3′ end with a molecular weight (MW) of 10.6 kDa [16]. Additionally, the Dz13 was labeled with 6FAM and black hole quencher 1 at the 5′ end and 3′ end, respectively to create FAM-Dz13-Q (Biomers, Ulm, Germany). The following listed substances were purchased by the suppliers in parentheses: *Ex vivo* full thickness skin (Across Barriers GmbH, Saarbruecken, Germany), Deoxyribonuclease I from bovine pancreas, deoxyribonuclease II type IV from porcine spleen, branched polyethylenimine (PEI) (MW: 25 kDa), chitosan oligosaccharide lactate (chitosan OSL) (degree of deacetylation (DD): 90%, Mn: 4–6 kDa), (Sigma–Aldrich, Munich, Germany), T5 exonuclease and micrococcal nuclease (New England Biolabs, Germany), Chitopharm S (chitosan S) (DD: 70%, MW: 50–1000 kDa) (Cognis, Monheim, Germany), Chitosan-HCl (chitosan XS) (DD: 70%, MW: 30–70 kDa) (Kraeber & Co, Ellerbek, Germany), Maxilon flavine 10 GFF/basic yellow 40 (Hemtsman, Germany).

2.2. DNAzyme analytics

The DNAzyme Dz13 was qualitatively and quantitatively analyzed by an anionic exchange high pressure liquid chromatography (AEX-HPLC), which has been previously described [9]. Briefly, samples were purified with phenol-chloroform extraction and ethanol precipitation. If it was necessary, samples were decomplexed using sodium hydroxide or heparin (1% (w/v)).

2.3. Identification of the DNAzyme-degrading enzyme

Cornified squames from the skin surface found on used dry-razor blades from healthy volunteers were collected. Prior to collection, volunteers had not washed or creamed their skin for 12 h and all hair was removed with a dry-shaver. The areas of collection were on the forearm and lower leg. The skin samples were either pooled (3 females and 3 males) or were individually tested (1 female and 2 males). The collected skin was suspended with a TEAA buffer (100 mM TEAA-acetic acid, 1 mM $MgCl_2$) at pH 5.0 or pH 6.6 to a concentration of 1% (w/v). The suspension was vigorously mixed and afterward centrifuged. The supernatant was incubated with a final Dz13 concentration of 50 μg/mL at 33 °C at 300 rpm for 15 min up to 3 h. Degradation products were analyzed with the AEX-HPLC method. The DNase I, DNase II and micrococcal nuclease were incubated at the same conditions with the Dz13. Only T5 exonuclease was incubated with the provided reaction buffer (50 mM potassium acetate, 20 mM Tris-acetate, 10 mM magnesium acetate, 1 mM DTT, pH 7.9). All experiments were done in triplicates.

2.4. Activity assay

The specific activity of the DNAzyme-degrading enzyme was determined with two different methods:

i. For a real-time fluorescence analysis the FAM-Dz13-Q was incubated at a final amount of 30 μg/mL with the pooled skin supernatant of Section 2.3 but using an acetic buffer (50 mM acetic acid, 1 mM $MgCl_2$, 0.1% IGEPAL, pH 5.0). To determine a calibration curve, the same amount of FAM-Dz13-Q was incubated in heat-inactivated skin supernatant with DNase II standards in a range from 2 to 10 Units/mL (33 °C, at least 1 h). The emission (480/520 nm) was measured every 30 s using the Synergy HTX plate reader (BioTek Instruments, Berlin, Germany). All data points of the samples were subtracted from corresponding samples incubated in heat-inactivated skin supernatant. All samples were tested six times, and standards and blanks were analyzed in triplicates. The data are presented as the mean with standard deviation (SD).
ii. For an endpoint analysis the AEX-HPLC was used. The Dz13 was incubated at a final amount of 50 μg/mL, with the pooled skin supernatant of Section 2.3. The reaction was done at 33 °C for up to 4 h in TEAA buffer (100 mM TEAA, 1 mM $MgCl_2$, pH 5.0). At each time point, the reaction was stopped and the sample was measured by the AEX-HPLC method. Calibration standards of DNase II were in a range of 2.5–10 Units/mL. The reaction was repeated six times and results are presented as the mean ± SD.

2.5. Preparation of polyplexes

The polyplexes were made by self-assembly complexation. The polycations chitosan XS, chitosan S, chitosan OSL, PEI and the polyanionic DNAzyme Dz13 were dissolved in a reaction buffer (100 mM TEAA-acetic acid, 1 mM $MgCl_2$, pH 5.0). The polycation solutions were each mixed with the Dz13 solution. The final Dz13 concentration was 100 μg/mL, whereas the polycation concentration was in a range between 5 and 500 μg/mL. The corresponding N/P ratio (ratio between phosphate groups of the DNA and free amino groups of a polycation) varied for each polycation.

2.6. Characterization of polyplexes

The degree of protonation of polycation's amino groups was determined with a potentiometric titration. First, 50 mg of polycation was dissolved in 100 mL of deionized water containing 100 mM NaCl. In case of chitosan, the water was acidified with additional 0.15 mL of 100 mM HCl and the solution was stepwise back-titrated with a solution of 100 mM NaOH. In case of PEI, no HCl was added and the titration was done with a solution of 100 mM HCl. The pH was measured with a pH meter (SG78, Mettler-Toledo, Giessen, Germany). The titration was done in duplicates. The acid dissociation constant (pK_a) was determined at the inflexion point of chitosan. The pK_a of PEI at each pH value was calculated using Eq. (1). The parameters α and β are the slope and the axis intercept of a linear relation between the common logarithm of the deprotonation quotient and pH [17].

$$pK_a = (1 - \alpha) \times pH - \beta \quad (1)$$

The polyplexes were characterized at about 30 min after polyplex formation. The size distribution was measured according to the dynamic light scattering and is indicated with z-average size (z-average) and polydispersity index (PDI) (Zetasizer Nano Z, Malvern, Worcestershire, UK). If the particle exceeded the size of 1 μm, the polyplexes were measured by static light scattering and the particle size is indicated as Sauter mean diameter (Mastersizer

2000, Malvern, Worcestershire, UK). The zeta potential was measured with the Zetasizer Nano Z. Samples of all measurements were diluted in TEAA buffer (100 mM TEAA-acetic acid, 1 mg $MgCl_2$, pH 5.0). All samples were tested in triplicates, and the data are presented as the mean ± SD. To visualize polyplexes at high ξ ratios the samples were dried and sputtered with gold. Images were taken with a scanning electron microscope (SEM) (EVO LS10, Zeiss, Jena, Germany) using an electron acceleration voltage of 20 kV.

To determine the degree of complexation of the polyplexes, a competitive displacement assay was developed. The fluorescent emission of the cationic fluorescent dye (basic yellow 40) increased if the dye bound to single-stranded DNA. Adding a competitive polycation such as chitosan or PEI released the dye from the Dz13 and the emission decreased. The fluorescent dye (final concentration 1% (w/v)) was incubated with different amounts of Dz13 standards (2.5–100 μg/mL) or with polyplexes at different N/P ratios using a TEAA buffer (100 mM TEAA-acetic acid, 1 mM $MgCl_2$, pH 5.0). The emission (485/528 nm) was measured with the plate reader (Synergy HTX, BioTek Instruments, Berlin, Germany). To decomplex the polyplexes, lithium-heparin was added for a final concentration of 0.1% (w/v). All samples were tested six times, and the data are presented as the mean ± SD.

The stability of the polyplexes was measured with the gel retardation assay. The method has been previously described with modifications [9]. In brief, the polyplexes were loaded into an agarose gel and an electric field was applied. Afterward, the DNAzyme of the polyplexes was stained with a fluorescent dye to document mobility. Modifications were made in terms of the TEA buffer and the loading buffer. The pH value of both buffers was set to 5.0 and the loading buffer was changed to 6% glycerol and 50% TEA buffer.

2.7. DNAzyme degradation assay

2.7.1. Skin surface

Polyplexes consisting of 100 μg/mL Dz13 and different polycations at a variety of N/P ratios were incubated with a final concentration of 5.9 Units/mL DNase II (33 °C, 300 rpm, 90 min). The reaction was stopped by phenol-chloroform extraction and analyzed by the AEX-HPLC method. The data are presented relative to untreated Dz13 standards. All experiments were repeated six times, and are presented as the mean ± SD.

2.7.2. Full thickness skin

Human facial skin was obtained from female Caucasian volunteers undergoing plastic reduction. The three donors have given their written permission to use the *ex vivo* samples for scientific examinations and the procedure was in accordance with the Ethical Conduct for Research Involving Humans. 0.5 g of each cryopreserved skin specimen was incubated in 1 mL extraction buffer (100 mM TEAA-acetic acid, 1 mg $MgCl_2$, pH 5.0) for 1 h and 300 rpm. 50 μL Dz13 (200 μg/mL) alone or with different chitosan S polyplexes (ξ ratio: 0.31, 0.63, 1.01, 1.26, 6.29) was incubated with 50 μL skin extract (33 °C, 300 rpm, 15 min). The reactions were stopped and purified by phenol-chloroform extraction. Non-treated controls were incubated with heat inactivated skin extracts of each donor. The results are summarized as the mean ± SD.

2.8. Statistics

Statistical analysis was performed with OriginPro 8. To determine significant differences in the mean of families, a one-way Analysis of Variance (ANOVA) was performed. The homogeneity of variance was tested with a Levene's test. As a post hoc test, the Bonferroni analysis was used. A significance level of $p < 0.05$ was used.

3. Results and discussion

3.1. Degradation of dermally applied DNAzymes

3.1.1. Identification of the degrading enzyme on human skin

The present study focused on the human skin surface to identify the most degrading enzyme against DNAzymes. In a previous study, it was shown that the skin surface is the most degrading layer during drug delivery [8]. On the skin, a variety of different degrading enzymes can cleave DNA-based APIs. The degradation with each enzyme will ideally result in different DNA fragments. Following this assumption analysis of a fragment pattern could in turn give information about the prevalent degrading enzyme. Therefore, the degradation pattern of the Dz13 on human skin was obtained and qualitatively analyzed by AEX-HPLC. The AEX-HPLC separated DNA fragments according to the amount of negatively charged phosphates. The resulting chromatogram shows DNA absorption peaks at different time points, according to the length of the DNA fragment (Fig. 1). The intact Dz13, with 34 nucleotides, had one characteristic peak at a retention time of about 16.2 min, whereas the enzymatically degraded Dz13 showed multiple DNA fragments, which generated characteristic degradation patterns. In order to associate the skin's degradation pattern with a DNase pattern, a broad range of DNase representatives was analyzed. The reaction parameter, time and pH value were varied to investigate robustness of the degradation patterns. Despite previous reports, monitoring the patterns at an initial and an advanced stage revealed no changes in the degradation mechanisms [18]. The pH value of the reaction was varied between 5.0 and 6.6 (data not shown), to represent the pH range of the whole skin [19]. The highest pH dependency was examined with T5 exonuclease, which was only active at a pH value of 7.9 and failed to be compared with a more acidic pH value. In contrast, the remaining DNases were active at both pH values and their specific degradation patterns remained unchanged. In fact, the degradation pattern was so consistent that a comparison of the pattern can be used to identify the degrading enzyme of DNAzymes on the human skin. To exclude individual skin abnormalities, the patterns of three individual persons (data not shown) and a pool of six persons were compared and, irrelevant of the origin, no variations were observed. The degradation pattern had characteristic DNA fragments at a range of n − 1 to n − 4 and products around n − 15. The n − 1 to n − 4 fragments could be an indication for an exonuclease activity. But in comparison with the purified DNases, neither the micrococcal exonuclease nor T5 exonuclease nor DNase I had similarities. However, the DNase II did have a comparable degradation pattern with DNA fragments of similar sizes. Moreover, the n − 1 to n − 4 fragments could be explained by the high concentration of purine at the 5′ end of the Dz13, which is a preference for DNase II cleavage [20]. Furthermore, the fragments of around n − 15 can be attributed to the CpG-A motif in the catalytic domain of the 10–23 DNAzymes, which is a cleavage site of DNase II [21]. Exchanging the CpG-A motif by a triplicate of deoxyadenosine resulted in the absence of the particular fragments. In conclusion, a DNase II-like activity was identified against the DNAzyme Dz13 on the human skin. This result is in agreement with Fischer et al., who identified DNase II as a main degrading enzyme of the stratum corneum but only when using double stranded DNA substrates of higher lengths [12].

3.1.2. Determination of the enzyme activity on human skin

The specific activity of the enzyme on the skin was determined by two independent methods. Using both methods would reduce the error of the determined specific activity value, because the specific errors of each analytic method would be diminished.

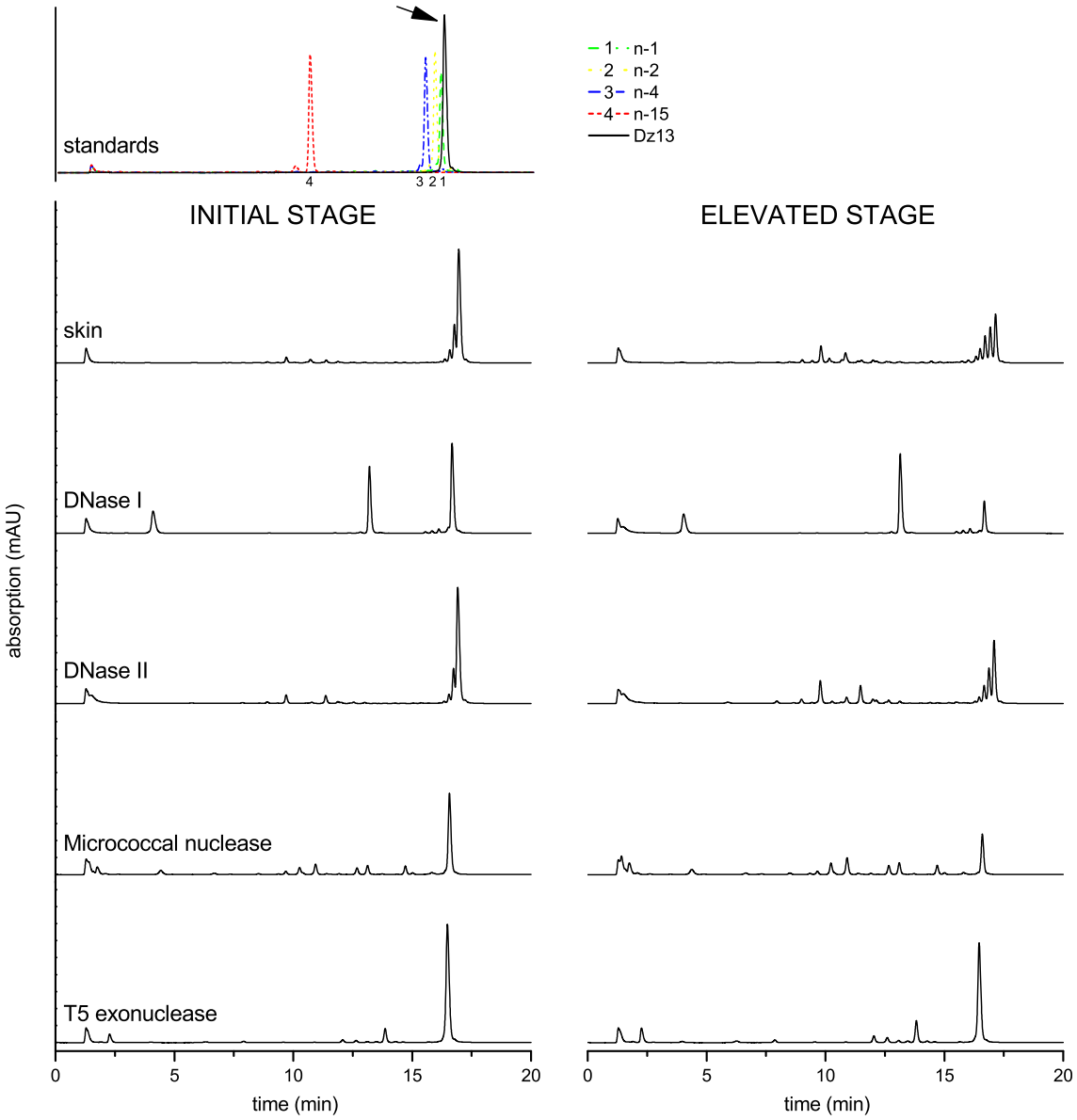

Fig. 1. AEX-HPLC chromatograms of Dz13 after degradation with different types of DNases and human skin. Chromatograms show degradation products at two different stages of degradation. The reactions were done at pH value 5.0, except T5 exonuclease (pH 7.9). Arrow indicates intact Dz13.

The real-time analysis used a developed fluorescence assay. The Dz13 was modified with a fluorescent dye and a corresponding dark quencher. If the FAM-Dz13-Q molecule was intact, the specific fluorescent emission was absorbed by the quencher. Degradation of the FAM-Dz13-Q separated the fluorescent dye from the corresponding quencher and an increased emission signal could be monitored. The curve of the resulting emission was fitted and the maximal slope represented the maximal conversion rate (Fig. 2A). The resulting specific activity of human skin was determined with 0.59 ± 0.01 Units/mg relative to DNase II standards. The endpoint analysis determined the integrity of Dz13 at different time points. Therefore, the intact Dz13 was quantified by AEX-HPLC (Fig. 2B). Using the endpoint analysis, the specific activity on the skin was determined with 0.59 ± 0.27 Units/mg relative to DNase II standards. However, to decelerate the activity of purified DNase II, suppliers use double stranded DNA by default. But double stranded DNA gets degraded faster than single stranded DNA such as DNAzymes [22]. The method can determine the actual activity without the need of DNase standards. The resulting actual activity was found to be $5.6 \cdot 10^{-5}$ Units/mg and therefore 10^5 fold lower than the activity relative to DNase standards. Although two different analytic methods were used, both methods revealed nearly equal results. However, comparable data could not be found in the literature to evaluate the determined values.

3.2. Characterization of polyplexes

The characterization of polyplexes is important, because the various properties have a large impact on different approaches. Size and zeta potential of the particles have influence on colloidal stability, skin penetration and cellular uptake [23–25]. The degree of complexation and complex stability will influence the protective effects and API release characteristics [26–28]. A characterization of polyplexes with different polycations in a broad range of N/P ratios was done using different kinds of biodegradable chitosans (Fig. 4). In addition, PEI was selected because the polycation is often considered as a gold standard in DNA delivery [29]. The degree of protonation of the polycation's amino groups is one of

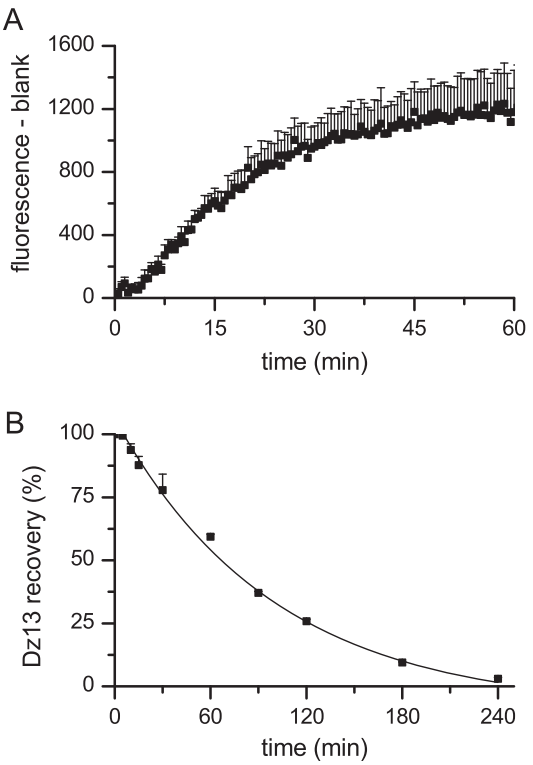

Fig. 2. Determination of Dz13 degrading activity of the skin (mean ± SD, $n = 6$). Degrading activity was monitored by real-time fluorescence analysis. The offset was set to zero (A). Degrading activity was measured by an endpoint analysis (B).

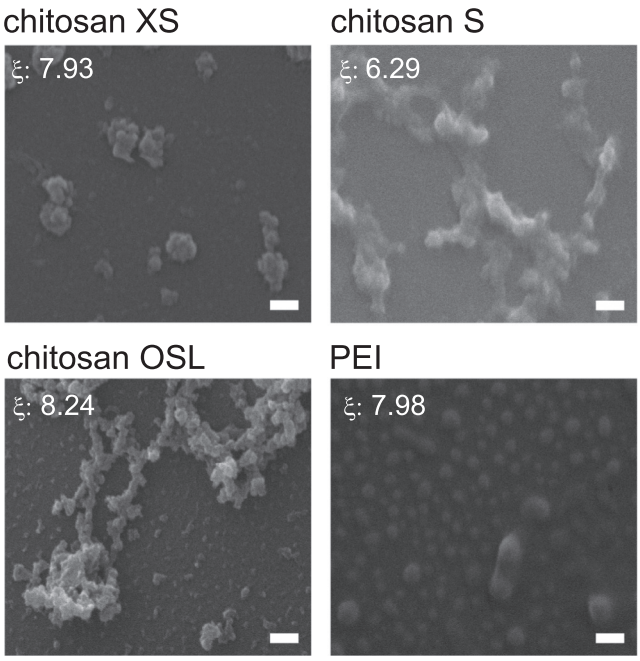

Fig. 3. SEM images of different polyplexes with high ξ ratios. Scale bars indicate 200 nm.

the main aspects of polyplex formation. The used chitosans possessed primary amino groups with similar residues, which resulted in specific pK_a values for each chitosan. The specific pK_a values revealed almost completely protonated amino groups at a pH value of 5.0 (Table 1). Under the particular conditions the N/P ratio was equal to the ξ ratio (N/P ratio = ξ_C ratio). On the contrary, the branched PEI possessed a high amount and high variety of amino groups with different residues, which complicates the determination of one specific pK_a. Therefore, potentiometric titration data had to be additionally fitted with a model proposed by Suh et al. [17]. The resulting $\alpha = 0.1895$ and $\beta = -1.0485$ were used to determine a pK_a value for each pH value. At a pH value between 5.0 and 5.1, only 55–56% of the groups were protonated. The partial protonation leads to the outcome, that the N/P ratio was unequal to the ξ ratio (N/P ratio ≠ ξ_P ratio).

The degree of protonation, and thus, the ξ ratio, influenced the zeta potential of the produced polyplexes. The zeta potential provided information about the surface potential of polyplexes. A low ξ ratio with an excess of the Dz13 resulted in negative zeta potentials, whereas a high ξ ratio with an excess of polycations

Table 1
Properties of different polyplexes at different ξ ratios. Particle size measured with DLS or SLS. The degree of protonation was determined with potentiometric titration.

	$\xi_{C,P}$ ratio	z-average (d nm)	PDI	Sauter mean diameter (nm)	pH value	Degree of protonation (%)
Chitosan XS	7.93	186 ± 34	0.3 ± 0.1		5.0 ± 0.0	98
	3.17	243 ± 45	0.2 ± 0.0		5.0 ± 0.0	98
	2.78	333 ± 108	0.3 ± 0.0		5.0 ± 0.0	98
	1.59			$(49 \pm 5) \cdot 10^3$	5.0 ± 0.0	98
	0.40			$(8 \pm 4) \cdot 10^3$	5.0 ± 0.0	98
Chitosan S	6.29	344 ± 125	0.3 ± 0.2		5.1 ± 0.0	98
	2.52	353 ± 109	0.3 ± 0.2		5.0 ± 0.0	99
	1.26	377 ± 130	0.2 ± 0.2		5.0 ± 0.0	99
	1.01			$(91 \pm 31) \cdot 10^3$	5.0 ± 0.0	99
	0.63			$(75 \pm 20) \cdot 10^3$	5.0 ± 0.0	99
	0.31			$(17 \pm 3) \cdot 10^3$	5.0 ± 0.0	99
Chitosan OSL	8.24	222 ± 19	0.3 ± 0.1		5.0 ± 0.0	98
	3.33	326 ± 68	0.2 ± 0.0		5.0 ± 0.0	98
	3.05	592 ± 75	0.7 ± 0.0		5.0 ± 0.0	98
	1.65			$(72 \pm 12) \cdot 10^3$	5.0 ± 0.0	98
	0.21			$(8 \pm 4) \cdot 10^3$	5.0 ± 0.0	98
PEI	19.95	114 ± 20	0.2 ± 0.0		5.1 ± 0.0	55
	7.98	152 ± 21	0.1 ± 0.0		5.1 ± 0.0	55
	4.06	148 ± 12	0.1 ± 0.0		5.0 ± 0.0	56
	1.62			$(83 \pm 20) \cdot 10^3$	5.0 ± 0.0	56
	1.22			$(56 \pm 12) \cdot 10^3$	5.0 ± 0.0	56
	0.51	200 ± 69	0.3 ± 0.2		5.0 ± 0.0	56
	0.20	89 ± 8	0.4 ± 0.0		5.0 ± 0.0	56

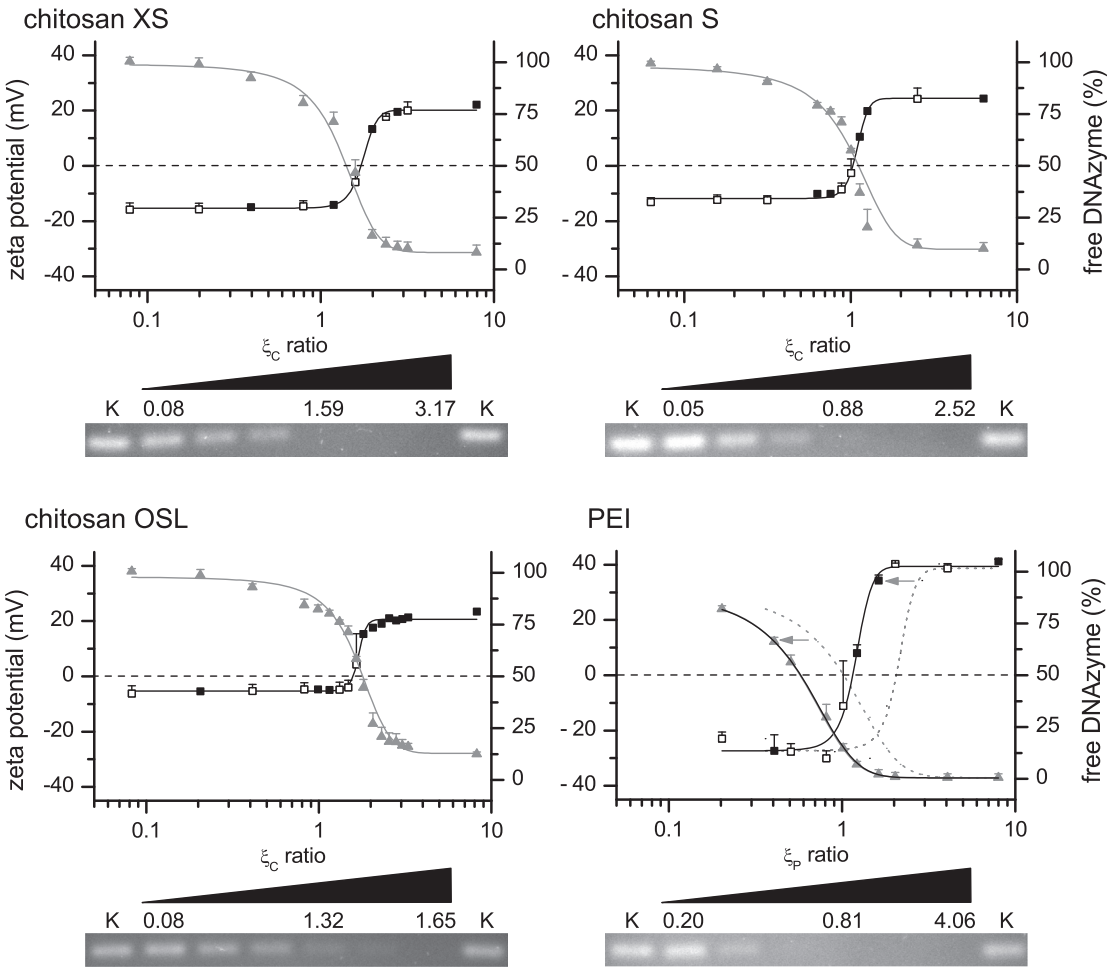

Fig. 4. Characterization of polyplexes from different polycations (mean ± SD, $n = 3$). Zeta potential (■) and degree of complexation in terms of free Dz13 (▲) at different ξ ratios are presented. Samples shown in the gel retardation assay are marked with □. The dotted graphs of PEI represent the dependency to N/P ratio.

resulted in positive values (Fig. 4). At ξ_{ISO}, the composition of polycation and polyanion neutralized each other resulting in a neutral zeta potential. The characteristic ξ_{ISO} values were at or near to an equal stoichiometric ratio and depended on the polycations. The specific ξ_{ISO} values followed the order: chitosan S ⩽ PEI < chitosan OSL ⩽ chitosan XS. The lower ξ_{ISO} values of chitosan S and PEI can be attributed to the formation of more stable polyplexes at lower ξ ratios due to a high MW of chitosan S or due to a high charge density, respectively. The stability of the polyplexes was visualized by a retarded mobility in the gel retardation assay as well. The polyplexes were able to cover the negative charge of the Dz13 in an applied electric field before the specific ξ_{ISO} values were acquired.

The degree of protonation is a primary parameter of complexation, but complexation is not restricted to the electrostatic interaction. In addition, a second hydrophobic binding mode between the polycation and the groove of DNA was reported for chitosan and PEI [30,31]. In the present study, the competitive displacement assay primarily monitored complexation via electrostatic binding. The assay revealed that the recovery of free DNAzyme was gradually reduced with the addition of polycations, whereas the degree of complexation increased (Fig. 4). In the case of chitosan, the ξ ratio at a degree of complexation of 50% (ξ_{50}) was at 1 or between 1 and 2. Consequently, about two amino groups of the chitosan polymer were necessary to complex one phosphate group of the Dz13. The degree of complexation levelled off at around 90% with positively overcharged polyplexes. The lower ξ_{50} value of chitosan S was related to the MW. The flexibility of polymers increased with the chain size [32]. Therefore, chitosan S needs less amino groups to entangle the DNA strand of Dz13. In comparison, PEI had a lower ξ_{50} value of 0.5 and at ξ_{ISO} the Dz13 was entirely complexed. The difference between the polycations can be related to the type of binding. Whereas the complex formation of PEI was driven by the electrostatic binding mode, the complexation with chitosan could be attributed to an additionally hydrophobic binding mode due to a lower charge density along with incomplete deacetylation. Charge density and MW are generally important factors in particle size formation [24]. The size of polyplexes generally depended on the zeta potential, despite the fact that different types of polycations were analyzed (Table 1). In near isoelectric conditions (ξ_{ISO}), polyplexes obtained the highest sizes and polyplexes agglomerated within hours. The smallest particle sizes were achieved at high ξ ratios with a positive zeta potential. Such size reduction is consistent with a gain in electrostatic repulsion of the particles. The visualization of the polyplexes showed grape like structures (Fig. 3). Polyplexes of PEI showed the least aggregation tendency, while SEM sample preparation. Polyplexes of chitosan S formed polymer films including spherical particles.

3.3. Validation of polyplexes on skin

Polyplexes have already been shown to protect DNA-based molecules against degradation on porcine skin [9], but the protective efficiency of polyplexes on human skin remains to be exam-

ined. In order to screen a higher amount of different kinds of polyplexes an *in vitro* degradation assay was developed. Therefore, the degrading activity of human skin was simulated using DNase II at the determined activity. The polyplexes of each polycation were tested in a wide variety of ξ ratios (Fig. 5). At a critical ξ ratio (ξ_{cri}), a complete protection could be achieved without significant difference to a corresponding control. The ξ_{cri} ratio depended on the selected polycation and the polyplex properties following the order: chitosan S < chitosan XS ⩽ chitosan OSL < PEI. At the ξ_{cri} ratios, the zeta potential and the degree of complexation were at the maximum levels. The high degree of complexation ensured that each DNAzyme molecule had been bound and shielded by the surrounding polycations. Only chitosan S protected the Dz13 at the lowest ξ_{cri} ratio without a complete complexation. The experiment revealed some protection at a ratio of 0.63 and full protection at 1.01, indicating that the specific threshold for sufficient protection was somewhere between the two ratios. The polycation could better entangle the nucleic acid, resulting in a more effective sterical hindrance, due to high molecular and flexible polymer chains [33]. This observation is in accordance with the high stability of the gel retardation assay. However, PEI possessed a high stability, and the highest complexation efficiency, but had the lowest protection efficiency. The high charge density, and hence, the high electrostatic binding, positively affected stability and complexation of the polyplexes, but did not efficiently shield the Dz13. This result supports the assumption that the sterical hindrance is not only affected by electrostatic binding, but also by the hydrophobic binding mode. Considering all empirical data, the following observation can be made: In terms of polycation properties, a high MW positively affected the protective efficiency. In addition, the ξ ratio controlled the physicochemical properties of a polyplex, whereas a levelled off zeta potential is a good indicator for a sufficient protection of DNAzymes. Concerning a therapeutic application, polyplexes based on chitosan, would be favorable due to biodegradability and low toxicity [34]. On the other hand, polyplexes with PEI are known to have a high transfection ability along with an endosomal escape, which would increase the amount of DNAzymes at the cytoplasm of skin cells [35]. But PEI is a non-degradable polycation which has a tendency to be toxic [36].

Concerning an appropriate dermal DDS, the protection of DNAzymes is one major part besides skin penetration and cellular uptake of the API. In a previous study a dermal DDS was developed that combined the penetration enhancing effects of a SME with the protective effects of chitosan-polyplexes [9]. The study showed that the dermal DDS was able to protect and enhance penetration of DNAzymes into *ex vivo* porcine skin. A first examination was done to determine the protective efficiency of Dz13 in human skin. Therefore, the most promising polyplexes with chitosan S were incubated with *ex vivo* full thickness skin to determine the protective efficiency. Without polyplex protection the Dz13 was degraded and only 39.7 ± 11.8% of intact Dz13 was recovered. At a ξ ratio between 0.63 and 1.01 the recovery rate raised from 56.0 ± 3.7% to 80.5 ± 2.9%. At a ξ ratio of 1.26 the recovery rate (94.1 ± 9.0%) did not show a significant difference to the non-treated control (heat inactivated skin extract) and was therefore declared as ξ_{crit} ratio. In comparison with skin surface, the higher degradation rates can be explained by a loss of complex stability due to competitive interferences of skin's polyelectrolytes [37].

The data of the present study confirmed the protective effects of polyplexes on and in human skin and will help to optimize further approaches of the dermal DDS. Aspects of penetration and cellular uptake of DNAzymes with the particular dermal DDS with human skin remain to be analyzed.

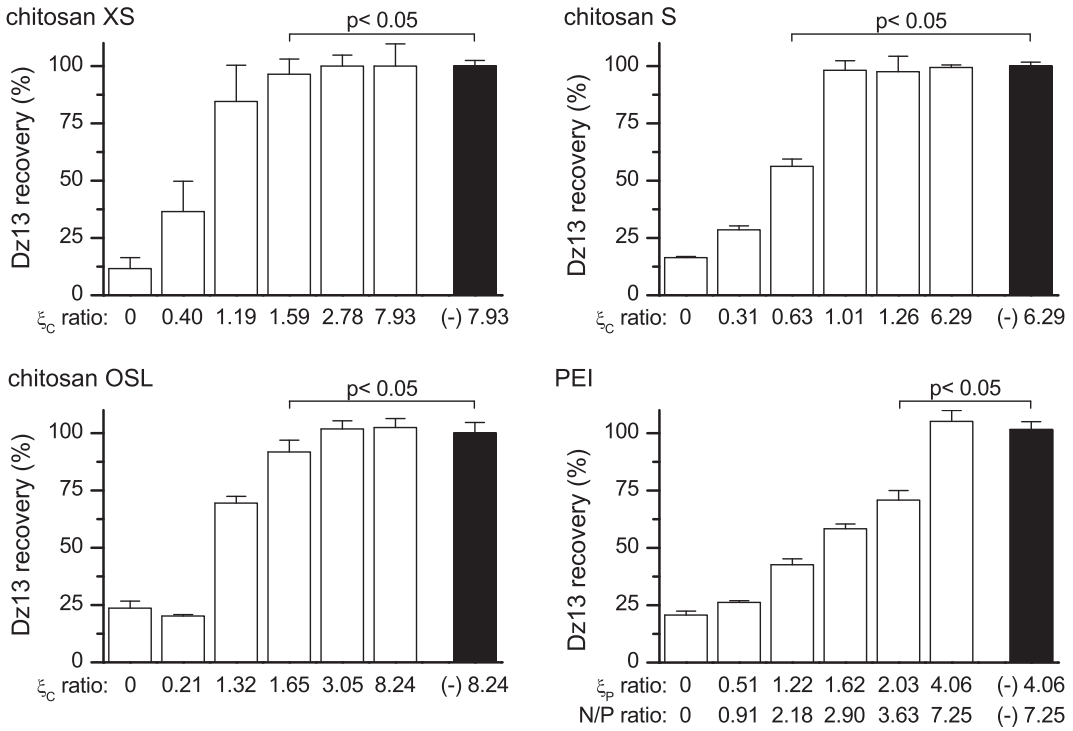

Fig. 5. Degradation assay was done with different polyplexes at different ξ ratios (mean ± SD, $n = 6$). The polyplexes with a fixed Dz13 amount were incubated in DNase II to simulate the human skin and the intact Dz13 was quantified afterward with AEX-HPLC. Data are presented relative to the corresponding control without DNase treatment. (–); indicates control without DNase II treatment. Significant differences were calculated by one-way ANOVA following a Bonferroni test.

4. Conclusion

In the present work, the degradation and protection of a DNA-based API on human skin were analyzed. The determination of the degradation pattern of a DNAzyme on the skin could be related to that of DNase II activity, with a specific activity of 0.59 Units/mg. The results were used to develop an *in vitro* degradation assay. The assay was successfully used to screen different polyplexes for the protective efficiency on human skin. Depending on the ξ ratio of the polyplexes, the DNAzyme could be sufficiently protected against degradation. The high MW of the biodegradable chitosan S resulted in the highest protective efficiency, whereas PEI had the lowest protective efficiency.

Acknowledgments

This work was supported by the German Federal Ministry of Education and Research [grant number 03FH031|3]. Furthermore, the authors would like to thank Sebastian Beer and Elke Landrock-Bill for SEM imaging.

References

[1] S.W. Santoro, G.F. Joyce, A general purpose RNA-cleaving DNA enzyme, Proc. Natl. Acad. Sci. USA 94 (9) (1997) 4262–4266.
[2] M.J. Cairns, T.M. Hopkins, C. Witherington, L. Wang, L.Q. Sun, Target site selection for an RNA-cleaving catalytic DNA, Nat. Biotechnol. 17 (5) (1999) 480–486, http://dx.doi.org/10.1038/8658.
[3] Y. Cao, L. Yang, W. Jiang, X. Wang, W. Liao, G. Tan, Y. Liao, Y. Qiu, D. Feng, F. Tang, B.L. Hou, L. Zhang, J. Fu, F. He, X. Liu, W. Jiang, T. Yang, L.-Q. Sun, Therapeutic evaluation of Epstein-Barr virus-encoded latent membrane protein-1 targeted DNAzyme for treating of nasopharyngeal carcinomas, Mol. Ther. 22 (2) (2014) 371–377, http://dx.doi.org/10.1038/mt.2013.257.
[4] U. Homburg, A. Turowska, J. Kuhlmann, A. Müller, J. Renz, J. Bille, H. Renz, H. Garn, Safety profile and pharmacokinetics of SB010, an inhaled GATA-3-specific DNAzyme, in phase I clinical trials in healthy and asthmatic subjects, Eur. Respir. J. 42 (Suppl. 57) (2013).
[5] E.-A. Cho, F.J. Moloney, H. Cai, A. Au-Yeung, C. China, R.A. Scolyer, B. Yosufi, M.J. Raftery, J.Z. Deng, S.W. Morton, P.T. Hammond, H.-T. Arkenau, D.L. Damian, D.J. Francis, C.N. Chesterman, Barnetson, C. Ross St, G.M. Halliday, L.M. Khachigian, Safety and tolerability of an intratumorally injected DNAzyme, Dz13, in patients with nodular basal-cell carcinoma: a phase 1 first-in-human trial (DISCOVER), Lancet 381 (9880) (2013) 1835–1843, http://dx.doi.org/10.1016/S0140-6736(12)62166-7.
[6] M.B. Appaiahgari, S. Vrati, DNAzyme-mediated inhibition of Japanese encephalitis virus replication in mouse brain, Mol. Ther. 15 (9) (2007) 1593–1599, http://dx.doi.org/10.1038/sj.mt.6300231.
[7] A.A. Fokina, D.A. Stetsenko, J.-C. François, DNA enzymes as potential therapeutics: towards clinical application of 10–23 DNAzymes, Expert Opin. Biol. Ther. 15 (5) (2015) 689–711, http://dx.doi.org/10.1517/14712598.2015.1025048.
[8] T. Schmidts, K. Marquardt, P. Schlupp, D. Dobler, F. Heinz, U. Mäder, H. Garn, H. Renz, J. Zeitvogel, T. Werfel, F. Runkel, Development of drug delivery systems for the dermal application of therapeutic DNAzymes, Int. J. Pharm. 431 (1–2) (2012) 61–69, http://dx.doi.org/10.1016/j.ijpharm.2012.04.034.
[9] K. Marquardt, A.-C. Eicher, D. Dobler, U. Mäder, T. Schmidts, H. Renz, F. Runkel, Development of a protective dermal drug delivery system for therapeutic DNAzymes, Int. J. Pharm. 479 (1) (2014) 150–158, http://dx.doi.org/10.1016/j.ijpharm.2014.12.043.
[10] L. Eckhart, H. Fischer, E. Tschachler, Mechanisms and emerging functions of DNA degradation in the epidermis, Front Biosci. (Landmark Ed) 17 (2012) 2461–2475.
[11] P. Santoianni, S. Rothman, Nucleic acid-splitting enzymes in human epidermis and their possible role in keratinization, J. Invest. Dermatol. 37 (1961) 489–495.
[12] H. Fischer, J. Scherz, S. Szabo, M. Mildner, C. Benarafa, A. Torriglia, E. Tschachler, L. Eckhart, DNase 2 is the main DNA-degrading enzyme of the stratum corneum, PLoS ONE 6 (3) (2011) e17581, http://dx.doi.org/10.1371/journal.pone.0017581.
[13] E.T. Berends, A.R. Horswill, N.M. Haste, M. Monestier, V. Nizet, M. von Köckritz-Blickwede, Nuclease expression by *Staphylococcus aureus* facilitates escape from neutrophil extracellular traps, J. Innate Immun. 2 (6) (2010) 576–586, http://dx.doi.org/10.1159/000319909.
[14] L. Eckhart, H. Fischer, K.B. Barken, T. Tolker-Nielsen, E. Tschachler, DNase1L2 suppresses biofilm formation by *Pseudomonas aeruginosa* and *Staphylococcus aureus*, Br. J. Dermatol. 156 (6) (2007) 1342–1345, http://dx.doi.org/10.1111/j.1365-2133.2007.07886.x.
[15] H. Dautzenberg, W. Jaeger, Effect of charge density on the formation and salt stability of polyelectrolyte complexes, Macromol. Chem. Phys. 203 (14) (2002) 2095–2102, http://dx.doi.org/10.1002/1521-3935(200210)203:14<2095:AID-MACP2095>3.0.CO;2-9.
[16] L.M. Khachigian, R.G. Fahmy, G. Zhang, Y.V. Bobryshev, A. Kaniaros, C-Jun regulates vascular smooth muscle cell growth and neointima formation after arterial injury. Inhibition by a novel DNA enzyme targeting c-Jun, J. Biol. Chem. 277 (25) (2002) 22985–22991, http://dx.doi.org/10.1074/jbc.M200977200.
[17] J. Suh, H.J. Paik, B.K. Hwang, Ionization of poly(ethylenimine) and poly (allylamine) at various pH′s, Bioorg. Chem. 22 (3) (1994) 318–327, http://dx.doi.org/10.1006/bioo.1994.1025.
[18] G. Bernardi, Spleen acid deoxyribonuclease, in: P.D. Boyer (Ed.), The Enzymes, Academic Press, New York, USA, 1971, pp. 271–287.
[19] H. Wagner, K.H. Kostka, C.M. Lehr, U.F. Schaefer, PH profiles in human skin: influence of two in vitro test systems for drug delivery testing, Eur. J. Pharm. Biopharm. 55 (1) (2003) 57–65.
[20] C.J. Evans, R.J. Aguilera, DNase II: genes, enzymes and function, Gene 322 (2003) 1–15.
[21] M.P. Chan, M. Onji, R. Fukui, K. Kawane, T. Shibata, S.-I. Saitoh, U. Ohto, T. Shimizu, G.N. Barber, K. Miyake, DNase II-dependent DNA digestion is required for DNA sensing by TLR9, Nat. Commun. 6 (2015) 5853, http://dx.doi.org/10.1038/ncomms6853.
[22] I. Harosh, D.M. Binninger, P.V. Harris, M. Mezzina, J.B. Boyd, Mechanism of action of deoxyribonuclease II from human lymphoblasts, Eur. J. Biochem. 202 (2) (1991) 479–484.
[23] Q. Gan, T. Wang, C. Cochrane, P. McCarron, Modulation of surface charge, particle size and morphological properties of chitosan—TPP nanoparticles intended for gene delivery, Colloids Surf B Biointerfaces 44 (2–3) (2005) 65–73, http://dx.doi.org/10.1016/j.colsurfb.2005.06.001.
[24] M.D. Buschmann, A. Merzouki, M. Lavertu, M. Thibault, M. Jean, V. Darras, Chitosans for delivery of nucleic acids, Adv. Drug Deliv. Rev. 65 (9) (2013) 1234–1270, http://dx.doi.org/10.1016/j.addr.2013.07.005.
[25] F. Rancan, Q. Gao, C. Graf, S. Troppens, S. Hadam, S. Hackbarth, C. Kembuan, U. Blume-Peytavi, E. Rühl, J. Lademann, A. Vogt, Skin penetration and cellular uptake of amorphous silica nanoparticles with variable size, surface functionalization, and colloidal stability, ACS Nano 6 (8) (2012) 6829–6842, http://dx.doi.org/10.1021/nn301622h.
[26] M. Bertschinger, G. Backliwal, A. Schertenleib, M. Jordan, D.L. Hacker, F.M. Wurm, Disassembly of polyethylenimine-DNA particles in vitro: implications for polyethylenimine-mediated DNA delivery, J. Control. Release 116 (1) (2006) 96–104, http://dx.doi.org/10.1016/j.jconrel.2006.09.006.
[27] M. Köping-Höggård, I. Tubulekas, H. Guan, K. Edwards, M. Nilsson, K.M. Vårum, P. Artursson, Chitosan as a nonviral gene delivery system. Structure-property relationships and characteristics compared with polyethylenimine in vitro and after lung administration in vivo, Gene Ther. 8 (14) (2001) 1108–1121, http://dx.doi.org/10.1038/sj.gt.3301492.
[28] F.C. MacLaughlin, R.J. Mumper, J. Wang, J.M. Tagliaferri, I. Gill, M. Hinchcliffe, A. P. Rolland, Chitosan and depolymerized chitosan oligomers as condensing carriers for in vivo plasmid delivery, J. Control. Release 56 (1–3) (1998) 259–272.
[29] S. Patnaik, K.C. Gupta, Novel polyethylenimine-derived nanoparticles for in vivo gene delivery, Expert Opin. Drug Deliv. 10 (2) (2013) 215–228, http://dx.doi.org/10.1517/17425247.2013.744964.
[30] W. Liu, S. Sun, Z. Cao, X. Zhang, K. Yao, W.W. Lu, K.D.K. Luk, An investigation on the physicochemical properties of chitosan/DNA polyelectrolyte complexes, Biomaterials 26 (15) (2005) 2705–2711, http://dx.doi.org/10.1016/j.biomaterials.2004.07.038.
[31] K. Utsuno, H. Uludağ, Thermodynamics of polyethylenimine-DNA binding and DNA condensation, Biophys. J. 99 (1) (2010) 201–207, http://dx.doi.org/10.1016/j.bpj.2010.04.016.
[32] X. Liu, K.A. Howard, M. Dong, M.Ø. Andersen, U.L. Rahbek, M.G. Johnsen, O.C. Hansen, F. Besenbacher, J. Kjems, The influence of polymeric properties on chitosan/siRNA nanoparticle formulation and gene silencing, Biomaterials 28 (6) (2007) 1280–1288, http://dx.doi.org/10.1016/j.biomaterials.2006.11.004.
[33] W.E. Rudzinski, T.M. Aminabhavi, Chitosan as a carrier for targeted delivery of small interfering RNA, Int. J. Pharm. 399 (1–2) (2010) 1–11, http://dx.doi.org/10.1016/j.ijpharm.2010.08.022.
[34] T. Kean, M. Thanou, Biodegradation, biodistribution and toxicity of chitosan, Adv. Drug Deliv. Rev. 62 (1) (2010) 3–11, http://dx.doi.org/10.1016/j.addr.2009.09.004.
[35] O. Boussif, F. Lezoualc'h, M.A. Zanta, M.D. Mergny, D. Scherman, B. Demeneix, J. P. Behr, A versatile vector for gene and oligonucleotide transfer into cells in culture and in vivo: polyethylenimine, Proc. Natl. Acad. Sci. USA 92 (16) (1995) 7297–7301.
[36] S. Kawakami, Y. Ito, P. Charoensit, F. Yamashita, M. Hashida, Evaluation of proinflammatory cytokine production induced by linear and branched polyethylenimine/plasmid DNA complexes in mice, J. Pharmacol. Exp. Ther. 317 (3) (2006) 1382–1390, http://dx.doi.org/10.1124/jpet.105.100669.
[37] S. Danielsen, S. Strand, C. de Lange Davies, B.T. Stokke, Glycosaminoglycan destabilization of DNA—chitosan polyplexes for gene delivery depends on chitosan chain length and GAG properties, Biochim. Biophys. Acta 1721 (1–3) (2005) 44–54, http://dx.doi.org/10.1016/j.bbagen.2004.10.011.

III. Evaluation and quantification of spectral information in tissue by confocal microscopy. In: *Journal of Biomedical Optics* 17 (10), S. 106011.

Journal of Biomedical Optics

SPIEDigitalLibrary.org/jbo

Evaluation and quantification of spectral information in tissue by confocal microscopy

Ulf Maeder
Kay Marquardt
Sebastian Beer
Thorsten Bergmann
Thomas Schmidts
Johannes T. Heverhagen
Klemens Zink
Frank Runkel
Martin Fiebich

Evaluation and quantification of spectral information in tissue by confocal microscopy

Ulf Maeder,[a] Kay Marquardt,[b] Sebastian Beer,[a] Thorsten Bergmann,[a] Thomas Schmidts,[b] Johannes T. Heverhagen,[c] Klemens Zink,[a] Frank Runkel,[b] and Martin Fiebich[a]
[a]Technische Hochschule Mittelhessen—University of Applied Sciences, Institute of Medical Physics and Radiation Protection, Wiesenstraße 14, 35390 Gießen, Germany
[b]Technische Hochschule Mittelhessen—University of Applied Sciences, Institute of Bioprocess Engineering and Pharmaceutical Technology, Wiesenstraße 14, 35390 Gießen, Germany
[c]Inselspital, University Hospital, Institute of Diagnostic, Interventional and Pediatric Radiology, Bern, Switzerland

Abstract. A confocal imaging and image processing scheme is introduced to visualize and evaluate the spatial distribution of spectral information in tissue. The image data are recorded using a confocal laser-scanning microscope equipped with a detection unit that provides high spectral resolution. The processing scheme is based on spectral data, is less error-prone than intensity-based visualization and evaluation methods, and provides quantitative information on the composition of the sample. The method is tested and validated in the context of the development of dermal drug delivery systems, introducing a quantitative uptake indicator to compare the performances of different delivery systems is introduced. A drug penetration study was performed *in vitro*. The results show that the method is able to detect, visualize and measure spectral information in tissue. In the penetration study, uptake efficiencies of different experiment setups could be discriminated and quantitatively described. The developed uptake indicator is a step towards a quantitative assessment and, in a more general view apart from pharmaceutical research, provides valuable information on tissue composition. It can potentially be used for clinical *in vitro* and *in vivo* applications. [DOI: 10.1117/1.JBO.17.10.106011]

Keywords: spectral imaging; skin visualization; drug delivery; skin penetration study; confocal microscopy; quantitative uptake indicator.

Paper 12276 received May 3, 2012; revised manuscript received Jul. 19, 2012; accepted for publication Sep. 7, 2012; published online Oct. 1, 2012.

1 Introduction

The visualization of intrinsic and extrinsic substances in biological tissue is a very common task in the area of biomedical imaging. Fluorescence microscopy is a widely used technique to assess the local distribution of either intrinsic autofluorescent structures or incorporated fluorescent molecules. In the field of investigating drug delivery into biological tissue, especially skin tissue, fluorescent dyes are utilized in many cases as model agents. Amongst other techniques confocal,[1] multiphoton[2–5] and widefield[6] microscopy is used to evaluate pharmaceutical transdermal and dermal delivery systems.[7–9] Amongst others, highly potent approaches for delivery and therapy are microemulsion[10–12] and nanoparticle[13] formulations. Transdermal delivery systems are used for systemic drug distribution. Therefore the amount that permeated through the skin is of interest. *In vivo* studies commonly analyze the drug concentration in blood while *in vitro* studies, for example, have to analyze the concentration in equivalent receptor fluids. The drug concentration is normally determined by enzyme-linked immunosorbent assay (ELISA) or high-performance liquid chromatography (HPLC). The focus of dermal delivery systems is the penetration of drugs into the skin layers. An important parameter that can be assessed microscopically using vertical slices of the tissue is the penetration depth. The origin of tissues can be from excised skin addressing *in vitro* studies or in case of *in vivo* studies from skin biopsies. However, elaborated approaches using tape-stripping and HPLC analysis are often used for evaluation. HPLC analysis allows quantification of the drug in the whole sample without showing the distribution. Microscopy on the other hand shows the pathways of the transport but lacks the possibility to quantify without further calibration efforts.[1]

Microscopic tissue imaging is very promising in terms of identifying pathways and providing further inside in penetration processes. However, a major problem is that tissue often shows strong autofluorescence. Especially skin is very complex and consists of various endogenous fluorophores, such as melanin, elastin, riboflavin and NAD(P)H[2] and possesses a broad autofluorescence spectrum that may interfere with incorporated external dyes. Due to the overlapping spectra, the origin of the fluorescence in microscopic images cannot be easily distinguished by signal intensity alone. Recording spectral information along with intensity images would help in the identification. Some approaches for recording spectral information by means of hyperspectral setups can be found in the literature.

Previous studies describe the penetration of fluorophores into skin, skin tumor and irradiation investigations and the assessment of bruised and traumatic skin injuries.[14–19] Numerous further reports on spectral imaging that do not cover skin research are available.[20–24]

In this work we present a new confocal imaging approach with microscopic spatial resolution to visualize spectral information in tissue. The appropriate image processing steps based on normalized cross-correlation and the derivation of a new

Address all correspondence to: Ulf Maeder, Technische Hochschule Mittelhessen—University of Applied Sciences, Institute of Medical Physics and Radiation Protection, Wiesenstraße 14, 35390 Gießen, Germany. Tel: ++49 641 3092675; Fax: ++49 641 3092977; E-mail: ulf.maeder@kmub.thm.de

0091-3286/2012/$25.00 © 2012 SPIE

quantitative measure is described. The method is tested in the context of pharmaceutical development of drug delivery systems. In this study it is used to localize and evaluate fluorescent dyes in vertical slices of excised porcine skin to quantify uptake efficiency of a submicron emulsion for dermal transport. Although the method is discussed in the field of pharmaceutics, the method can be useful in more general applications in life-science imaging. Therefore, in addition to the presented *in vitro* considerations, potential *in vivo* applications are discussed.

2 Material and Methods

2.1 *Fluorescent Probe and Skin Autofluorescence*

Nile Red (Sigma-Aldrich, Germany) was used as a lipophilic fluorescent dye in the prepared submicron emulsion. The fluorescence spectrum of Nile Red remains stable over a wide pH range while influenced by the polarity of its solvents.[25] Figure 1 shows the emissions spectra of the dye, solved in 70% ethanol, in comparison to natural porcine skin measured by the confocal laser-scanning microscope. Nile Red has an emission peak at 580 nm excited with the 476 nm line of an argon laser. The broad autofluorescence spectrum of skin exists due to the numerous intrinsic fluorophores.

2.2 *Drug Delivery System Preparation*

Submicron emulsions were chosen as a delivery system because they have shown to enhance the penetration of substances into skin due to their particle size and surfactants.[26] Submicron emulsions are oil-in-water emulsions with a droplet size below one micrometer. It is a kinetic stable emulsion in which the droplet size is achieved by an incorporation of emulsifiers.[27] The oil phase consisted of oleth-3, -10, ethyloleat (Croda, Germany), coco-caprylat/caprat, cetearyl isononanoat (Cognis, Germany) and 0.002% Nile Red, while the aqueous phase consisted of sodium chloride, citric acid, potassium sorbate (Fagron, Germany), magnesium sulfate and glycerol (Caelo, Germany). The surfactant concentration was adjusted to achieve a hydrophilic-lipophilic balance value of 11. All ingredients obtained were of pharmaceutical grade. The physico-chemical properties were recorded to characterize the delivery system. The dynamic light scattering analyzing method (Zetasizer Nano ZS 90, Malvern Instruments, UK) showed a z-average size of 258 ± 3 nm with a polydispersity index of 0.16 ± 0.01. The viscosity of 2.4 ± 0.2 mPa $\cdot$ s was determined by RheoStress 300 Rheometer (ThermoHaake, Germany). Due to the preservation with potassium sorbate, the pH value was adjusted to 4.8 ± 0.2.

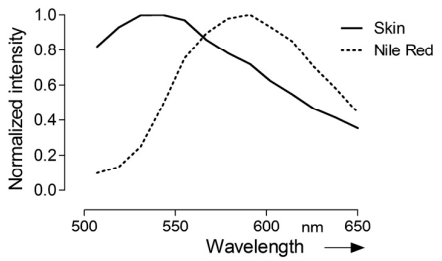

Fig. 1 Emission spectra of untreated porcine skin and the fluorescent dye Nile Red (Excitation: 476 nm). The spectral data was measured using the confocal microscope. The normalized presentation of the data shows the distinguishable emission peaks and the spectral overlap.

2.3 *Porcine Skin Samples*

Porcine ear skin is quite similar to human skin and was therefore used in this study.[28] Fresh ears of domestic pigs were obtained from a local abattoir and kept on ice during transport to the laboratory. After slaughtering, porcine ears were cleaned with water and shaved to remove the bristles. The full thickness skin was displaced with a scalpel and stored at −20 °C for less than three months.

Two preparation methods were used to obtain reference skin samples for validation measurements and penetration skin samples. The latter were used for the penetration study that evaluates delivery system performance.

2.4 *Reference Skin Samples*

The frozen skin specimens were cut into 10-μm thick slices using a cryo-microtom (Leica Microsystems, Germany) and then transferred into 70% ethanol with different Nile Red concentrations for 10 min. The dye was soaked up and excessive dye was removed from the skin under flowing water. The dye concentrations (0.2, 1, and 2 µg/mL) were chosen to cover a common recovery range of agents in the specimens of drug penetration studies. These reference skin samples were used to derive the sensitivity of the imaging scheme.

2.5 *Penetration Skin Samples*

The penetration of Nile Red into skin was performed on a Franz diffusion cell setup. On the day of experiment the frozen skin was thawed and fixed between the donor and receptor chamber of the Franz diffusion cell (Gauer Glas, Puettlingen, Germany). The penetration area had a diameter of 1.767 cm^2 and was in contact to 12 mL phosphate buffered saline (PBS) temperatured to 32.5 °C on the dermis side. The submicron emulsion was applied as infinite-dose (300 μL) for 3 h, 6 h, 8 h and 24 h to three porcine skin samples each to get a total of 12 experiment samples. After each time period, the skin was removed from the diffusion cell, wiped and washed with 50 mL aqua dest. The specimen was mounted into a freezing medium (Leica, Germany), shock frozen by fluid nitrogen and cut into various 10 μm thick vertical slices in order to prepare penetration samples for microscopy.

2.6 *Spectral Imaging*

Spectral imaging was performed using a TCS SP5 confocal laser-scanning microscope (Leica Microsystems, Mannheim, Germany) equipped with a detection unit that allows spectral discrimination to selectively detect narrow wavelength bands. The recorded fluorescence emission region (excitation at 476 nm) starting at 495 nm up to 650 nm (divided into 10 single detection bands that are 20 nm wide) was chosen to cover the spectra of porcine skin and Nile Red. A 0.7 NA water immersion objective (20×) was used and the image resolution was set to 512×512 pixel with a pixel size of 1.51 µm^2, resulting in a field of view of 775×775 µm^2. The generated image stacks were of the dimensions $xy\lambda$. The reference spectrum of Nile Red was recorded in the same way. Figures 2 and 3 give an overview of a 24 h penetration sample in comparison to natural (untreated) skin. The series of λ-stack pictures and an exemplary spectrum of the selected regions of interest (ROI) are shown to illustrate the different spectra. These spectral differences are used for the image processing scheme.

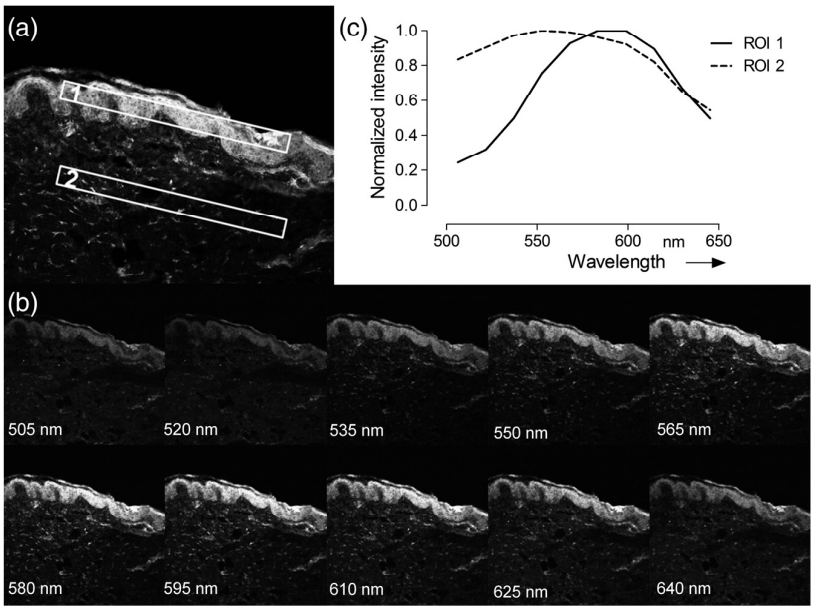

Fig. 2 Overview (a), images of the λ-stack (b) and spectra of ROI 1 and 2 (c) of a 24 h penetration skin sample. The given wavelengths of the λ-stack describe the center of the 20 nm wide wavebands.

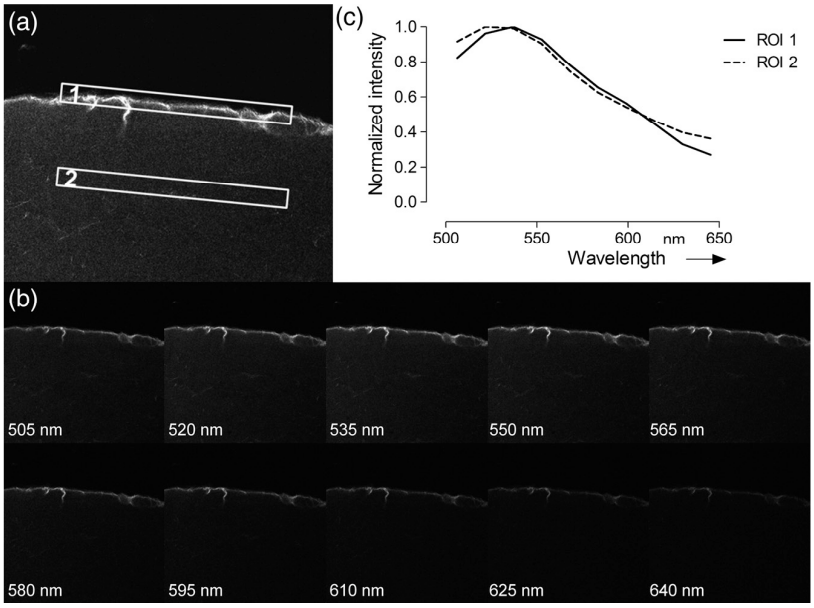

Fig. 3 Overview (a), images of the λ-Stack, (b) spectra of ROI 1 and 2, (c) of an untreated skin sample. The given wavelengths of the λ-stack describe the center of the 20 nm wide wavebands.

2.7 *Image Processing Scheme*

The image processing starts with the application of a threshold to exclude pixels with low intensities. The background or noisy image regions are excluded from the calculations. In the next step, the intensity data are normalized along the λ-axis to calculate intensity independent spectra for each image pixel. The normalized cross correlation (CC) metric is used to quantify the similarity between the normalized sample spectra and the reference spectra of Nile Red.

$$CC = \frac{\sum [S_{Ref}(i) - \bar{S}_{Ref}] * [S_{Sample}(i) - \bar{S}_{Sample}]}{\left\{\sum [S_{Ref}(i) - \bar{S}_{Ref}]^2\right\} * \left\{\sum [S_{Sample}(i) - \bar{S}_{Sample}]^2\right\}}, \quad (1)$$

where $S_{ref}(i)$ is the normalized intensity at position i of the reference spectrum, $S_{sample}(i)$ is the normalized intensity at position i of the sample spectrum, $\bar{S}_{ref}$ is the mean intensity value of the

normalized reference spectrum and $\bar{S}_{sample}$ is the mean intensity value of the normalized sample spectrum.

The resulting correlation coefficient map of the image is built on the spectral information in the sample and is therefore based on dye distribution. Hereby, the highest CC value of one represents complete accordance between sample and reference spectrum. Decreasing CC values indicate decreasing correlation of the spectra.

To enable a comparison of the different images, the uptake indicator UI_x is introduced. It represents the quantity of coefficients higher than a threshold normalized to the total number of pixels representing tissue.

$$UI_x = \frac{\text{Number of correlation coefficients higher } x}{\text{Number of tissue pixels}} \quad (2)$$

These tissue pixels are derived by calculating the standard deviation of the normalized spectral data for every pixel. A uniformly distributed intensity profile along the λ-axis indicates background pixels that are not included in the calculations.

Because UI_x depends on an arbitrary threshold, two evaluation experiments were carried out. In the first experiment untreated skin samples were used to calculate the fraction that is false positively classified as Nile Red pixels with increasing threshold values (see Table 1).

Table 1 indicates the fraction of pixels of an untreated skin sample that are false positively calculated to be similar to the dye reference spectrum.

In the second experiment the reference skin samples were used to evaluate the highest threshold that allows a clear discrimination between the used concentrations.

Figure 4 shows the results of the reference samples indicating that $UI_{0.9}$ is not suitable to allow discrimination of the two lowest concentrations, whereas it is possible when using $UI_{0.8}$. Considering the very low false positive classification of. 02%, $UI_{0.8}$ was used as the evaluation parameter for further experiments.

2.8 *Validation Measurements*

To confirm that the scheme is not depending on absolute intensity values, the samples were imaged with different intensification by varying photomultiplier (PMT) voltages in a range from 500 V to 1200 V in eight steps. $UI_{0.8}$ was calculated for every image and was expected to be constant for different image intensity levels. For the second experiment the focal depth was changed during imaging of two skin samples and $UI_{0.8}$ was calculated to assess the influence of focusing.

Table 1 Measurements of untreated skin samples ($n = 5$) for the evaluation of the 0 parameter.

	$UI_{0.4}$	$UI_{0.5}$	$UI_{0.6}$	$UI_{0.7}$	$UI_{0.8}$	$UI_{0.9}$
Mean (%)	3.6	.9	.4	.09	.02	.0002
StdDev (%)	.9	.4	.1	.03	.01	.0002

Table 2 Presentation of the skin penetration results in mean $UI_{0.8}$ and standard deviation for the four time periods.

$UI_{0.8}$	3 h	6 h	8 h	24 h
Mean (%)	0.7	1.5	3.0	13.8
StdDev (%)	0.6	1.1	2.6	4.8

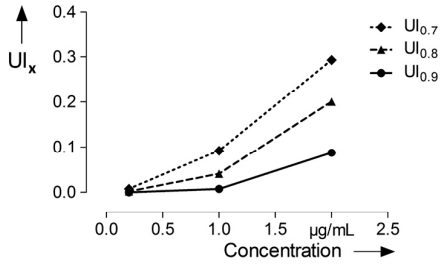

Fig. 4 Determination of the appropriate value for UI_x. The graph shows the $UI_{0.7}$, $UI_{0.8}$ and $UI_{0.9}$ values for 0.2 µg/mL, 1 µg/mL and 2 µg/mL Nile Red reference skin samples. It is not possible to discriminate the 0.2 µg/mL and 1 µg/mL sample when using $UI_{0.9}$.

3 Results

3.1 *Scheme Validation*

The results of the validation experiment for varying signal intensities are shown in Fig. 5(a). Regarding the variation of the PMT voltage to modify the image intensity, $UI_{0.8}$ is nearly constant over a 200 to 300 V region for the 24 h and 8 h samples. The $UI_{0.8}$ increase at 500 to 600 V can be explained with the very low overall intensity of the spectral images at 500 V. Thus, the spectra cannot be properly measured. The $UI_{0.8}$ decrease starting at 900 to 1000 V can be observed due to a strong signal saturation effect in single spectral bands for the 8 h and 24 h samples. Therefore, the spectral information is lost because of detector saturation. The 6 h sample has a $UI_{0.8}$ value that is constant over the range of 600 to 1200 V.

These measurements indicate that the $UI_{0.8}$ values do not change significantly over a broad intensity interval when using reasonable imaging parameters.

Focus position, in contrast, is a very sensitive parameter. The graph in Fig. 5(b) shows a Gaussian-like distribution of $UI_{0.8}$ with varying focus depths for the 10 μm thick sample. The measurements indicate that it is important to focus carefully for getting reliable results. Considering the moderate $UI_{0.8}$ change around the -1 µm to 1 μm relative focus position, a roughly 3-μm tolerance margin for focusing can be supposed.

3.2 *Skin Penetration Study*

The results of the penetration study show a strong time dependence of dye uptake in skin (see Fig. 6 and Table 2). The assessment of this uptake using the $UI_{0.8}$ parameter allows the quantitative comparison of the four time periods. It shows that the 24 h samples have a more than four times higher mean $UI_{0.8}$ value compared to the 8 h samples.

The overlay intensity-based images and the spectrally resolved dye distribution are shown in Fig. 7. The intensity-based images were recorded with optimized parameters to achieve high image quality. The dye distribution was visualized using the correlation coefficient map and the $UI_{0.8}$ parameter as a threshold. The epidermal skin layer can be distinguished from the lower dermal layer due to its bright gray appearance. The

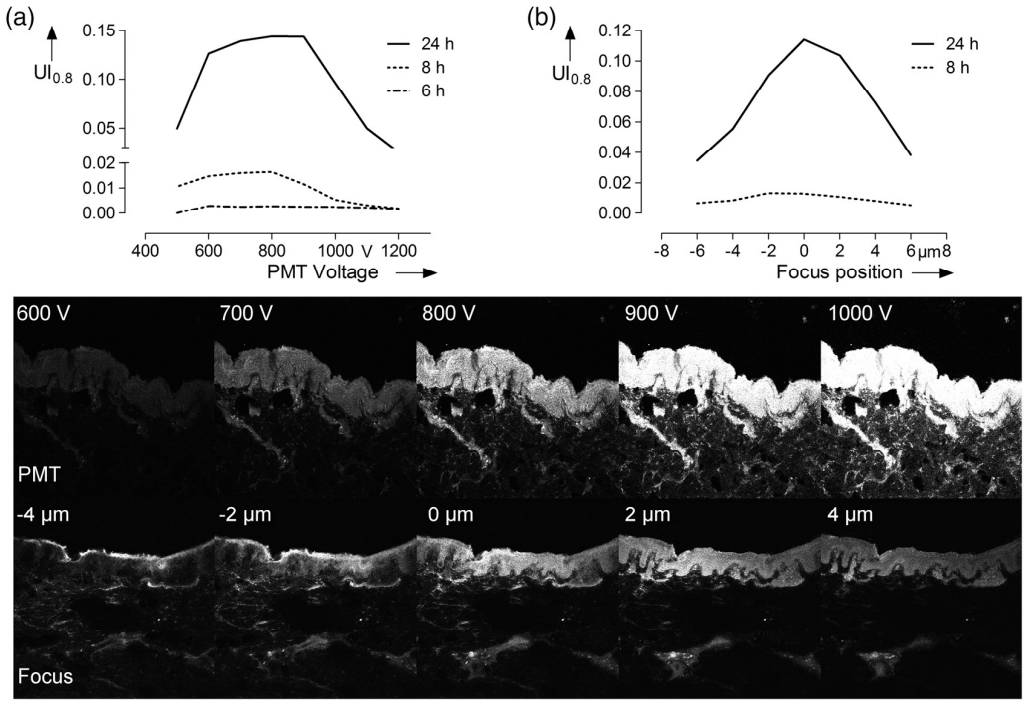

Fig. 5 The graphs show the results of the varying PMT (a) and focus (b) settings. The image sequences illustrate the changes in the data when varying the PMT voltage and the focus depth, respectively.

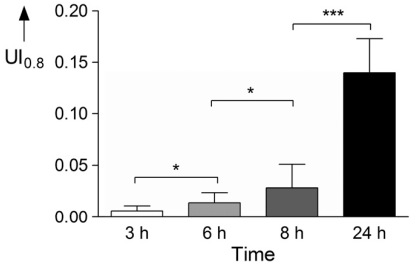

Fig. 6 Skin penetration study results ($n = 20$ per penetration period). Data are presented in mean ±SD. $^{*}P < 0.05$ and $^{***}P < 0.001$ evaluated by paired Student's t-test. The 24 h samples show a significantly higher uptake of Nile Red.

darker dermal layer, however, shows brighter structures throughout the whole area. Dye distribution, shown in red, indicates that for the 3 h, 6 h and 8 h samples, the uptake does not cover the whole epidermis in the way that the $UI_{0.8}$ criteria is fulfilled. The 24 h sample shows complete uptake in the epidermis and additional uptake in the dermis layer.

4 Discussion

It was shown that a spectrally resolved imaging and processing method can be used to assess and compare spectral information in tissue. The processing scheme calculates the introduced uptake indicator that derives from spectral correlation analysis. It can be used for mapping spectral information in microscopic images of tissue. The method is developed and validated in the context of a very frequently performed penetration experiment according to the OECD Guidelines for Testing of Chemicals in pharmaceutical research. However, the scope of the method is not limited to drug delivery studies but can be transferred to further applications that need spectral discrimination at a microscopic scale.

4.1 *Pharmaceutical In Vitro Experiments*

High dermal transport is important to address skin diseases occurring in the upper layers. Tape-stripping methods are commonly used to stepwise ablate small parts of the outer skin for quantitatively analyze depth profiles.[29] However, it is limited to the stratum corneum and does not give any information of the homogeneity and the distribution of drugs in the skin layer itself. In contrast, microscopic evaluation of vertical slices has the capability to show profiles directly throughout the whole skin, but lacks the possibility to quantify the amount of penetrated substances. Schmidts[30] presented a skin penetration study that correlated an ELISA based quantification with an intensity-based microscopy evaluation method. The results were of good qualitative accordance indicating the suitability of the microscopy approach for evaluating dermal delivery systems. The developed uptake indicator of this paper was a consequent advancement of Schmidts' microscopy analysis. It allows indirect quantitative measurements and is a step towards the quantitative evaluation of dermal delivery systems and processes. The results of the presented penetration study support this statement as they show a clear discrimination of the four time periods.

Our proposed method may also be beneficial to studies involving applications of spectral and hyperspectral imaging of penetration studies. Roberts; et al.; performed delivery studies using a FLIM multiphoton system[4] that is capable of spectrally detecting fluorescence signal to compare liposome systems. They concluded that the deformability of the liposomes increases penetration based on visual evaluation. In this case, the uptake

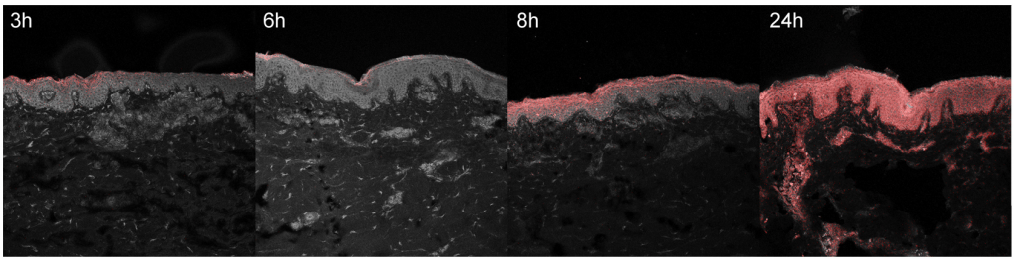

Fig. 7 Overlay of the intensity based confocal images of the skin and the spectrally resolved dye distribution (shown in red, please refer to the online version of this manuscript) for the four time periods.

indicator could be used to obtain comparable results and further increase insight into underlying penetration processes.

Hernandez-Palacios[14] introduced a hyperspectral camera system with 20 μm spatial resolution to evaluate penetration studies. The hyperspectral camera detected the emission peak of Alexa 488 (518 to 524 nm) and therefore avoided the use of fluorescence filters. However, the evaluation is based on the fluorescence intensity that is composed of Alexa dye and skin autofluorescence background. Skin structures like melanin and keratin, with an emission peak at 520 nm,[2,4] contribute to this intensity. Subtraction of a constant offset value compensates the overlaying signal. Figure 7 illustrates that, when using microscopic resolution, structures of the skin are brightly visible that are not covered with dye. In this case, the overlapping and superimposing signal of the skin and dye vary depending on microscopic structures that are not equally distributed. Hence, a constant autofluorescent background offset cannot be defined and mapping of the dye based on intensity in the microscopic scale is not possible.

4.2 *Advantages and Drawbacks for Delivery Studies*

The spectral imaging scheme has several benefits. Additional to the advantage of accurate dye mapping, spectral analysis is superior to intensity-based methods in terms of experiment procedures because it does not require standardized imaging. In general, the emission intensity in confocal microscopy depends on various parameters. Therefore, when using intensity-based methods, it is a comprehensive but very important task to use constant settings in order to assure the comparability of the results. This standardization process requires the assessment and control of imaging setup and sample conditions. While the setup may be kept constant for a whole experiment with certain effort, the sample conditions cannot be controlled easily due to their biological nature.

It is known that the pH-value changes in different skin layers[31] and may influence the intensity of dyes that have a strong pH-dependency. Apart from the pH value, fluorescence emission can also be affected by polarity. In the case of Nile Red, the fluorescence is unaffected by pH-values between 4.5 and 8.5 but the emission peak shifts depending on the polarity of the environment.[25] A possible shift must be considered for choosing the appropriate reference spectrum for image processing calculations. Additionally, photobleaching is a serious problem that requires attention. Borgia[6] reports a 4 to 16% bleaching rate after a one second illumination of Nile Red. It is concluded that the images have to be taken within 10 ms to avoid a strong signal variation.

The spectral data do not depend on absolute intensity values but on relative intensity changes between single wavebands. Consequently they are less sensitive to condition variations and photobleaching resulting in a high robustness of the calculated results. Figure 5 shows that the calculated assessment parameter is constant for reasonable changes of the imaging parameters. This allows measuring every sample with individual settings without the need to use standardized imaging parameters for comparing the results. The advantage is a broad, analyzable concentration range of fluorescent dye in skin specimens. This is especially useful for comparing completely independent experiment setups.

Another advantage of the spectral method is that it is still applicable whenever dyes with emission spectra that are clearly separated from the skin spectrum are not available. Although the spectra overlap, an explicit correlation to either dye or tissue can still be performed. As a result, a reliable assessment of the spatial distribution of dye in tissue is possible.

The $UI_{0.8}$ parameter that is chosen for the evaluation of the penetration study is an arbitrary measure. It is important to understand that it cannot be used to quantitatively assess the total amount of dye in skin. Due to the overlapping dye and skin spectra, it is difficult to determine the exact correlation coefficient that describes the transition between the two possible signal origins. The $UI_{0.x}$ parameters are used to arbitrarily classify the calculation results into dye and tissue pixels according to a threshold value. For this reason the proposed spectral method is not applicable for tasks that need exact quantitative results. In these cases intensity-based methods can be used that need to be calibrated or intensity corrected. Monte Carlo simulations that determine and compensate for effects of signal attenuation due to scattering and absorption[32] are often applied for these applications. Combining these techniques with the spectral evaluation for penetration studies would add valuable information to the localization and penetration depth of dye and agents.

4.3 *Pharmaceutical In Vivo Experiments*

It is arguable that *in vitro* results can be used to assess delivery systems designed for *in vivo* use. No clear data is available in the literature as there are many studies with good and poor correlation between *in vitro* and *in vivo* results.[33] Therefore, *in vitro* results for drug delivery cannot be transferred directly to *in vivo* considerations without further investigation. For this reason, studies are performed with a parallel *in vivo/in vitro* setup[34–36] using living mice for the application and penetration of delivery systems and substances. The mice either are sacrificed or biopsies are taken for analysis afterwards. An approach

for *in vivo* imaging without sacrificing the animals is the use of animal window models.[37,38] Here, the living animal can be microscopically examined directly through windows that are surgically inserted into the region of interest. Whenever living animals are observed motion artifacts have to be considered and either fixation or synchronizing the scanning system to the heartbeat needs to be performed. Amornphimoltham[39] reviewed further *in vivo* applications for drug delivery research and showed the technical efforts that have to be made for data acquisition.

4.4 *Feasibility for Clinical In Vivo Applications*

Gareau[40] presented an approach of *in vivo* confocal reflectance microscopy for the detection of early-stage melanoma of murine skin without further surgical interventions. Lange-Asschenfeld[41] and Caspers[42] showed confocal laser-scanning microscopes for *in vivo* imaging of human skin morphology and wound healing. Both studies mention the potential use for pharmaceutical research on drug delivery. A combination of the proposed microscope setup and our spectrally resolved detection unit could be used for optical sectioning and evaluation of fluorescent dyes in living tissue. Additionally, the *in vivo* microscopy scheme presented by Gareau combined with our proposed spectral uptake indicator could be used in clinical applications like melanoma detection presented by Kuzmina[15] for monitoring size and shape variations.

Extending established microscopic *in vivo* imaging schemes with our proposed spectral evaluation method has the chance to provide additional information for pharmaceutical and clinical applications. However, further investigation is necessary to validate these potential approaches.

Acknowledgments

We would like to thank the Hessen State Ministry of Higher Education, Research and the Arts for the financial support within the Hessen initiative for scientific and economic excellence (LOEWE-Program).

References

1. R. Alvarez-Román et al., "Visualization of skin penetration using confocal laser scanning microscopy," *Eur. J. Pharm. Biopharm.* **58**(2), 301–316 (2004).
2. K. Schenke-Layland et al., "Two-photon microscopes and in vivo multiphoton tomographs—powerful diagnostic tools for tissue engineering and drug delivery," *Advanced Drug Delivery Reviews* **58**(7), 878–896 (2006).
3. S.-J. Lin, S.-H. Jee, and C.-Y. Dong, "Multiphoton microscopy: a new paradigm in dermatological imaging," *Eur. J. Dermatol.* **17**(5), 361–366 (2007).
4. M. S. Roberts et al., "Non-invasive imaging of skin physiology and percutaneous penetration using fluorescence spectral and lifetime imaging with multiphoton and confocal microscopy," *Eur. J. Pharm. Biopharm.* **77**(3), 469–488 (2011).
5. H. I. Labouta et al., "Combined multiphoton imaging-pixel analysis for semiquantitation of skin penetration of gold nanoparticles," *Int. J. Pharm.* **413**(1–2), 279–282 (2011).
6. S. L. Borgia et al., "Lipid nanoparticles for skin penetration enhancement-correlation to drug localization within the particle matrix as determined by fluorescence and parelectric spectroscopy," *J. Contr. Release* **110**(1), 151–163 (2005).
7. M. R. Prausnitz and R. Langer, "Transdermal drug delivery," *Nat. Biotechnol.* **26**(11), 1261–1268 (2008).
8. P. L. Honeywell-Nguyen and J. A. Bouwstra, "Vesicles as a tool for transdermal and dermal delivery," *Drug Discov. Today Tech.* **2**(1), 67–74 (2005).
9. R. H. H. Neubert, "Potentials of new nanocarriers for dermal and transdermal drug delivery," *Eur. J. Pharm. Biopharm.* **77**(1), 1–2 (2011).
10. M. Kreilgaard, "Influence of microemulsions on cutaneous drug delivery," *Advanced Drug Delivery Reviews* **54**(Suppl. 1), S77–S98 (2002).
11. M. Kreilgaard, E. J. Pedersen, and J. W. Jaroszewski, "NMR characterisation and transdermal drug delivery potential of microemulsion systems," *J. Contr. Release* **69**(3), 421–433 (2000).
12. M. J. Lawrence and G. D. Rees, "Microemulsion-based media as novel drug delivery systems," *Advanced Drug Delivery Reviews* **45**(1), 89–121 (2000).
13. T. W. Prow et al., "Nanoparticles and microparticles for skin drug delivery," *Advanced Drug Delivery Reviews* **63**(6), 470–491 (2011).
14. J. Hernandez-Palacios et al., "Hyperspectral characterization of fluorophore diffusion in human skin using a sCMOS based hyperspectral camera," *Proc. SPIE* **8087**, 808717 (2011).
15. I. Kuzmina et al., "Towards noncontact skin melanoma selection by multispectral imaging analysis," *J. Biomed. Opt.* **16**(6), 060502 (2011).
16. S.-G. Kong, "Inspection of poultry skin tumor using hyperspectral fluorescence imaging," *Proc. SPIE* **5132**, 455–463 (2003).
17. M. S. Chin et al., "Hyperspectral imaging for early detection of oxygenation and perfusion changes in irradiated skin," *J. Biomed. Opt.* **17**(2), 026010 (2012).
18. L. L. Randeberg, "Hyperspectral imaging of bruised skin," *Proc. SPIE* **6078**, 60780O (2006).
19. L. L. Randeberg et al., "In vivo hyperspectral imaging of traumatic skin injuries in a porcine model," *Proc. SPIE* **6424**, 642408 (2012).
20. J. M. Beach, "Portable hyperspectral imager for assessment of skin disorders: preliminary measurements," *Proc. SPIE* **5686**, 111–118 (2005).
21. B. Park et al., "AOTF hyperspectral microscopic imaging for foodborne pathogenic bacteria detection," *Proc. SPIE* **8027**, 802707 (2011).
22. R. Arora, G. I. Petrov, and V. V. Yakovlev, "Hyperspectral coherent anti-Stokes Raman scattering microscopy imaging through turbid medium," *J. Biomed. Opt.* **16**(2), 021116 (2011).
23. G. N. Stamatas and N. Kollias, "In vivo documentation of cutaneous inflammation using spectral imaging," *J. Biomed. Opt.* **12**(5), 051603 (2007).
24. C. Zakian et al., "In vivo quantification of gingival inflammation using spectral imaging," *J. Biomed. Opt.* **13**(5), 054045 (2008).
25. D. L. Sackett and J. Wolff, "Nile red as a polarity-sensitive fluorescent probe of hydrophobic protein surfaces," *Anal. Biochem.* **167**(2), 228–234 (1987).
26. D. I. Friedman, J. S. Schwarz, and M. Weisspapir, "Submicron emulsion vehicle for enhanced transdermal delivery of steroidal and nonsteroidal antiinflammatory drugs," *J. Pharm. Sci.* **84**(3), 324–329 (1995).
27. T. Schmidts, "Protective effect of drug delivery systems against the enzymatic degradation of dermally applied DNAzyme," *Inter. J. Pharm.* **410**(1–2), 75–82 (2011).
28. C. Herkenne et al., "Pig ear skin ex vivo as a model for in vivo dermatopharmacokinetic studies in man," *Pharm. Res.* **23**(8), 1850–1856 (2006).
29. J. Lademann et al., "The tape stripping procedure—evaluation of some critical parameters," *Eur. J. Pharm. Biopharm.* **72**(2), 317–323 (2009).
30. T. Schmidts et al., "Development of drug delivery systems for the dermal application of therapeutic DNAzymes," *Inter. J. Pharm.* **431**(1–2), 61–69 (2012).
31. H. Wagner et al., "pH profiles in human skin: influence of two in vitro test systems for drug delivery testing," *Eur. J. Pharm. Biopharm.* **55**(1), 57–65 (2003).
32. U. Maeder, "Feasibility of Monte Carlo simulations in quantitative tissue imaging," *International Journal of Artifical Organs* **33**(4), 253–259 (2010).
33. B. Godin and E. Touitou, "Transdermal skin delivery: predictions for humans from in vivo, ex vivo and animal models," *Advanced Drug Delivery Reviews* **59**(11), 1152–1161 (2007).
34. Z.-R. Huang et al., "In vitro and in vivo evaluation of topical delivery and potential dermal use of soy isoflavones genistein and daidzein," *Inter. J. Pharm.* **364**(1), 36–44 (2008).

35. F. C. Rossetti, "A delivery system to avoid self-aggregation and to improve in vitro and in vivo skin delivery of a phthalocyanine derivative used in the photodynamic therapy," *J. Contr. Release* **155**(3), 400–408 (2011).
36. M. E. M. J van Kuijk-Meuwissen et al., "Application of vesicles to rat skin in vivo: a confocal laser scanning microscopy study," *J. Contr. Release* **56**(1–3), 189–196 (1998).
37. M.-A. Abdul-Karim et al., "Automated tracing and change analysis of angiogenic vasculature from in vivo multiphoton confocal image time series," *Microvascular Research* **66**(2), 113–125 (2003).
38. S. Schlosser et al., "Paracrine effects of mesenchymal stem cells enhance vascular regeneration in ischemic murine skin," *Microvasc. Res.* **83**(3), 267–275 (2012).
39. P. Amornphimoltham, A. Masedunskas, and R. Weigert, "Intravital microscopy as a tool to study drug delivery in preclinical studies," *Advanced Drug Delivery Reviews* **63**(1–2), 119–128 (2011).
40. D. S. Gareau et al., "Noninvasive imaging of melanoma with reflectance mode confocal scanning laser microscopy in a murine model," *J. Investig. Dermatol.* **127**(9), 2184–2190 (2007).
41. S. Lange-Asschenfeldt et al., "Applicability of confocal laser scanning microscopy for evaluation and monitoring of cutaneous wound healing," *J. Biomed. Opt.* **17**(7), 076016 (2012).
42. P. J. Caspers, G. W. Lucassen, and G. J. Puppels, "Combined in vivo confocal Raman spectroscopy and confocal microscopy of human skin," *Biophys J.* **85**(1), 572–580 (2003).

IV. Development of a protective dermal drug delivery system for therapeutic DNAzymes. In: *International Journal Pharmaceutics* 479 (1), S. 150–158.

International Journal of Pharmaceutics 479 (2015) 150–158

Contents lists available at ScienceDirect

International Journal of Pharmaceutics

journal homepage: www.elsevier.com/locate/ijpharm

Development of a protective dermal drug delivery system for therapeutic DNAzymes

Kay Marquardt [a,*], Anna-Carola Eicher [a], Dorota Dobler [a], Ulf Mäder [b], Thomas Schmidts [a], Harald Renz [c], Frank Runkel [a]

[a] Institute of Bioprocess Engineering and Pharmaceutical Technology, University of Applied Sciences Mittelhessen, Wiesenstrasse 14, 35390 Giessen, Germany
[b] Institute of Medical Physics and Radiation Protection, University of Applied Sciences Mittelhessen, Wiesenstrasse 14, 35390 Giessen, Germany
[c] Institute of Laboratory Medicine and Pathobiochemistry, Molecular Diagnostic, Baldinger Strasse, 35043 Marburg, Philipps-University Marburg, Germany

ARTICLE INFO

Article history:
Received 22 October 2014
Received in revised form 16 December 2014
Accepted 19 December 2014
Available online 23 December 2014

Chemical compounds studied in this article:
Benzoic acid (PubChem CID: 243)
Benzyl alcohol (PubChem CID: 244)
Chitosan (PubChem CID: 21896651)
Methylparaben (PubChem CID: 7456)
Phenoxy ethanol (PubChem CID: 31236)
Phosphatidylcholin (PubChem CID: 45266626)
Propylene glycol (PubChem CID: 1030)
Propylparaben (PubChem CID: 7175)
Oleyl oleate (PubChem CID: 543844)

Keywords:
Drug delivery system
DNAzyme
Chitosan
Polyplex
Submicron emulsion
DNase

ABSTRACT

RNA-cleaving DNAzymes are a potential novel class of nucleic acid-based active pharmaceutical ingredients (API). However, developing an appropriate drug delivery system (DDS) that achieves high bioavailability is challenging. Especially in a dermal application, DNAzymes have to overcome physiological barriers composed of penetration barriers and degrading enzymes. The focus of the present study was the development of a protective and penetration-enhanced dermal DDS that was tailor made for DNAzymes. DNAzyme Dz13 was used as a potential API for topical therapy against actinic keratosis. In the progress of development and selection, different preservatives, submicron emulsions (SMEs) and the physiological pH range were validated with respect to the API's integrity. A physicochemical stable SME of a pharmaceutical grade along with a high API integrity was achieved. Additionally, two developed protective systems, consisting of a liposomal formulation or chitosan-polyplexes, reduced the degradation of Dz13 in vitro. A combination of SME and polyplexes was finally validated at the skin and cellular level by in vitro model systems. Properties of penetration, degradation and distribution were determined. The result was enhanced skin penetration efficiency and increased cellular uptake with a high protective efficiency for DNAzymes due to the developed protective DDS.

1. Introduction

DNAzymes represent a novel class of nucleic acid-based potentially active pharmaceutical ingredients (API). The synthetic molecules can be grouped into different subclasses. The molecules of the 10–23 DNAzyme subclass consist of a single DNA strand that can be divided into a conserved catalytic domain and two flanking binding domains (Breaker and Joyce, 1994; Santoro and Joyce, 1997). The catalytic domain is able to cleave the transcripts of gene expressions (post-transcriptional silencing). Variations of the binding domain can specifically address different pathogen gene expression patterns, resulting in a high number of potential therapeutic approaches (Cairns et al., 1999; Tan et al., 2009). Promising approaches have been made towards developing therapies for different skin diseases, for instance, atopic dermatitis or basal cell and squamous cell carcinomas (Cai et al., 2012; Schmidts et al., 2012).

A new dermally applied API could be DNAzyme Dz13. Dz13 is a typical representative of the 10–23 DNAzymes with hydrophilic properties, a high molecular weight (MW) of 10.6 kDa and a negative charge (Khachigian et al., 2002; Santoro and Joyce, 1997). Studies revealed that Dz13 can inhibit the translation of the overexpressed protein c-Jun consequently suppressing the growth of squamous and basal cell carcinomas (SCC and BCC) (Cai et al., 2012; Cho et al., 2013; Zhang et al., 2004). Similar results are expected for the treatment of actinic keratosis, a precursor form of

* Corresponding author. Tel.: +49 641 309 2630; fax: +49 641 309 2553.
E-mail address: Kay.Marquardt@kmub.thm.de (K. Marquardt).

http://dx.doi.org/10.1016/j.ijpharm.2014.12.043
0378-5173/

SCC and BCC (Criscione et al., 2009). In this context, Dz13 was chosen as a promising API candidate for topical treatment of actinic keratosis.

The target of Dz13 is the messenger RNA of c-Jun in the cytoplasm of keratinocytes located within the outer skin layers. Dermally applied Dz13 is at the site of action but is separated by multiple physiological barriers compromising therapeutic outcomes. The stratum corneum is the outermost skin layer and forms a first lipid barrier (Jepps et al., 2013), restraining DNAzymes from penetration. The second main barrier of the skin is enzymatically active. Enzymes of exogene and endogene origin on the surface and in the skin can irreversibly degrade DNA (reviewed by Eckhart et al., 2012). If DNAzyme overcomes the two barriers, a high bioavailability in the top skin layers will be helpful to sufficiently internalize Dz13 into cells. A variety of approaches may be possible to pass through the crucial barriers, despite the challenging properties of DNAzymes, including the following strategies. (i) Enhancing the permeability of the stratum corneum by hydration or disruption. In this setting, using penetration enhancers, for instance propylene glycol, oleic acid or even whole galenic formulations, such as submicron emulsions (SME), could be possible (Mohammed et al., 2014; Ongpipattanakul et al., 1991). SMEs have excellent penetration enhancement properties due to their compositions and nano-scaled droplet size, which have already shown an ability to transport and accumulate a DNAzyme into the first skin layers (Amselem and Friedman, 1998; Schmidts et al., 2012). (ii) Maintaining the integrity of DNAzymes by using protective systems. For example, the systems could consist of liposomal formulations or chitosan-polyplexes that could counteract the degradation of DNAzymes by encapsulation or complexation, respectively (Richardson et al., 1999; Semple et al., 2001). Furthermore, an advantage of both systems could be that they enhance cellular uptake. It is expected that a combination of the approaches in one protective drug delivery system (DDS) will increase the topical bioavailability of DNAzymes, resulting in an increase in therapeutic efficiency (Elsabahy et al., 2011; Zhu and Mahato, 2010).

The present study focused on an advancement towards a protective DDS for the dermally applied Dz13. In preliminary examinations, the compatibility and suitability of different preservatives and pH range with Dz13 was investigated. Subsequently, a SME with an appropriate preservation was developed to enhance the penetration of the API. The SME was investigated in terms of physicochemical stability and the integrity of Dz13. To protect the DNAzyme against degradation, a liposomal formulation and chitosan-polyplexes were developed and validated. Finally, a combination of the SME and polyplexes generated a novel protective DDS. Aspects of penetration, degradation and distribution with and without the protective DDS were determined on the skin and cellular level with in vitro model systems.

2. Materials and methods

2.1. Materials

Triethylammonium acetate and phenol–chloroform–isoamyl alcohol were provided by Applichem Lifescience (Germany). Phosphatidylcholin and phosphatidylglycerol were thankfully provided by Lipoid (Germany). Deoxyribonuclease I from bovine pancreas, 10x TAE buffer, and agarose were purchased from Sigma–Aldrich (USA). DNAzyme Dz13 sodium salt was synthesized by Integrated DNA Technologies (Belgium). Dz13 consists of 34 deoxyribonucleotides including an inverted thymidine with a MW of 10.6 kDa (Khachigian et al., 2002). Especially for fluorescence analytics, a 5'FAM-labelled DNAzyme (FAM-DNAzyme) with similar characteristics was synthesized by Biospring (Germany). The fluorescence-labelled FAM-DNAzyme (MW: 10.6 kDa) consists of 34 deoxyribonucleotides and an inverted thymidine (Turowska et al., 2013). In addition, SYBR Gold nucleic acid gel stain was bought from Life Technologies (Germany). PBS buffer with and without Mg^{2+} and Ca^{2+}, Dulbecco's modified eagle's medium, fetal bovine serum, and trypsin/EDTA solution were purchased from Biochrom AG (Germany). The human keratinocyte cell line HaCaT was kindly provided by Prof. Dr. Weindl of the Institute of Pharmacy (Pharmacology and Toxicology), Freie Universität Berlin, Germany. The following ingredients were obtained at pharmaceutical grade. Phenoxy ethanol and benzoic acid were purchased from FrankenChemie (Germany) and OTC Pharma (Germany), respectively. Glycerol, magnesium sulphate were purchased from Fagron (Germany). Glyceryl stearate, stearyl alcohol and ceteareth-20 were supplied by Evonik (Germany). Benzyl alcohol, methylparaben, propylparaben, propylene glycol, laureth-12 and caprylic/capric triglyceride were bought from Caelo (Germany). Cetearyl isononanoate, oleyl oleate and chitosan (Chitopharm S) were provided by Cognis (Germany). The chitosan has a MW range of 50–1000 kDa and a degree of deacetylation of 70%. The following ingredients were obtained at HPLC grade. Acetonitrile, ethanol, sodium perchlorate, hydrochloric acid, sodium hydroxide, potassium dihydrogen phosphate, disodium hydrogen phosphate and sodium acetate were supplied by VWR BDH Prolabo (Germany).

2.2. DNAzyme analytics

For the present examinations, Dz13 and the alternative 5'FAM-labelled DNAzyme (FAM-DNAzyme) were analysed by the following four different methods.

(i) The quality and quantity of Dz13 and the FAM-DNAzyme were analysed by using anionic exchange high pressure liquid chromatography (AEX-HPLC). Prior to analysis, samples were purified using phenol-chloroform extraction and an ethanol-sodium acetate precipitation. The purified samples were analysed with a DNAPac PA200 column (Thermo Fisher Scientific, Germany). The HPLC system was a LaChrom Elite system with a fluorescence detector and UV–vis (VWR-HITACHI, Germany). The UV–vis detector wavelength was set to 260 nm. Calibration detector was performed between 15 and 200 μg/mL ($r^2 = 0.999$) with a limit of quantification (LOQ) of 3.7 μg/mL and a limit of detection (LOD) of 11.4 μg/mL. The fluorescence signal was measured using a 490 nm excitation wavelength and 520 nm emission wavelength. The calibration curve was established in a range from 4 to 40 μg/mL ($r^2 = 0.999$). The LOQ and LOD can be specified with 1.0 μg/mL and 0.3 μg/mL, respectively. The equilibration buffer consisted of 20% acetonitrile and 4% triethylammonium acetate (pH 7.0), while the elution buffer also included 0.2 M acetate sodium perchlorate. The AEX-11;HPLC system was performed in gradient mode, starting with 45% elution buffer and, after 18 min, ending with 100% elution buffer. The flow rate was 1 mL/min at a temperature of 60 °C. The EZChrome Elite Software was used for peak integration. The quantification was performed using a standard calibration curve at the investigated concentration range and above the quantification limit.

(ii) The quantities of intact Dz13 and FAM-DNAzyme were measured by hybridization-ELISA as previously described (Schmidts et al., 2012). Hybridization probes were adjusted to Dz13 or FAM-DNAzyme, and the substrate was exchanged to ABTS solution.

(iii) FAM-DNAzyme was detected using confocal laser-scanning microscopy (CLSM) using the TCS SP5CLSM (Leica, Germany). To distinguish between the specific fluorescence of the dye and

autofluorescence of skin specimens or cell extracts, a spectral analysis of each pixel was performed according to Maeder et al. (2012). The method was adapted to the FAM dye. Therefore, the excitation wavelength and emission wavelength spectrum were set to 488 nm and 500–600 nm, respectively. The method-specific *p*-value was set to 0.85. After identifying the dye, the specific intensity was summed and is presented as a mean intensity per summed pixel ± SD.

(iv) The fluorescences of FAM-DNAzyme in the HaCaT keratinocytes were detected using flow cytometry (guava easyCyte 5HT, EMD Millipore, Germany) and analysed using corresponding software (GuavaSoft 2.5). After 5000 events per sample, the cell population was defined in the forward-scattering and sideward-scattering diagram. The fluorescence emission of 488 nm excitation wavelength of the gated cell population was used to identify FAM-DNAzyme positive cells. The threshold was adjusted to obtain the lowest signal of the medium control.

2.3. Preparation of drug delivery systems

2.3.1. Submicron emulsion

The SMEs were produced by high-energy emulsification. The blend of the emulsifiers of the SME without preservatives was previously optimized regarding most thermo-stable droplet size. The SMEs were manufactured in triplicate with and without Dz13 according to Table 1 and each was conserved using different preservatives analogous to Table 2. In the case of the parabens, a blend of methylparaben and propylparaben was used. The aqueous phase and oil phase of the SME were separately heated to 65 °C until all ingredients were dissolved. The aqueous phase was added to the oil phase and homogenized for 2 min at 24,000 rpm by a rotor/stator homogenizer (D-15 homogenizer with DS-20/PF-EMR, MICCRA, Germany).

2.4. Preparation of protective systems

2.4.1. Liposomes

Liposomes were manufactured using a combination of the lipid film method and high pressure homogenization. A mixture of 4 wt % phosphatidylcholine and 1 wt% phosphatidylglycerol were dissolved in chloroform in a round bottom flask. The organic solvent was completely removed using rotary evaporation (BUCHI, Germany). Dz13 was encapsulated using the passive loading technique. For that purpose, the remaining thin lipid film was hydrated with a 0.01 M Sorensen's buffer and 4 mg/mL Dz13 at 40 °C resulting in large multilamellar vesicles (LMV). The LMVs were homogenized in a high pressure homogenizer (EmulsiFlex-C5, AVESTIN, Germany). The homogenization process was performed for 30 cycles at 40 °C and 1000 bar. A control group (spiked liposomes) was produced without Dz13. Therefore, Dz13 was spiked to the formulation to a final concentration of 4 mg/mL after liposome manufacturing process.

Table 1
Composition of the submicron emulsion.

Ingredient	wt%
Aqua	ad 100
DNAzyme	0.40
Caprylic/capric triglyceride	10.0
Cetearyl isononanoate	6.00
Ceteareth-20	3.85
Glycerol 85%	3.00
Glyceryl stearate	0.65
Laureth-12	1.00
Magnesium sulphate	0.30
Oleyl oleate	4.00
Preservatives	[a]
Stearyl alcohol	1.00

[a] For preservatives' concentration, see Table 2.

Table 2
Concentration of the preservatives.

Preservatives	wt%
Benzoic acid	0.10
Benzyl alcohol	1.00
Phenoxy ethanol	1.00
Propylene glycol	20.0
Parabens	
Methylparaben	0.15
Propylparaben	0.05

2.4.2. Chitosan-DNAzyme polyplexes

Chitosan-DNAzyme polyplexes were prepared in the following manner. Chitosan was dissolved in 1 M sodium acetate buffer with a pH value of 5.0. A concentrated, aqueous DNAzyme solution was added to the chitosan solution to a final DNAzyme concentration of 4 mg/mL. The final chitosan concentrations were in a range between 0.1 and 2 mg/mL equal to a N/P ratio of 0.035 and 0.7. A stepwise mixing of both solutions at 25 °C and 1300 rpm in a Thermomixer (Eppendorf, Germany) formed coarsely dispersed polyplexes.

2.5. Preparation of a protective drug delivery system

To generate a protective DDS, the developed SMEs and polyplexes were combined. Placebo SMEs with preservatives were manufactured according to Section 2.3.1. The polyplexes with DNAzymes were produced as described in Section 2.4.2 and dried overnight. The dried polyplexes were resuspended in the SMEs. Final concentrations of the DNAzymes and chitosan in the protective drug delivery system were 4 mg/mL and 2 mg/mL, respectively.

2.6. Stability of DNAzymes

The influence of different matrices on the integrity of DNAzymes was investigated. Therefore, Dz13 was incubated at a final concentration of 4 mg/mL with the following matrices: (i) Aqueous solutions were in a range of the physiologic pH values. The pH values from 5 to 7 in 0.5 steps were maintained by a 67 mM Sorensen's buffer. (ii) Aqueous solutions with different preservatives were used. The preservatives and their concentrations were used according to Table 2. (iii) SMEs were used with different preservatives. SMEs were produced as described in Section 2.3.1. All samples were selectively incubated at 8 °C, 25 °C at a 60% relative humidity (RH) or 40 °C with 75% RH. Each condition was performed in triplicate and analysed at fixed time intervals over a period of 3 months. Dz13 was qualified and quantified by AEX-HPLC. The data are presented as the mean with SD relative to the mean after 1 day.

2.7. Characterization of drug delivery systems and protective systems

The characterization of the DDSs and protective systems was selectively performed with regard to physicochemical properties, sufficient preservation and complexation efficiency. The physicochemical properties were determined as described in the following steps. The mean droplet size and droplet size distribution of diluted SMEs or liposomes were analysed using dynamic light

scattering (DLS) with the Zetasizer Nano Z (Malvern, UK). The droplet size and droplet distribution were presented as the z-average size (z-average) and polydispersity index (PDI), respectively. The pH value was monitored with a pH probe (FE20, Mettler-Toledo, Germany) or pH indicator strips (pH-Fix 2.0–9.0, MACHEREY-NAGEL, Germany), depending on the sample volume. Viscosity measurements were conducted at 25 °C with a cone and plate geometry of 2.2 cm in diameter and 2° cone angle (RheoStress 300, ThermoHaake, Germany). The share rate ramp was 0.1–100/s. The test of sufficient preservation was restricted to placebo SMEs. The preservation efficiency tests were conducted according to the European Pharmacopoeia using the microbial strains *Staphylococcus aureus*,*Escherichia coli*, *Pseudomonas aeruginosa* and *Candida albicans* (Council of Europe, 2013). The test of efficient complexation was restricted to polyplexes. A gel retardation assay was performed to visualize the degree of complexation. A 1.5% agarose gel was run in a Tris-acetate-EDTA (TAE) buffer (pH 8.3) for 1 h at 100 V (EV 200, Consort bvba, Belgium), and Dz13 was stained with 1x SYBR Gold. Each sample in the gel contained approximately 10 ng of Dz13 premixed with loading buffer. Furthermore, the degree of complexation was quantified by AEX-HPLC. The samples were centrifuged for 5 s at 13,000 rpm, and the recovery of Dz13 in the supernatant was analysed. To analyse Dz13, the polyplexes were decomplexed by adding sodium hydroxide to the samples until obtaining a final molarity of 1 M. All experiments were performed in triplicates and are presented as the mean with SD.

2.8. DNAzyme degradation assay

The degradation of Dz13 was investigated with deoxyribonuclease I (DNase I, EC 3.1.21.1). A 0.45 M Sorensen's buffer (pH 7.4) with a 10 mM magnesium sulphate was produced. The DNase I was diluted with Sorensen's buffer to a concentration of 400 units/mL and stored on ice until use. The different samples including 4 mg/mL Dz13 were incubated at a ratio 1:2 with the DNase I solution. The incubation parameters were 25 °C at 300 rpm for 0.5, 1 or 2 h in a Thermomixer (Eppendorf, Germany). The degrading reaction was immediately stopped by adding phenol-chloroform solution following an extraction and ethanol-sodium acetate precipitation. Negative control groups of each sample were equally treated without adding DNase I. The purified samples were analysed by AEX-2011;HPLC, allowing a qualitative and quantitative measurement of the degradation of Dz13. Each sample was tested in triplicate, and the data are presented as the mean with SD.

2.9. In vitro studies

2.9.1. Skin penetration study

The in vitro penetration study was performed in a Franz diffusion cell with fresh and intact porcine skin (*sus scrofa domestica*) in accordance with OECD guidelines and as previously described (OECD, 2004a,b,b; Schmidts et al., 2012). Infinite doses (0.5 mL) of 4 mg/mL Dz13 and FAM-DNAzyme at a 9:1 ratio were applied. After 24 h, the penetration study was stopped and analysed by multiple methods. The remaining formulation in the donor chamber was completely washed off the skin and was analysed using AEX-HPLC. Dz13 and the FAM-DNAzyme were detected simultaneously. A skin area of 0.5 cm^2 was snap frozen and vertically sliced in 15 specimens using the Leica CM 1850UV cryostat (Leica, Germany) and analysed by CLSM. The remaining skin (1.26 cm^2) was analysed using hybridization-ELISA. For this purpose, the skin was lysed by proteinase K, and the amount of intact Dz13 was quantified using specific probes. Each sample was tested in 5 Franz diffusion cells. The data are presented as the means with SDs.

2.9.2. Cell uptake study

HaCaT cells were cultivated in 24-well plates (2 cm^2/well) in DMEM medium with 10% FBS at 37 °C, 5% CO_2. At a confluence level of more than 75%, the cell monolayer was washed with PBS. The cells were treated with different media (0.5 mL). For this purpose, the total amount of Dz13 was replaced by the FAM-DNAzyme at a final concentration of 1 μg/cm^2. The FAM-DNAzyme was complexed with chitosan to polyplexes (N/P ratio: 0.7) and diluted with DMEM ($n = 18$). Control groups consisted of FAM-DNAzyme without chitosan ($n = 18$), chitosan itself ($n = 6$) or medium only ($n = 6$). After 24 h, the cell monolayer was washed twice with PBS, and the distribution of the FAM-DNAzyme was monitored by CLSM. Therefore, cells were stained with 4′,6-diamidino-2-phenylindole (DAPI) and Alexa Fluor 555 Phalloidin. Additionally, trypsinized cell suspension was analysed by flow cytometry. The cell extract of 9 wells were pooled to 3 samples, lysed with Proteinase K, and analysed by hybridization-ELISA.

2.9.3. Statistics

Statistical analysis was performed with OriginPro 8. To determine significant differences in the mean of families the one-way Analysis of Variance (ANOVA) was performed. The homogeneity of variance was tested with the Levene's test. As a post hoc test the Bonferroni analysis was used. $p < 0.05$ was considered as significant.

3. Results and discussion

3.1. Stability of DNAzymes

In preliminary investigations, the influence of different matrices on the Dz13's integrity was investigated. Matrices or ingredients could interact with the API or trigger degradation, resulting in decreased therapeutic activity. Dz13 was tested over a pH range similar to the physiologic gradient of the skin (Wagner et al., 2003) and conventional for a final DDS. No different alteration in comparison with each pH value could be observed (data not shown). Especially, no degradation of the DNA's phosphodiester bonds by acid hydrolysis was monitored, which would be one degradation pathway. In a further analysis, appropriate preservatives and their concentrations were selected according to the German Pharmaceutical Codex. The integrity of Dz13 was unaffected by the tested preservatives with the exception of benzoic acid (Table 3). Samples with benzoic acid continually lost Dz13 recovery. An interaction between DNAzyme and benzoic acid is conceivable because Zhang and Ma, (2013) discovered that the sodium salt of benzoic acid is able to interact with DNA by hydrophobic and hydrogen binding. This interaction can change the retention time of Dz13 in the AEX-HPLC analysis, which led to a decreased detection of the DNAzyme. As a result, all tested preservatives, except benzoic acid, can be used for further formulations containing Dz13.

Table 3
Dz13 recovery from aqueous solutions with different preservatives after 3 months. The means of triplicate samples with SDs relative to the corresponding means after 1 day. O, not performed.

	DNAzyme recovery (%)		
Preservatives	8 °C	25 °C	40 °C
Without	98 ± 1	103 ± 3	101 ± 4
Benzoic acid	O	58 ± 1	O
Parabens	O	101 ± 3	O
Benzyl alcohol	O	100 ± 3	O
Phenoxy ethanol	100 ± 1	100 ± 3	107 ± 4
Propylene glycol	97 ± 1	101 ± 5	101 ± 2

Table 4
Physicochemical properties of SMEs with different preservatives with or without Dz13 measured by DLS, pH indicators or a pH probe (mean ± SD, $n = 3$). PE test, preservative efficacy test; O, not performed.

		SME without DNAzyme				SME with DNAzyme		
Preservative		pH	z-average (d.nm)	PDI	PE test	pH	z-average (d.nm)	PDI
Without	1 day	6.7	303 ± 29	0.3 ± 0.1	O	O	O	O
	1 month	7.0	223 ± 2	0.1 ± 0.0				
	3 months	7.0	223 ± 1	0.1 ± 0.0				
Parabens	1 day	5.7	243 ± 8	0.1 ± 0.0	Fail	6.2	258 ± 38	0.1 ± 0.1
	1 month	6.2	315 ± 19	0.2 ± 0.0		6.2	305 ± 82	0.2 ± 0.1
	3 months	6.0	300 ± 13	0.1 ± 0.1		6.3	286 ± 70	0.2 ± 0.0
Benzyl alcohol	1 day	6.6	243 ± 12	0.1 ± 0.1	Fail	7.0	268 ± 35	0.1 ± 0.1
	1 moth	7.0	326 ± 7	0.2 ± 0.0		7.0	267 ± 30	0.1 ± 0.1
	3 months	7.0	288 ± 14	0.2 ± 0.0		7.0	259 ± 30	0.1 ± 0.0
Phenoxy ethanol	1 day	6.8	261 ± 5	0.1 ± 0.0	Fail	6.8	330 ± 13	0.3 ± 0.1
	1 month	7.0	334 ± 8	0.3 ± 0.1		6.8	347 ± 15	0.2 ± 0.1
	3 months	7.0	319 ± 21	0.1 ± 0.1		6.8	324 ± 2	0.2 ± 0.1
Propylene glycol	1 day	6.7	225 ± 1	0.1 ± 0.1	Pass	7.0	223 ± 10	0.1 ± 0.0
	1 month	7.0	255 ± 0	0.1 ± 0.0		7.0	235 ± 28	0.1 ± 0.1
	3 months	7.0	249 ± 3	0.2 ± 0.1		7.0	211 ± 35	0.1 ± 0.1

The SME formulations of Section 2.3.1 (except benzoic acid) were chosen as the DDS. The integrity of Dz13 in all SMEs was over a range of 100 ± 12% after a period of 3 months. Thus, the ingredients of the particular SME did not affect the stability of Dz13.

3.2. Development of a drug delivery system

The SME as a promising DDS was further characterized. Therefore, a selection of compatible preservatives was added to the basic SME formulation according to Section 2.3.1. The stability of the DDSs were monitored with regard to physicochemical properties (Table 4). The droplet size of the formulation without preservatives and Dz13 was approximately 300 nm and decreased slightly within the first weeks of storage. The addition of preservatives and Dz13 did not significantly influence the droplet size and droplet size distribution ($p < 0.05$). Furthermore, the parameters of all SMEs did not change significantly with $p < 0.05$ over the period of time. The viscosity of most SMEs was in a range of 21 ± 7.6 mPa s. SMEs containing propylene glycol had the highest viscosity of 46.5 ± 8.7 mPa s. The preservative efficacy test revealed sufficient preservation only by the SMEs that contained propylene glycol. Overall, the SME represents an appropriate DDS for DNAzymes due to the physicochemical stability along with the compatibility with Dz13.

3.3. Development and validation of the protective systems

3.3.1. Liposomes

Liposomes are able to encapsulate hydrophilic APIs into the aqueous inner phase. A lipid bilayer separated the inner phase from the external phase, resulting in a protection against degrading enzymes located in the external phase. Therefore, a liposomal formulation with DNAzymes was produced. The incorporation of Dz13 into the liposomal formulation increased the liposome size (z-average) from 36 ± 2 nm to 52 ± 12 nm. However, the droplet size distribution of both formulations remained similar with a PDI of 0.4. Encapsulating DNAzymes into liposomes is challenging using the passive loading technique, especially at high API concentrations and small liposome sizes (Xu et al., 2012a). Purifying the liposomes by diafiltration determined a Dz13 encapsulation efficiency of less than 6% (data not shown). A theoretical encapsulation efficiency of 9.2% based on the calculation by Xu et al. (2012b) affirmed the result. Therefore, the majority of the DNAzymes were present in the external aqueous phase and unprotected towards DNase activity. In the DNAzyme degradation assay with DNase I, the liposomal formulation was validated to be suitable as a potential protective system. The liposomal formulation with encapsulated Dz13 was compared to a liposomal formulation with spiked Dz13 after the liposome formation (Fig. 1). The formulation with encapsulated Dz13 was significantly more protective than the liposomal formulation with spiked Dz13 and an aqueous solution ($p < 0.05$). After 2 h, Dz13 in the aqueous solution was completely degraded, while 8.7 ± 0.8% and 5.0 ± 0.5% of Dz13 in the encapsulated and spiked formulation, respectively, was intact. Although the DNAzyme of the spiked formulation was not encapsulated, protective properties were monitored. This might be explainable by the observations by Gregoriadis et al. (1996). The group described that DNA was able to adsorb onto similar liposomal lipids and thus protected against degradation to a certain extent (Gregoriadis et al., 1996). Nevertheless, the recovery of Dz13 from the liposomal formulations was reduced over the time, indicating that the majority of the DNAzyme was insufficiently protected.

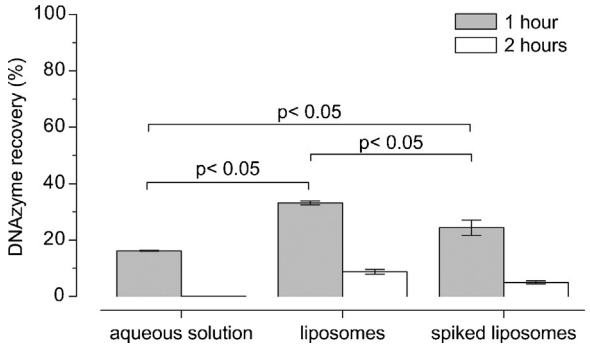

Fig. 1. DNAzyme degradation assay with liposomal formulations. Comparison of liposomes directly manufactured with Dz13 versus liposomes spiked with Dz13 after liposome formation. The Dz13 was analysed by AEX-HPLC (mean ± SD, $n = 3$). Significant differences were calculated by one-way ANOVA following a Bonfferroni test ($p < 0.05$).

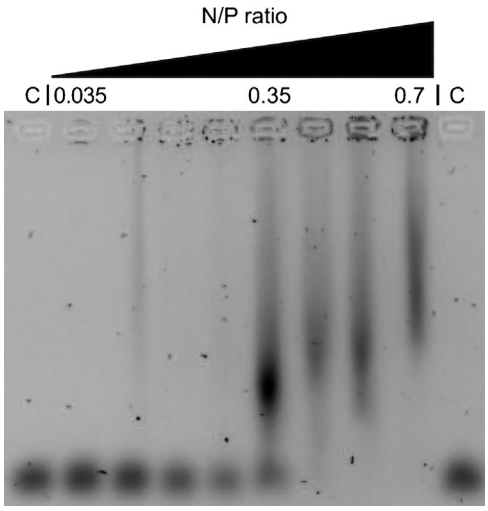

Fig. 2. Gel retardation assay with polyplexes at different N/P ratios. A fixed Dz13 concentration was complexed with different concentrations of chitosan resulting in different N/P ratios. The samples were analysed by gel electrophoresis. Lane C: Dz13 without chitosan.

3.3.2. Chitosan-DNAzyme polyplexes

The complexation between DNAzyme and cationic chitosan to polyplexes spontaneously occurs by electrostatic attraction (Dautzenberg and Jaeger, 2002). The resulting close bond may be able to shield the DNAzyme against enzymatic degradation. Investigation in the present study revealed that the properties of the chitosan-DNAzyme polyplexes depended on the ratio of chitosan's amino groups to DNAzyme phosphate groups (N/P ratio). The stability of the polyplexes increased with higher N/P ratios. Stable polyplexes had the ability to cover the negative charge of Dz13 as visualized by a retarded gel mobility in the electric field (Fig. 2). In contrast, Dz13 without chitosan or decomplexed Dz13 (sample not shown) had an unhindered run length.

The degree of complexation of the polyplexes was measured by AEX-HPLC (Fig. 3A). Using this method, free Dz13 in the supernatant of polyplex samples was detectable, while complexed Dz13 was not detected. Therefore, the degree of complexation was reciprocally proportional to the recovery of the free DNAzyme. An increased amount of chitosan did increase the degree of complexation. At a N/P ratio above 0.61, maximal complexation efficiency was achieved. The protective properties of the polyplexes for DNAzymes were further tested in the DNAzyme degradation assay. The recovery of Dz13 was monitored at multiple time points (Fig. 3B). At a N/P ratio of 0.7, no time-dependent degradation of Dz13 was observed, and a maximal integrity of $81 \pm 2\%$ was maintained. The observed loss might be due to partial exposure of outer complexed Dz13 to DNase activity. A correlation between degradation and degree of complexation after 2 h of DNAzyme degradation assay could be generated (Fig. 3C). The correlation demonstrated that polyplexes with a high N/P ratio represent sufficient protective systems for DNAzymes.

3.4. Protective drug delivery system

Compared to the liposomal formulation, the polyplex samples (N/P ratio: 0.7) provided a significant higher and time-independent protective efficiency. Therefore, the promising polyplexes were incorporated into a SME containing propylene glycol to generate a protective DDS. Propylene glycol was selected as a compatible agent with sufficient preservative activity. The polyplexes maintained the degree of complexation ($97 \pm 2\%$) while also incorporating into the protective DDS. The protective property of the system was finally validated by the DNAzyme degradation assay (Table 5). A high DNase concentration was subjected to the samples to maximise the degrading stress and exceed the activity of human skin (Reimer et al., 1978). At that concentration, unprotected Dz13 was almost fully degraded in every sample after 2 h. In contrast, the protective DDS obtained significant higher protection efficiency ($p < 0.05$). The complexation of Dz13 increased the protective efficiency similar to the previous results of Section 3.3.2. However, unlike the polyplexes in aqueous solution,

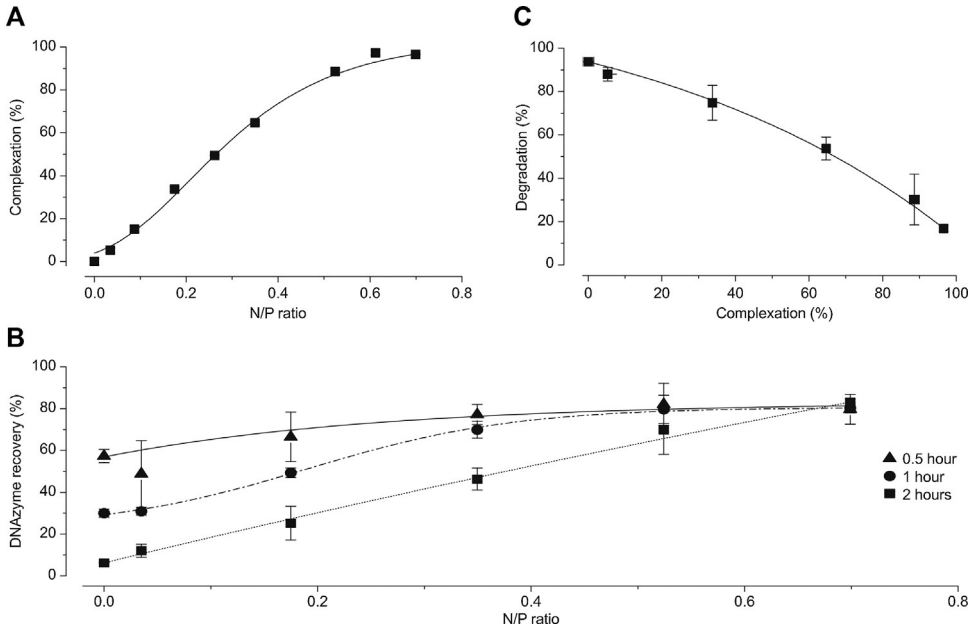

Fig. 3. Polyplex samples with a fixed Dz13 concentration in sodium acetate buffer analysed by AEX-HPLC (mean ± SD, $n = 3$). A: Complexation efficiency between Dz13 and chitosan at different N/P ratios. B: DNAzyme degradation assay with Dz13 in polyplexes at different N/P ratios. C: Correlation between DNAzyme degradation after 2 h and degree of complexation of Dz13 and chitosan.

Table 5
DNAzyme degradation assay of different samples with Dz13 (mean ± SD, $n = 3$). Protective DDS consisted of SME with propylene glycol and polyplexes (N/P: 0.7).

	DNAzyme recovery (%)		
Samples	0.5 h	1.0 h	2.0 h
Aqueous solut.	44 ± 1	22 ± 2	7 ± 0
Acetate buffer	57 ± 3	30 ± 2	6 ± 0
SME	25 ± 1	10 ± 1	2 ± 0
Protective DDS	101 ± 5	84 ± 6	70 ± 3

a time-dependent degradation of Dz13 was observed. The ingredients of the SMEs might led to temporary destabilisation and dissociations of the polyplex compounds. Bordi et al. (2013) observed a similar destabilisation of the electrostatic interaction between chitosan and DNA in the presence of a high ionic strength medium. Furthermore, the efficiency of enzymatic reactions is generally sensitive towards the reaction medium. In the present study, matrix effects of the protective DDS influenced DNase I activity. A decreased pH value by the sodium acetate buffer of polyplex samples (Mori et al., 2001) had an inhibitory effect on the DNAzyme degradation. In contrast, a high magnesium concentration (Pan et al., 1998) of the SMEs increased the enzymatic activity. Nevertheless, the data clearly demonstrated that incorporating the polyplexes into the SME compensated for the SME's lack of a protective characteristic, resulting in a protective DDS. Additionally, the approach using polyplexes could be adaptable for other DDSs where the DNAzyme is unprotected (Schmidts et al., 2011).

3.5. In vitro studies

3.5.1. Skin penetration study

DNAzyme applied with the protective DDS was subjected to a skin penetration study. In this study, aspects of degradation, penetration and distribution were examined using different analytic methods (Fig. 4). AEX-HPLC analysis of the remaining formulation revealed that polyplexes could maintain the integrity of Dz13 on the skin surface. By contrast, the unprotected Dz13 in aqueous solution were nearly fully degraded after 24 h (Fig. 4A). To calculate the distinct degradation of each sample, the ratio between the peak area of the intact Dz13 to the whole peak area of the chromatogram was compared relative to the ratio of HPLC calibration standards. The aqueous solution had a relative recovery of 6 ± 7%, the polyplexes in aqua of 97 ± 1% and the polyplexes in SME of 99 ± 2%. Similar results were observed with the FAM-DNAzyme (data not shown). The reduction of intact DNAzymes in aqueous solution is triggered by commensal bacteria and the skin. The penetration of intact Dz13 into the skin was quantified using hybridization-ELISA. The polyplexes themselves did not positively affect the penetration efficiency compared with the aqueous solution. However, the combination of polyplexes and SME as protective DDS increased the skin uptake from 0.3 ± 0.3 μg/cm² to a value of 1.0 ± 0.5 μg/cm² (Fig. 4B). The CLSM visualised the distribution of FAM-DNAzyme in the skin. The pictures of vertically cross-sectioned skin specimens revealed that the identified fluorescence signal was located within the outermost skin layers (Fig. 4C). However, the CLSM was unable to verify the integrity of the FAM-DNAzyme. Therefore, the quantified and summarized CLSM data indicated a similarly enhanced penetration efficiency of the FAM-DNAzyme from aqueous solution and the protective DDS (Fig. 4D). Degraded FAM-DNAzyme can penetrate with less difficulty into the skin due to a smaller MW, resulting in a false-positive signal. Therefore, the fluorescence analysis can only be utilised if a potential degradation of the fluorescence-labelled molecule is monitored. In conclusion, the protective DDS can protect DNAzyme from degradation on the skin surface and can enhance the penetration of intact DNAzyme into the layers of the skin.

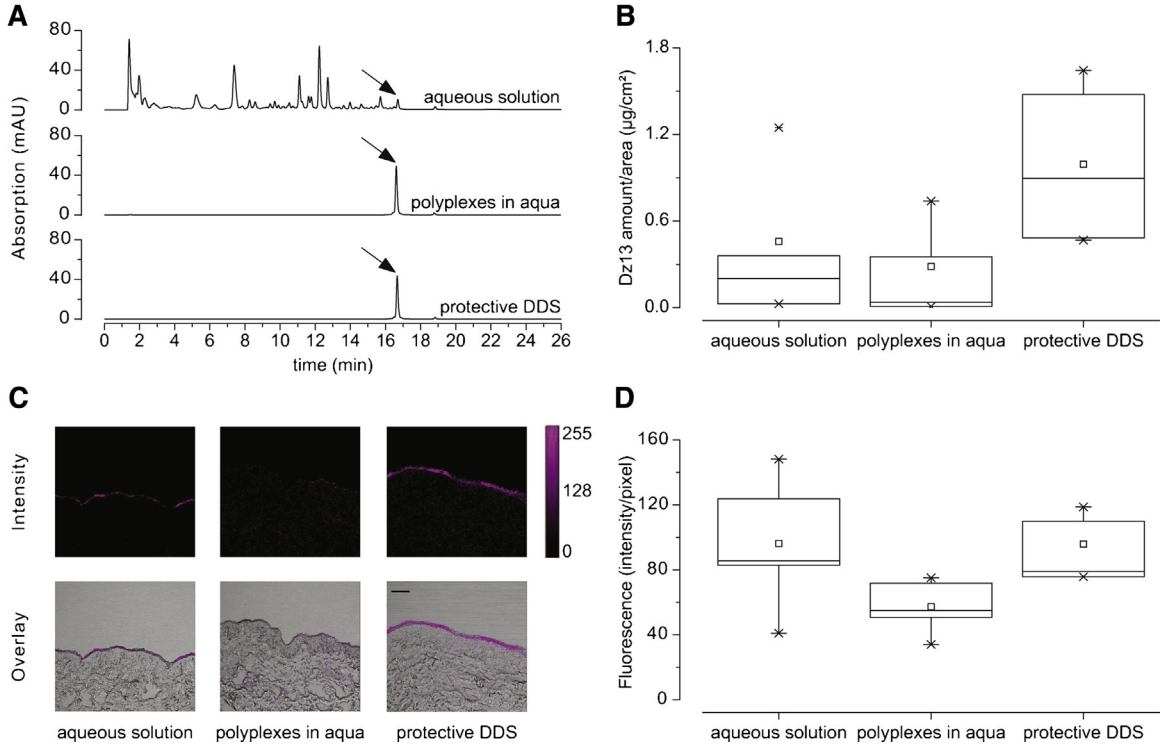

Fig. 4. Penetration study with Dz13 in aqueous solution, polyplexes in aqueous solution or polyplexes in SME. A: AEX-HPLC chromatograms of Dz13 in the applied formulations after the penetration study. Arrows indicate the intact DNAzyme. B: Intact Dz13 recovery in skin samples measured by hybridization-ELISA ($n = 5$). C: CLSM pictures of skin specimens. Spectral analysis (upper picture) and overlay with transmitted light picture (lower picture). The scale bar represents 100 μm. D: Summed data of all spectral analysis CLSM pictures ($n = 5$).

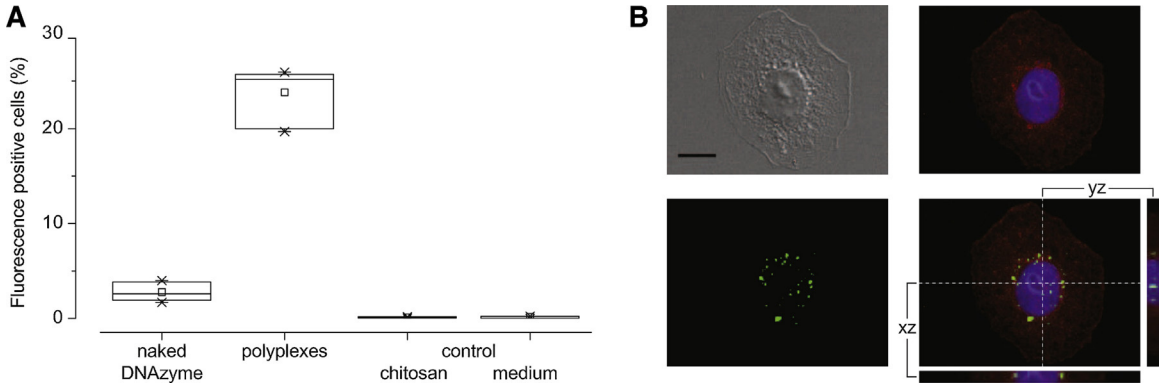

Fig. 5. Cellular uptake of the FAM-DNAzyme with polyplexes into HaCaT keratinocytes after 24 h of incubation. A: Percentage of fluorescence positive cell measured by flow cytometry (controls $n = 3$, samples $n = 9$). B: Pictures of HaCaT keratinocyte incubated with polyplexes. FAM-DNAzyme are represented in green. Nucleic DNA and F-actin filament of the cytoskeletons were stained with DAPI (blue) and Alexa Fluor 555 Phalloidin (red), respectively. The scale bar represents 10 μm. Orthogonal section yz and xz are corresponding to the cross. (For interpretation of the references to color in this figure legend, the reader is referred to the web version of this article.)

3.5.2. Cell uptake study

On the cellular level, the penetration and distribution of DNAzyme with the polyplexes (N/P: 0.7) were compared to naked DNAzymes with HaCaT keratinocytes. To simulate the cell uptake after penetration into the skin, the concentration of FAM-DNAzyme in the cell medium was adjusted to 1.0 μg/cm^2 (according to Section 3.5.1). The results of the flow cytometry demonstrated an enhanced uptake of FAM-DNAzyme by polyplexes into the keratinocytes (Fig. 5A). The data are in accordance to the summed data of CLSM analytic (data not shown). The results indicated that polyplexes were able to cover anionic properties of DNAzymes (see Section 3.3.2), which might have enhanced the internalization progress. The concentration of the intact FAM-DNAzyme in cells was determined to be 0.12 ± 0.00 μg/cm^2 by hybridization-ELISA. The internalized FAM-DNAzyme was distributed into the cytoplasm at the side of action (Fig. 5B).

4. Conclusion

In the present study, a physicochemical stable SME with sufficient preservation was developed as an appropriate DDS for DNAzyme Dz13. To protect Dz13 against enzymatic degradation, a liposomal formulation and chitosan-DNAzyme polyplexes were developed. In a validation process, the integrity of Dz13 was monitored in different samples in the presence of degrading DNase I. The assay revealed that the protective properties of the liposomes were mainly driven by the lipid ingredients rather than by encapsulating the Dz13. The superior polyplexes indicated that the stability and charge of the complex and the protective characteristic depend on the N/P ratio. The combination of developed SME and the polyplexes was able to compensate for the SME's lack of protection. In general, using the polyplexes may be possible for other DDS with insufficient protection of DNAzymes. The developed protective DDS was examined in in vitro model systems at the skin and cellular level. The protective DDS was able to protect Dz13 and FAM-DNAzyme against degradation on the skin surface. The penetration of the intact Dz13 and FAM-DNAzyme into the skin and subsequently into keratinocytes was enhanced compared with the control samples. Topically applied FAM-DNAzyme was distributed into the outermost layers of skin, and in the case of the cell culture, FAM-DNAzyme was mainly located in the cytoplasm at the site of action. The presented results confirm that the developed protective DDS is an appropriate system for the dermally applied DNAzyme towards a therapy against actinic keratosis. Finally, the protective DDS could be adaptable for other nucleic acid-based APIs.

Acknowledgments

The authors would like to thank the Federal Ministry of Education and Research for the financial support (grant no. 03FH031 3).

References

Amselem, S., Friedman, D., 1998. Submicron emulsions as drug carriers for topical administration. Submicron Emulsions in Drug Targeting and Delivery. Harwood Academic Publishers, London, pp. 153–173.
Bordi, F., Chronopoulou, L., Palocci, C., Bomboi, F., Di Martino, A., Cifani, N., Pompili, B., Ascenzioni, F., Sennato, S., 2013. Chitosan–DNA complexes: effect of molecular parameters on the efficiency of delivery. Colloids Surf. A .
Breaker, R.R., Joyce, G.F., 1994. A DNA enzyme that cleaves RNA. Chem. Biol. 1, 223–229.
Cai, H., Santiago, F.S., Prado-Lourenco, L., Wang, B., Patrikakis, M., Davenport, M.P., Maghzal, G.J., Stocker, R., Parish, C.R., Chong, B.H., Wong, G.J., Wong, T.-W., Chesterman, C.N., Francis, D.J., Moloney, F.J., Barnetson, Ross St C., Halliday, G.M., Khachigian, L.M., 2012. DNAzyme targeting c-jun suppresses skin cancer growth. Sci. Transl. Med. 4, 139ra82.
Cairns, M.J., Hopkins, T.M., Witherington, C., Wang, L., Sun, L.Q., 1999. Target site selection for an RNA-cleaving catalytic DNA. Nat. Biotechnol. 17, 480–486.
Cho, E.-A., Moloney, F.J., Cai, H., Au-Yeung, A., China, C., Scolyer, R.A., Yosufi, B., Raftery, M.J., Deng, J.Z., Morton, S.W., Hammond, P.T., Arkenau, H.-T., Damian, D. L., Francis, D.J., Chesterman, C.N., Barnetson, Ross St C., Halliday, G.M., Khachigian, L.M., 2013. Safety and tolerability of an intratumorally injected DNAzyme, Dz13, in patients with nodular basal-cell carcinoma: a phase 1 first-in-human trial (DISCOVER). Lancet 381 (9880), 1835–1843.
Council of Europe, 2013. European Pharmacopoeia, 8th ed. European Pharmacopoeia, Strasbourg.
Criscione, Weinstock, M.A., Naylor, M.F., Luque, C., Eide, M.J., Bingham, S.F., 2009. Actinic keratoses: natural history and risk of malignant transformation in the veterans affairs topical tretinoin chemoprevention trial. Cancer 115, 2523–2530.
Dautzenberg, H., Jaeger, W., 2002. Effect of charge density on the formation and salt stability of polyelectrolyte complexes. Macromol. Chem. Phys. 203, 2095–2102.
Eckhart, L., Fischer, H., Tschachler, E., 2012. Mechanisms and emerging functions of DNA degradation in the epidermis. Front Biosci. (Landmark Ed) 17, 2461–2475.
Elsabahy, M., Nazarali, A., Foldvari, M., 2011. Non-viral nucleic acid delivery: key challenges and future directions. Curr. Drug Deliv. 8, 235–244.
Gregoriadis, G., Saffie, R., Hart, S.L., 1996. High yield incorporation of plasmid DNA within liposomes: effect on DNA integrity and transfection efficiency. J. Drug Target 3, 469–475.
Jepps, O.G., Dancik, Y., Anissimov, Y.G., Roberts, M.S., 2013. Modeling the human skin barrier–towards a better understanding of dermal absorption. Adv. Drug Deliv. Rev. 65, 152–168.
Khachigian, L.M., Fahmy, R.G., Zhang, G., Bobryshev, Y.V., Kaniaros, A., 2002. c-Jun regulates vascular smooth muscle cell growth and neointima formation after arterial injury. Inhibition by a novel DNA enzyme targeting c-Jun. J. Biol. Chem. 277, 22985–22991.
Maeder, U., Marquardt, K., Beer, S., Bergmann, T., Schmidts, T., Heverhagen, J.T., Zink, K., Runkel, F., Fiebich, M., 2012. Evaluation and quantification of spectral information in tissue by confocal microscopy. J. Biomed. Opt. 10, 106011.
Mohammed, D., Hirata, K., Hadgraft, J., Lane, M.E., 2014. Influence of skin penetration enhancers on skin barrier function and skin protease activity. Eur. J. Pharm. Sci. 51, 118–122.

Mori, S., Yasuda, T., Takeshita, H., Nakajima, T., Nakazato, E., Mogi, K., Kaneko, Y., Kishi, K., 2001. Molecular, biochemical and immunological analyses of porcine pancreatic DNase I. Biochim. Biophys. Acta 1547, 275–287.

OECD, 2004a. Guidance Document for the Conduct of Skin Absorption Studies. OECD Publishing.

OECD, 2004b. Test No. 428: Skin Absorption: In Vitro Method. OECD Publishing.

Ongpipattanakul, B., Burnette, R.R., Potts, R.O., Francoeur, M.L., 1991. Evidence that oleic acid exists in a separate phase within stratum corneum lipids. Pharm. Res. 8, 350–354.

Pan, C.Q., Ulmer, J.S., Herzka, A., Lazarus, R.A., 1998. Mutational analysis of human DNase I at the DNA binding interface: implications for DNA recognition, catalysis, and metal ion dependence. Protein Sci. 7, 628–636.

Reimer, G., Zöllner, E.J., Reitz, M., Schwulera, U., Leonhardi, G., 1978. Comparison of DNase, DNA-polymerase and RNA-polymerase activities present in the DNA-binding proteins of normal human dermis, epidermis, horny layer and psoriatic scales. Arch. Dermatol. Res. 263, 317–324.

Richardson, S.C., Kolbe, H.V., Duncan, R., 1999. Potential of low molecular mass chitosan as a DNA delivery system: biocompatibility, body distribution and ability to complex and protect DNA. Int. J. Pharm. 178, 231–243.

Santoro, S.W., Joyce, G.F., 1997. A general purpose RNA-cleaving DNA enzyme. Proc. Natl. Acad. Sci. U. S. A. 94, 4262–4266.

Schmidts, T., Dobler, D., von den Hoff, S., Schlupp, P., Garn, H., Runkel, F., 2011. Protective effect of drug delivery systems against the enzymatic degradation of dermally applied DNAzyme. Int. J. Pharm. 410, 75–82.

Schmidts, T., Marquardt, K., Schlupp, P., Dobler, D., Heinz, F., Mäder, U., Garn, H., Renz, H., Zeitvogel, J., Werfel, T., Runkel, F., 2012. Development of drug delivery systems for the dermal application of therapeutic DNAzymes. Int. J. Pharm. 431, 61–69.

Semple, S.C., Klimuk, S.K., Harasym, T.O., Dos Santos, N., Ansell, S.M., Wong, K.F., Maurer, N., Stark, H., Cullis, P.R., Hope, M.J., Scherrer, P., 2001. Efficient encapsulation of antisense oligonucleotides in lipid vesicles using ionizable aminolipids: formation of novel small multilamellar vesicle structures. Biochim. Biophys. Acta 1510, 152–166.

Tan, M.L., Choong Peter, F.M., Dass, C.R., 2009. DNAzyme delivery systems: getting past first base. Expert Opin. Drug Deliv. 6, 127–138.

Turowska, A., Librizzi, D., Baumgartl, N., Kuhlmann, J., Dicke, T., Merkel, O., Homburg, U., Höffken, H., Renz, H., Garn, H., 2013. Biodistribution of the GATA-3-specific DNAzyme hgd40 after inhalative exposure in mice, rats and dogs. Toxicol. Appl. Pharmacol. 272 (2), 365–372.

Wagner, H., Kostka, K.H., Lehr, C.M., Schaefer, U.F., 2003. pH profiles in human skin: influence of two in vitro test systems for drug delivery testing. Eur. J. Pharm. Biopharm. 55 (1), 57–65.

Xu, X., Khan, M.A., Burgess, D.J., 2012a. A quality by design (QbD) case study on liposomes containing hydrophilic API: II. Screening of critical variables, and establishment of design space at laboratory scale. Int. J. Pharm. 423, 543–553.

Xu, X., Khan, M.A., Burgess, D.J., 2012b. Predicting hydrophilic drug encapsulation inside unilamellar liposomes. Int. J. Pharm. 423, 410–418.

Zhang, G., Dass, C.R., Sumithran, E., Di Girolamo, N., Sun, L.-Q., Khachigian, L.M., 2004. Effect of deoxyribozymes targeting c-jun on solid tumor growth and angiogenesis in rodents. JNCI-J. Natl. Cancer Inst. 96, 683–696.

Zhang, G., Ma, Y., 2013. Spectroscopic studies on the interaction of sodium benzoate, a food preservative, with calf thymus DNA. Food Chem. 141, 41–47.

Zhu, L., Mahato, R.I., 2010. Lipid and polymeric carrier-mediated nucleic acid delivery. Expert Opin. Drug Deliv. 7, 1209–1226.

Verzeichnis der akademischen Lehrer

Meine akademischen Lehrer waren Frau/Herr Breckow, Bergmann, Czermak, Dammann, Gokorsch, Heimrich, Hemberger, Kitzrow, Kirschbaum, Kleinöder, Kügler, Lauwerth, Leicht, Maas, Metz, Nietert, Platen, Röhm, Röhricht, Runkel, Stadlbauer in Gießen und Herr Renz in Marburg.

Danksagung
Eine Doktorarbeit entsteht nicht in der Isolation. Obwohl nur ein Name als Autor auf der Titelseite zu finden ist, bedarf es doch vieler helfender Hände diese zu vollenden. Daher möchte ich mich an dieser Stelle bei allen herzlich bedanken, die zu der Entstehung dieser Arbeit beigetragen haben.

Bei Herrn Prof. Frank Runkel möchte ich mich bedanken für das frühzeitige Vertrauen, dass du in mich gesteckt hast und das sich über Jahre hinweg zwischen uns gefestigt hat. Bei Dir steht die Person im Vordergrund und das weiß ich zu schätzen. Besonders bedanken will ich mich auch für die Freiheit, die du mir während der gesamten Forschungsarbeiten gewährtest, was zum einen zu wissenschaftlich-spannenden Exkursionen in andere Bereiche führte aber auch maßgeblich zum Gelingen dieser Arbeit beitrug. Ich danke Herrn Prof. Dr. Harald Renz für die herzlich hilfsbereite und wissenschaftliche Betreuung. Herrn Prof. Dr. Wolfgang Pfützner danke ich für die Übernahme des Zweitgutachtens. Mein ganz besonderer Dank gilt institutsübergreifend meinen Kollegen für die immer ausgesprochen angenehme Atmosphäre, die wissenschaftlichen Diskussionen und die außerordentlich freundschaftliche und gute Zusammenarbeit. Unvergessen bleibt für mich euer sportliches und besonders schweißtreibendes Engagement und die aus der hautfahrenden Quälereien im Zeichen meiner Doktorarbeit oder auch die Abende im wissenschaftlichen Umfeld. So habe ich während meiner Zeit als Doktorand viele neue Freundschaften gewonnen und alte Freundschaften gefestigt. Diese Freundschaften haben auch abseits der Arbeit die Zeit zu einer unvergesslichen gemacht und diese wie im Fluge vergehen lassen. Da meine Freundschaften Teil meines Lebens sind, sind auch sie Teil meiner Doktorarbeit und verdienen meinen uneingeschränkten Dank. Des Weiteren möchte ich mich bei Herrn Dr. Thomas Schmidts für die zahlreichen konstruktiven Gespräche und deine pragmatischen Lösungsansätze bedanken. Ebenso gilt mein Dank Frau Dr. Dorota Dobler die stets ihren wissenschaftlichen Rat uneigennützig angeboten hat und mir somit bewiesen hat, was für eine tolle Persönlichkeit sie ist. Zusätzlich möchte ich mich bei Anna-Carola Eicher für die tatkräftige Unterstützung im Labor bedanken. Mein Dank geht ebenso an die Mitglieder der Verwaltung der Fachbereiche in Gießen und Marburg.

Herzlichst möchte ich mich bei meiner Familie bedanken. Insbesondere meinen Eltern, die schon in der Grundschule den Grundstein für meine akademische Laufbahn gelegt hatten. Vielen Dank für eure fortwährende Unterstützung und das

unerschütterliche elterliche Vertrauen in mich. Bei meiner Partnerin möchte ich mich für die uneingeschränkte, liebevolle und vielseitige Unterstützung herzlich bedanken. Deine Unterstützung ging so weit, dass du versucht hast mir zuliebe die Welt der Naturwissenschaft für dich neu zu entdecken und für mich versucht hast, obwohl es oft nicht einfach ist, selbst zwischen den Zeilen zu lesen. Ich verspreche es dir, es hat sich schon jetzt gelohnt.